# Development and Characterisation of a Rat Model of Parkinson's Disease

Negrini, Matilde

2022

*Document Version:*
Publisher's PDF, also known as Version of record

# Development and Characterisation of a Rat Model of Parkinson's Disease

MATILDE NEGRINI
DEPARTMENT OF EXPERIMENTAL MEDICAL SCIENCE | LUND UNIVERSITY

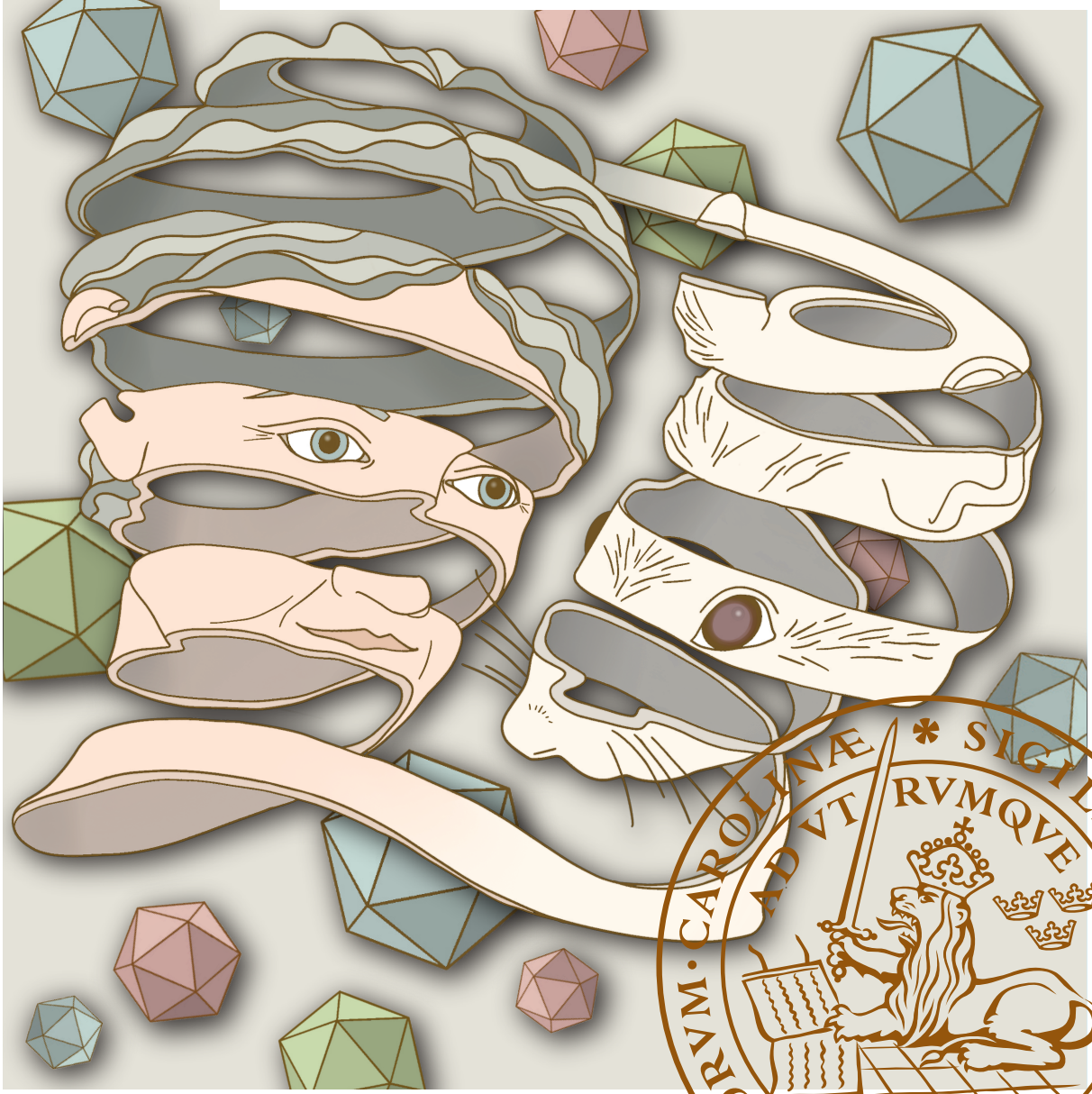

Printed by Media-Tryck, Lund 2022 NORDIC SWAN ECOLABEL 3041 0903

## About the author

**MATILDE NEGRINI** completed her MSc degree in cellular and molecular biotechnology in 2017 at Trento University and thereafter undertook a PhD under the supervision of Andreas Heuer in the Behavioural Neuroscience Laboratory. Her work centered on developing and characterising a rat model of Parkinson's Disease based on AAV-induced overexpression of alpha-synuclein.

LUND UNIVERSITY

FACULTY OF MEDICINE

Department of Experimental Mediacl Science

Lund University, Faculty of Medicine
Doctoral Dissertation Series 2022:143
ISBN 978-91-8021-305-9
ISSN 1652-8220

# Development and characterisation of a rat model of Parkinson's Disease

Matilde Negrini


LUND
UNIVERSITY

DOCTORAL DISSERTATION
by due permission of the Faculty of Medicine at Lund University this thesis will be defended on November 4th at 13.00 in Segerfalksalen, BMC A19, Lund, Sweden.

FACULTY OPPONENT

**Mikko Airavaara**
Neuroscience Center
University of Helsinki, Finland

| | |
|---|---|
| **Organization**<br>LUND UNIVERSITY<br>Behaviouar Neuroscience Laboratory<br>Department of Experimental Medical Sciences<br>Faculty of Medicine | **Document name**<br>DOCTORAL DISSERTATION<br>**Date of issue**<br>04/11/2022 |
| Author(s)<br>Matilde Negrini | Sponsoring organization |


**Title and subtitle**
Development and characterisation of a rat model of Parkinson's Disease


**Abstract**

Preclinical rodent models of Parkinson's Disease (PD) based on alpha-synuclein (αSyn) present some of the pathological hallmarks of the human condition, such as the progressive loss of dopaminergic neurons in the substantia nigra (SN) and the development of behavioural deficits. However, numerous reports on these models highlighted the variable outcomes that might originate from them if not validated properly. This thesis seeks to develop and characterise a rat model of PD, which present stable and relevant pathology and to be utilised for the investigation of disease progression and the assessment of therapeutic interventions. At first, we compared different αSyn models based on the injection of an adeno-associated virus (AAV) overexpressing human αSyn and/or the inoculation of preformed fibrils (PFFs). Although some additional pathology (i.e. increased protein aggregation and inflammation) could be obtained by combining AAV-αSyn and PFFs, AAV-αSyn alone was sufficient to generate a model that would present neuronal loss, Lewy-like pathology, and behavioural impairments. We, therefore, further investigated the ability of AAV-αSyn to model early stages of PD. We could detect a progressive development of motor and cognitive symptoms by using simple drug-free behavioural tests and concomitant neuronal loss in the SN. Subsequently, we demonstrated, for the first time in an AAV-αSyn model, attentional neglect, as well as deficits in movement initiation and movement completion using a lateralised choice reaction time task. Eventually, we tested whether our newly characterised model could be useful in the assessment of disease-modifying therapies, such as the injection of neurotrophic factors. We, therefore, tested the potential beneficial effects of a new candidate among them, the growth differentiation factor 5 (GDF5). Unfortunately, the injection of AAV-GDF5 did not exert any neuroprotective effect in our model. Taken together, these results show that it was possible to replicate our AAV-αSyn rat model between studies, and it presents stable neurodegeneration, synucleinopathy, as well as motor and cognitive deficits which can be assessed by a wide battery of simple and complex behavioural tests.



**Key words**
Parkinson's Disease, AAV, gene therapy, behaviour, rat model, dopamine, alpha-synuclein, PFFs

Classification system and/or index terms (if any)

| | | |
|---|---|---|
| Supplementary bibliographical information | | **Language** English |
| **ISSN** and key title 1652-8220 | | **ISBN** 978-91-8021-305-9 |
| Recipient's notes | **Number of pages** 87 | Price |
| | Security classification | |




Signature  Date 2022-09-28

# Development and characterisation of a rat model of Parkinson's Disease

Matilde Negrini


LUND
UNIVERSITY

Cover by Matilde Negrini representing a patient affected by Parkinson's Disease and the respective rat model, both surrounded by viral capsids. The two faces complete each other, symbolizing the bond between clinical and preclinical research. (Artwork inspired by M.C. Escher, *Bond of Union*, 1956)



Faculty of Medicine
Department of Experimental Medical Sciences

ISBN 978-91-8021-305-9
ISSN 1652-8220

Printed in Sweden by Media-Tryck, Lund University
Lund 2022

*To the students who supported me,*

"Anything that can go wrong, will go wrong"
*Murphy's Law*

# Table of Contents

# Original papers and manuscripts

I. **Negrini M**, Tomasello G, Davidsson M, Fenyi A, Adant C, Hauser S, Espa E, Gubinelli F, Manfredsson FP, Melki R, Heuer A. Sequential or simultaneous injection of preformed fibrils and AAV overexpression of alpha-synuclein are equipotent in producing relevant pathology and behavioural deficits (2022) *Journal of Parkinson's Disease*.

II. Gubinelli F, Cazzolla G, **Negrini M**, Kulacz I, Mehrdadian A, Tomasello G, Sarauskyte L, Venuti C, Jacobs F, Manfredsson FP, Davidsson M, Heuer A. Lateralized deficits after unilateral AAV-vector based overexpression of alpha-synuclein in the midbrain of rats on drug-free behavioural tests (2022) *Behavioural Brain Research*.

III. Gubinelli F, Sarauskyte S, Venuti C, Kulacz I, Cazzolla G, **Negrini M**, Answer D, Manfredsson FP, Davidsson M, Heuer A. Characterisation of functional deficits induced by AAV overexpression of alpha-synuclein in rats (2022) *Current Research in Neurobiology* (In review).

IV. **Negrini M**, Vecchio I, Sannio A, Jacobs F, Brignone D, Manfredsson, F, Davidsson M, O'Keeffe GW, Heuer A. AAV Vector Delivery of GDF5 to the Substantia Nigra: Implications for Gene Therapy on an alpha-Synuclein Rat Model of Parkinson's Disease (2022) *Manuscript in preparation*.

## Published papers outside the thesis

V. **Negrini M**, Wang G, Heuer A, Björklund T & Davidsson, M. AAV Production Everywhere: A Simple, Fast, and Reliable Protocol for In-house AAV Vector Production Based on Chloroform Extraction (2020) *Current Protocols in Neuroscience.*

VI. Davidsson M, **Negrini M,** Hauser S, Svanbergsson A, Lockowandt M, Tomasello G, Manfredsson FP & Heuer, A. A comparison of AAV-vector production methods for gene therapy and preclinical assessment (2020) *Scientific Reports*.

# Summary

Many efforts have been made to prevent Parkinson's Disease, but science is still far from finding a solution, and despite 200 years of research, someone is diagnosed with Parkinsonism every nine minutes. One of the reasons why this neurodegenerative disease is still incurable is the lack of a comprehensive animal model. Animals do not develop Parkinson's Disease naturally; therefore, it has to be induced artificially. One common approach is to inject toxins into the brain, which can induce death in the neurons releasing dopamine, mimicking what happens in the brains of patients at an advanced stage of parkinsonism. Even though it has been a golden standard for many years, nowadays, there is an interest in finding a model where this disease develops more similarly to the human condition. Many scientists have started using a protein called alpha-synuclein, which is known to play a key role in this disease. Patients with Parkinson's Disease accumulate insoluble deposits mainly composed of this protein, and this is linked to the death of dopamine-releasing neurons with consequences on movement and cognition. An efficient way to deliver alpha-synuclein in animal models is by using adeno-associated viruses, which in the past years have become the go-to vehicle for delivering genes to target tissues. In this thesis, we validated a new virus to express high levels of alpha-synuclein in the brain of rats to achieve stable behavioural deficits and relevant pathology. We demonstrated that our model develops stable motor and cognitive deficits similar to what is observed in humans by using a battery of simple and complex behavioural tests. Additionally, our model presents the typical pathological hallmarks that are present in patients, such as abnormal protein accumulation and neuronal death. The development and characterization of a reliable rat model of Parkinson's Disease are crucial for getting new insights about this incurable disease and for finding and testing new future treatments, such as neurotrophic factors. Neurotrophic factors are small proteins capable of both preventing neuronal death and promoting their survival. Many of them have already reached the stage of being tested in clinical trials, but scientists are still looking for new proteins with more specific and stronger beneficial effects. For this reason, the last part of this work was dedicated to testing the effects of a new candidate within neurotrophic factors, named GDF5.

# Sammanfattning

Stora ansträngningar och insatser har gjorts för att förebygga Parkinsons sjukdom, men trots det är forskningen fortfarande långt ifrån att hitta en lösning. Trots 200 år av intensiv forskning får var nionde minut en patient diagnosen Parkinsonism. En av anledningarna till att denna neurodegenerativa sjukdom fortfarande inte går att bota är avsaknaden av en djurmodell av Parkinsons sjukdom som efterliknar sjukdomen hos människor. Djur utvecklar inte Parkinsons sjukdom naturligt, därför måste sjukdomen induceras på konstgjord väg. Ett vanligt tillvägagångssätt är att injicera toxiner i hjärnan, dessa toxiner kan leda till att neuronerna som frisätter dopamin dör, vilket efterliknar vad som händer i patienternas hjärnor i ett framskridet stadium. Även om den här modellen har varit standard i många år, finns det numera ett intresse att hitta en modell där sjukdomen mer liknar det som sker hos patienter. Många forskare har börjat använda ett protein som kallas alfa-synuklein, detta protein är känt för att spela en viktig roll i sjukdomen. Patienter med Parkinsons sjukdom ackumulerar den toxiska formen av proteinet och detta är kopplat till att nervceller som frisätter dopamin dör, vilket leder till konsekvenser för bland annat rörelse och kognition. Ett effektivt sätt att leverera alfa-synuklein till nervceller i djurmodeller är att använda adeno-associerade virus. Dessa har under de senaste åren blivit det vanligaste sättet att leverera gener till olika celltyper. I den här avhandlingen utvecklade vi ett nytt virus för att uttrycka höga nivåer av alfa-synuklein i hjärnan på råttor. Målet med studierna var att uppnå stabila beteendeförändringar och relevant patologi hos råttorna. Vi visade att vår modell utvecklar stabila motoriska och kognitiva symptom, på samma sätt som det som observerats hos patienter genom både enkla och komplexa beteendetester. Dessutom visar vår modell de typiska patologiska kännetecknen som finns hos patienter, som onormal proteinackumulering och nervceller som dör. Utvecklingen och karakteriseringen av en reproducerbar råttmodell av Parkinsons sjukdom är avgörande för att få nya insikter om denna obotliga sjukdom och för att hitta och testa nya behandlingar, såsom till exempel neurotrofiska faktorer. Neurotrofiska faktorer är små proteiner som kan förhindra nervcellers död och främja deras överlevnad. Många av dessa faktorer har redan testats i kliniska försök, men forskare letar fortfarande efter nya proteiner med mer specifika och bättre effekter. Av denna anledning ägnades den sista delen av avhandlingen åt att testa effekterna av en ny kandidat inom neurotrofiska faktorer, nämligen GDF5.

# Riassunto

Sono stati fatti molti sforzi per prevenire il morbo di Parkinson, ma il mondo della scienza è ancora lontano dal trovare una soluzione. Nonostante 200 anni di ricerca, infatti, ogni nove minuti a una persona viene diagnosticata questa malattia. Uno dei motivi per cui questa patologia neurodegenerativa è ancora incurabile è la mancanza di un modello animale che racchiuda le sue principali caratteristiche patologiche. Gli animali, come è noto, non sviluppano la malattia di Parkinson in modo naturale, perciò deve essere indotta artificialmente. Un approccio comunemente utilizzato per fare ciò consiste nell'iniettare una tossina nel cervello che può indurre la morte nei neuroni che rilasciano dopamina, imitando ciò che accade nel cervello dei pazienti in uno stadio avanzato. Anche se per molti anni questa è stata una pratica standard, al giorno d'oggi i ricercatori stanno cercando altre vie, sviluppando modelli in cui la malattia si sviluppi in modo più naturale, similmente alla condizione umana. Molti scienziati hanno iniziato quindi ad utilizzare una proteina, chiamata alfa-sinucleina, che è nota per il suo ruolo chiave nello sviluppo di questa malattia. I cervelli dei pazienti affetti dal morbo di Parkinson, infatti, accumulano depositi insolubili di questa proteina: questo fattore è connesso alla morte dei neuroni che rilasciano dopamina, producendo conseguenze sul movimento e sulla cognizione. Un modo efficiente per somministrare l'alfa-sinucleina in modelli animali consiste nell'usare virus adeno-associati, che negli ultimi anni sono diventati il veicolo prediletto per esprimere geni in tessuti bersaglio. In questa tesi, abbiamo validato un nuovo virus per esprimere alti livelli di alfa-sinucleina nel cervello di ratto, in modo tale da ottenere deficit comportamentali e una patologia rilevante. Abbiamo dimostrato – utilizzando una batteria di test comportamentali semplici e complessi – che il nostro modello sviluppa deficit motori e cognitivi stabili in modo simile a quanto osservato negli esseri umani. Inoltre, il nostro modello presenta i tipici segni patologici presenti nei pazienti, come l'accumulo anomalo di proteine e la morte neuronale. Lo sviluppo e la caratterizzazione di un modello di ratto affidabile per il morbo di Parkinson è fondamentale per ottenere nuove conoscenze su questa malattia incurabile e per trovare e testare nuovi trattamenti, come ad esempio i fattori neurotrofici: piccole proteine solubili in grado di prevenire la morte neuronale e favorirne la sopravvivenza. Molti di loro hanno già raggiunto la fase di sperimentazione clinica, ma gli scienziati continuano a cercare nuove proteine con effetti benefici più specifici e più forti. Per questo motivo, l'ultima parte di questo lavoro è stata dedicata all'investigazione degli effetti di un nuovo candidato tra i fattori neurotrofici, chiamato GDF5.

# Abbreviations

| | |
|---|---|
| 6-OHDA | 6-hydroxydopamine |
| αSyn | alpha-synuclein |
| AADC | aromatic L-amino acid decarboxylase |
| AAV | adeno-associated virus |
| ACC | accuracy |
| BMPR | bone morphogenetic protein receptor |
| CA | catecholamine |
| CBA | chicken beta actin |
| cDNA | complementray DNA |
| CDNF | cerebral dopamine neurotrophic factor |
| COMT | catechol-o-methyl-transferase |
| DAB | 3,3'-diaminobenzidine |
| DAT | dopamine transporter |
| DBS | deep brain stimulation |
| ddPCR | digital droplet PCR |
| DJ-1 | parkinson associated deglycase |
| EFF | efficiency |
| ER | endoplasmic reticulum |
| GABA | gamma-aminobutyric acid |
| GAPDH | glyceraldehyde phosphate dehydrogenase |
| GDF5 | growth differentiation factor 5 |
| GDNF | glial cell line-derived neurotrophic factor |
| GFP | green fluorescent protein |
| GPe | external globus pallidus |
| GPi | internal globus pallidus |
| h | human |
| L-DOPA | levodopa |
| LB | Lewy Body |
| LN | Lewy Neurite |
| LOD | limit of detection |
| LRKK2 | leucine-rich repeat kinase 2 |
| LV | lateral ventricle |
| MAO-B | monoamine oxidase type B |
| MB | midbrain |

| | |
|---|---|
| MFB | medial forebrain bundle |
| MPTP | 1-methyl-4-phenyl-1,2,3,6-tetrahydropyridine |
| MRI | magnetic resonance imaging |
| MT | movement time |
| NGF | neurite growth factor |
| noTG | no transgene |
| NRTN | neurturin |
| NTF | neurotrophic factor |
| OD | optical density |
| PCR | polymerase chain reaction |
| PD | Parkinson's Disease |
| PDGF-BB | platelet-derived growth factor BB |
| PEI | polyethylenimine |
| PFA | paraformaldehyde |
| PFF | preformed fibril |
| PINK1 | PTEN-induced putative kinase 1 |
| pK | proteinase K |
| PRKN | parkin |
| pSer129 | phosphorylated serine 129 |
| PUT | putamen |
| qPCR | quantitative PCR |
| RRF | retrorubral field |
| RT | reaction time |
| SN | substantia nigra |
| SNc | substantia nigra pars compacta |
| SNr | substantia nigra pars reticulata |
| ST | striatum |
| STN | subthalamic nucleus |
| TGF-β | transforming growth factor beta |
| TH | tyrosine hydroxylase |
| ThioS | thioflavin S |
| TLR | toll-like receptor |
| TTI | total trials initiated |
| TTU | total trials usable |
| Ub | ubiquitin |
| VMAT2 | vescicula monoamine transporter 2 |
| VPS35 | vacuolar protein sorting-associated protein 35 |
| VTA | ventral tegmental area |
| WT | wild-type |

# Introduction

## Parkinson's Disease

### Aetiology

Parkinson's Disease (PD) is a progressive neurodegenerative disorder affecting more than 10 million people worldwide. About 90% of all PD cases are considered sporadic and they are determined by a complex interplay between genetic variants, environmental factors, lifestyle, as well as epigenetic factors (Sulzer, 2007). Among the greatest environmental risk factors there are ageing, head trauma, and exposure to compounds such as rotenone, paraquat and 1-methyl-4-phenyl-1,2,3,6-tetrahydropyridine (MPTP) (Noyce et al., 2012). The remaining cases are caused by monogenic mutations and several genetic variants have been identified in families with PD causing both autosomal dominant and recessive forms of the disease. Among them, the first being discovered was an autosomal dominant mutation (A53T) affecting the SNCA gene, encoding for α-synuclein (αSyn) (Polymeropoulos et al., 1997). Later, SNCA duplications and triplications have been reported, which suggested that αSyn is linked to PD in a dose-dependent manner (Ibanez et al., 2004; Singleton et al., 2003). Other known genetic variants with high penetrance affect leucine-rich repeat kinase 2 (LRRK2), Parkinson-associated deglycase (DJ-1), vacuolar protein sorting-associated protein 35 (VPS35), PTEN-induced putative kinase 1 (PINK1) and Parkin (PRKN). For an extensive review about PD please refer to (Kalia & Lang, 2015).

### Pathophysiology

PD results mainly from the dysregulation of dopamine transmission because of changes in the biological activity of the brain. This decrease in dopamine levels correlates with the progressive dysfunction and eventually death of dopaminergic neurons in the substantia nigra pars compacta (SNc) (Graybiel et al., 1990; Trétiakoff, 1919). One of the proposed major mechanisms for neuronal dysfunction and neuronal death in PD includes abnormal protein aggregation, which results in the intracellular formation of inclusions called Lewy bodies (LBs) and Lewy neurites (LNs). These inclusions are rich in filamentous structures mainly composed

of αSyn, which undergoes a conformational shift followed by polymerization into long protein fibrils (Spillantini et al., 1997; Wood et al., 1999). The exact mechanism by which αSyn starts aggregating is still unknown, but several point mutations, environmental factors, and post-translational modifications have been identified, which give rise to an increased tendency towards aggregation. For example, phosphorylation of serine 129 (pSer129) is the most reported post-translational modification and it can be found in different synucleinopathies (Fujiwara et al., 2002). Other common post-translational modifications include ubiquitination, truncation, nitration, and O-linked-N-acetylglucosaminylation (Manzanza et al., 2021).

To date, the exact process whereby αSyn aggregation causes neuronal cell loss is poorly understood, but some studies suggest that αSyn might disrupt the function of multiple cellular organelles such as synaptic vesicles, mitochondria, endoplasmic reticulum (ER) and Golgi, lysosomes, autophagosomes and the nucleus (Wong & Krainc, 2017). Figure 1 summarizes the major pathways implicated in αSyn toxicity.

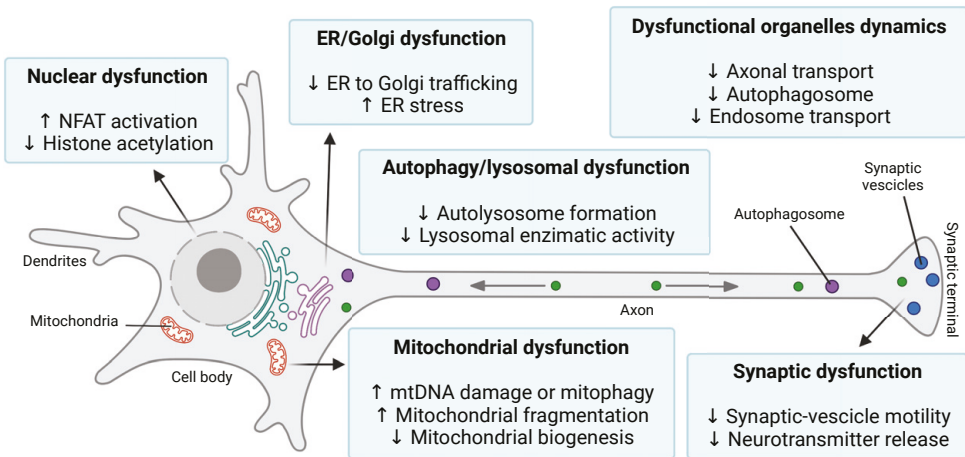


**Figure 1 | Pathways implicated in αSyn toxicity.** Dysfunction of the mitochondria, organelles and their dynamics, the Endoplasmic Reticulum (ER), the Golgi, the nucleus, the synapses, and of autophagy as well as the lysosomes have been implicated in αSyn toxicity. (adapted from Wong and Kranic 2017) (created with BioRender.com.)

Although several cellular mechanisms have been implicated in αSyn toxicity, multiple contributing factors might be crucial in determining the onset and the progression of the pathology. Among them are aging, the selective vulnerability of dopaminergic neurons in the SNc, the prion-like spreading of αSyn, and neuroinflammation (Wong & Krainc, 2017).

For example, activated microglia, the innate immune cells of the central nervous system, have been found in close contact with αSyn neuronal deposits in specimens from PD patients (Ouchi et al., 2005). Moreover, αSyn is able to bind Toll-like receptors (TLRs), a class of proteins that play a key role in the innate immune

system and microglia activation (Kim et al., 2013), and to act as a chemoattractant able to promote microglia migration (Wang et al., 2015).

As the severity of PD increases, the depletion of dopamine, the progressive neuronal dysfunction, and the neuronal loss lead to further changes in the brain, which alter the function of other important neurotransmitters such as glutamate, γ-aminobutyric acid (GABA), and serotonin. The interplay between these heterogeneous factors leads to the development of motor and non-motor symptoms (Barone, 2010).

## Motor and non-motor symptoms in PD

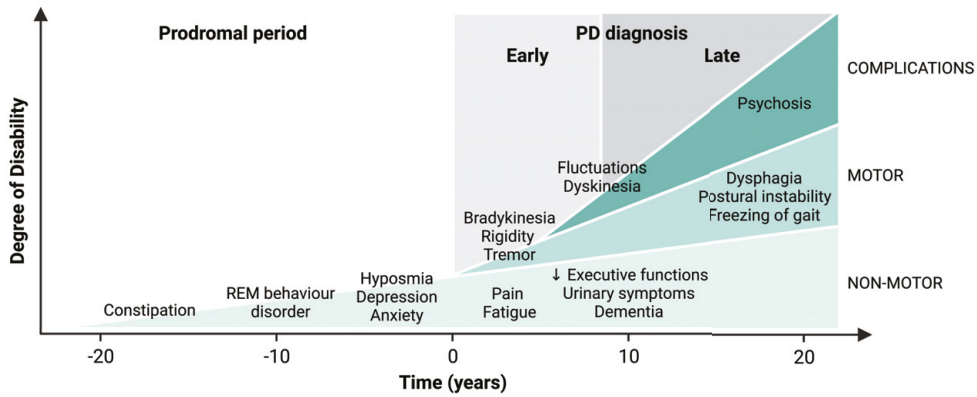


**Figure 2 | Clinical symptoms and time course of PD progression**. The onset of non-motor symptoms starts decades before the appearance of the motor symptoms and the time of disagnosis. The late stage of PD is characterised by the worsening of motor and non-motor symptoms and by the appearance of complications (adapted from Kalia et al. 2015). (created with BioRender.com.)

The first description of PD symptoms was given by James Parkinson in 1817. *An Essay on the Shaking Palsy* focuses on six individuals presenting the characteristic resting tremor, abnormal posture and gait, slowness of movement (bradykinesia), diminished muscle strength, and rigidity (Parkinson, 2002). Two centuries later, these cardinal motor features are still considered the hallmark of PD. However, they appear at an advanced stage of the disease when already 30% of the nigral neurons are dead and 50-70% of the striatal dopaminergic terminals are affected (Fearnley & Lees, 1991; Greffard et al., 2006; Ma et al., 1997). On the other hand, several non-motor symptoms, such as loss of smell (hyposmia), sleep disturbances, and constipation, can develop many years before the onset of motor symptoms and do not require that level of neuronal loss. In addition, neuropsychiatric and cognitive deficits play an important role in worsening patients' quality of life, and they, as well, are not necessarily related to neurodegeneration. Among them, depression and anxiety may develop before the onset of motor symptoms, while apathy, attention and memory deficits, loss of inhibitory control, and dementia usually start

developing after the time of diagnosis (Khoo et al., 2013). Figure 2 summarizes the development of clinical symptoms in PD over time.

*Braak Staging*

Braak and colleagues have suggested that the development of motor and non-motor symptoms correlates with the spatial and temporal distribution of LBs pathology, which follows a specific pattern that was eventually termed Braak staging (Braak et al., 2003). At Stages I and II, αSyn pathology can be found in the dorsal motor nucleus of the vagal nerve, in the medulla oblongata, in the anterior olfactory structures, in the lower raphe nuclei, and in the locus coeruleus. These regions are responsible for olfactory loss, autonomic dysfunction, depression, anxiety, and sleep disturbances. At Stages III and IV, the pathology spreads to the SNc, the amygdala, the nucleus basilis of Meynert, and the temporal mesocortex causing motor impairments and emotional disturbances. At Stages V and VI, the disease invades the temporal neocortex affecting the sensory and premotor areas, worsening the motor symptoms, and inducing further cognitive changes. However, Parkkinen and colleagues in 2005 suggested that this theory might not be accurate, as several observations made on post-mortem human brain tissues revealed that 30 % of patients had brain synucleinopathy without having developed any neurological disorder during their life (Parkkinen et al., 2005). A larger retrospective study made on 1720 autopsy samples by the same researchers showed that, among the αSyn-positive cases, 17 % of them were not following the canonical Braak staging, and 43 % of them had no neurological impairment (Parkkinen et al., 2008). Later, a study comparing the neuronal loss in the SNc and the presence of LBs showed that neither the Braak stages nor the increase in cortical LBs density correlated with the loss in the SNc (Parkkinen et al., 2011). Taken together, these observations suggest that LBs might not be the primary cause of cell loss and pathology progression in PD, and further studies focusing on how LBs relate to neurodegeneration are therefore warranted.

*Basal Ganglia*

For the purpose of this thesis, emphasis will be placed on the basal ganglia, a group of subcortical nuclei primarily responsible for voluntary movements, as well as procedural learning, executive functions, habitual and conditional behaviour. Anatomically, the main components of the basal ganglia are the striatum, the subthalamic nucleus (STN), the external and internal globus pallidus (GPe and GPi, respectively), and the substantia nigra pars compacta and reticulata (SNc and SNr, respectively). For ease of understanding, the classical model of the basal ganglia will be presented, although nowadays it is becoming evident that it is a rather simplified view of a more complex organization in which it is less easy to predict which inputs will generate a certain output (Bolam et al., 2000). Despite its limitations, this original model has critically shaped the understating of dopamine

contribution to motor output and how changes in dopamine levels lead to motor symptoms in PD (Albin et al., 1989; Alexander et al., 1986; DeLong, 1990).

In this model, inputs arriving from the cortex reach the striatum, and the GPi, together with the SNr, act as the principal output nuclei. Striatal neuronal activity is conveyed to the output nuclei (GPi and SNr) through GABA signalling mediated by the direct medium spiny neurons (dMSNs) and by a polysynaptic indirect pathway that involves connections to the GPe and the STN. GABAergic neurons in the GPi and SNr target the thalamus and brainstem, causing tonic inhibition of these structures. This inhibition is paused by the activity of the direct striato-nigral-pallidal projection, which decreases the GPi and SNr activity, thereby releasing the thalamus and brainstem from inhibition and allowing movement to happen. Dopaminergic neurons in the SNc project to the striatum, where they exert a dual effect on the striatal neuronal population. Striatal dopamine excites dMSNs expressing dopamine D1 receptors, substance P, and dynorphin and activates the direct pathway, whereas it inhibits striatal indirect medium spiny neurons (iMSNs) expressing dopamine D2 receptors and encephalin, deactivating the indirect pathway (Gerfen et al., 1990; Gerfen et al., 1991). Basically, according to this model, the activation of the indirect circuits would result in movement inhibition, while activation of the direct circuit would facilitate movement initiation.

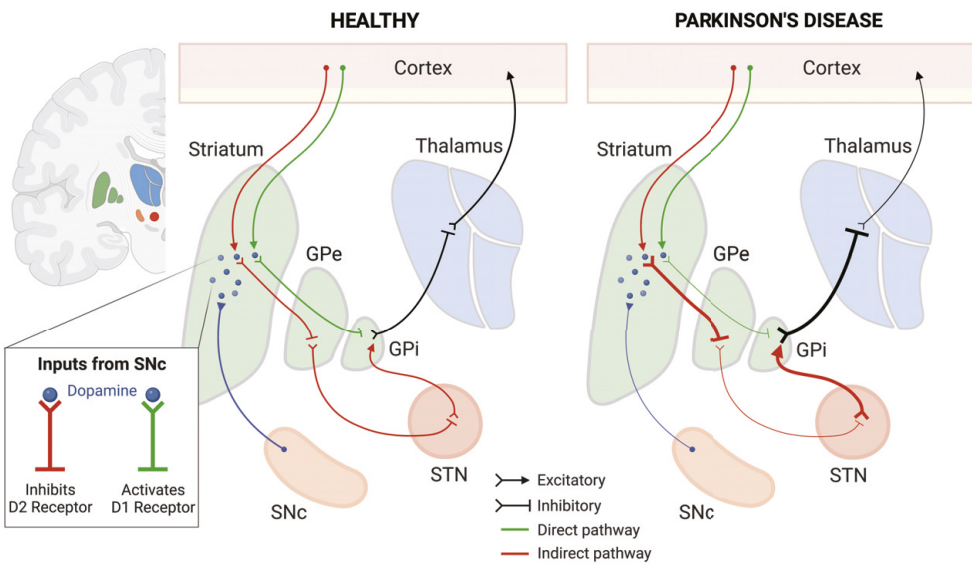


**Figure 3 | Classical model for the basal ganglia circuit in healthy and PD patients.** Reduction in dopaminergic signalling acting on the direct (D1) and indirect (D2) pathways results in a decrease in the inhibition of the STN and GPi. This results in a stronger inhibitory activity on the thalamus which in turn reduces the activation of the motor cortex. (created with BioRender.com.)

In the parkinsonian state, neurodegeneration in the SNc leads to a decrease in dopamine levels, facilitating the activation of the indirect pathway and reducing the activity of the direct pathway neurons. The inhibitory effect of the indirect neurons in the striatum targets the GPe, which results in increased activity of the STN. The STN will stimulate inhibitory neurons in the GPi and SNr, and in parallel, the decreased activation of the dMSNs will reduce the inhibitory control on the GPi and SNr, thereby contributing to an excessive inhibitory BG output at the cortical level.

However, accumulating evidence nowadays indicates that BG are essential in both action initiation and action selection. A new model has emerged, which emphasizes the complementary function of the direct and indirect pathways in movement initiation and action selection. This theory is well in line with the discovery of the simultaneous activation of the direct and indirect pathways during action initiation (Cui et al., 2013; Tecuapetla et al., 2009). Additionally, the striatum contains two neurochemically diverse compartments termed striosomes (or patches) and matrix; they receive different inputs and generate distinct outputs, indicating that the striatal synapses included in those regions might have different physiological functions (Gerfen, 1984, 1985; Graybiel & Ragsdale, 1978). Recently, the view of the GPe has also been updated; in fact, the GPe is targeted by dMSNs as well, and two distinct cell populations are residing in it having different characteristics and afferent projections (Cazorla et al., 2014; Mallet et al., 2012; Mastro et al., 2014).

*Dopaminergic neurons in the basal ganglia*

The identification of catecholamines (CAs) in the mammalian brain traces back to the early 1960s thanks to the work of Carlsson, Falck and Hillarp (Carlsson et al., 1962; Falck et al., 1962). By using their newly developed formaldehyde histofluorescence method, they managed to identify the two main CAs, dopamine and noradrenaline. Later, twelve groups of CA cells, numbered from A1 to A12, and their distribution in the rat brain were described (Dahlstroem & Fuxe, 1964), and twenty years later, five additional populations of CA cells (A13 to A17) have been included (Hökfelt, 1984). Immunohistochemical techniques able to identify dopamine-related enzymes and proteins, such as the tyrosine hydroxylase (TH), the aromatic amino acid decarboxylase (AADC), the dopamine transporter (DAT), and the vescicular monoamine transporter 2 (VMAT2), boosted the identification of this neuronal populations and mainly confirmed the original mapping, albeit with some discrepancies (Dubach, 1994; Gaspar et al., 1987). The A8, A9 and A10 dopaminergic populations are the ones mainly involved in the basal ganglia circuitry and they reside in the retrorubral field (RRF), in the SNc, and in the ventral tegmental area (VTA), respectively. Together they heavily innervate the striatum and the cortex, forming the nigrostriatal, mesolimbic and mesocortical pathways, which sustain sensorimotor, limbic, and associative functions, respectively. In brief, the A9 neurons residing in the SNc project mainly to the striatum, while the A10 neurons residing in the VTA project to the limbic and cortical areas. The A8 cell

groups project to striatal, limbic, and cortical areas. However, this is an oversimplification as accumulating evidence nowadays suggests that these connections are partially intermixed and the dopaminergic neurons residing in the midbrain can be additionally divided into dorsal and ventral tier. For an update regarding the dopaminergic system please refer to (Bjorklund & Dunnett, 2007).

In Parkinson's Disease, the nigrostriatal pathway is mainly affected and the A9 neurons degenerate preferentially (Damier et al., 1999; Fearnley & Lees, 1991). However, there are indications that aberrant neuronal activity in the limbic and associative systems may as well be present in PD patients and contribute to cognitive and behavioural impairments. For an extensive review on the topic, please refer to (McGregor & Nelson, 2019).

## Current therapeutic strategies

The main therapeutic strategies available for treating PD utilise pharmacological or surgical approaches for symptomatic relief. The gold standard pharmacological therapy for PD is levodopa (L-DOPA), a precursor of dopamine (Hornykiewicz, 2002). Usually, L-DOPA is prescribed together with carbidopa, which prevents or reduces the side effects of this therapy and decreases the amount of levodopa necessary to induce motor improvements (Greig & McKeage, 2016). The major side effect of this treatment is the development of motor fluctuations and involuntary movements, or L-DOPA-induced dyskinesias (Olanow et al., 2004). Other medications used to treat PD patients are dopamine agonists that mimic dopamine effects, monoamine oxidase type B (MAO-B) (Rabey et al., 2000; Rascol et al., 2005), and catechol-o-methyl-transferase (COMT) inhibitors that prevent dopamine breakdown (Nutt et al., 1994), amantadine to treat early-stage symptoms and dyskinesias (Crosby et al., 2003), and anticholinergics that reduce tremors and rigidity (Katzenschlager et al., 2003). The main surgical approach currently available for treating PD patients not responding well to medications is deep brain stimulation (DBS) which implants electrodes in the target brain region (usually STN or GPi) and connects them to a neurostimulator (Dougherty, 2018). The stimulation of these areas can relieve some of the motor symptoms, such as tremors, on/off fluctuations, and L-DOPA-induced dyskinesias. Another technique that recently received the Food and Drug Administration's approval is focused ultrasound, which uses magnetic resonance imaging (MRI)-guided ultrasound beams directed to target regions, such as the thalamus and the globus pallidus. It relieves tremor, stiffness or slowness, as well as dyskinesia. However, it can be applied on only one side of the brain, as the bilateral treatment can cause speech, swallowing or memory issues (Lennon & Hassan, 2021). Other therapies may be used to help reduce PD symptoms, such as physical, occupational, and speech therapies, as well as supportive therapies like a healthy diet and muscle exercises (Ransmayr, 2011).

# Rodent models of PD

Animal models are essential to obtain information about complex diseases and their prevention, diagnosis, and treatment. By using animals, researchers can carry out experiments that would be unethical, morally unacceptable, or technically impractical to perform on human subjects. Clearly, the use of laboratory animals should strictly follow the international and national guidelines and the principles of the 3 Rs (Replacement, Reduction, and Refinement) in order to perform more considerate animal research. Thus, it is of utmost importance to select the most appropriate model for the disease of interest to produce results that could be quickly translated into the human condition. In PD research, numerous rodent models have been generated, aiming to recapitulate some of the pathological hallmarks of this neurodegenerative disorder as seen in patients (Airavaara et al., 2020). Here I will focus on the most relevant rodent models used for behavioural and neuroprotective studies.

## Neurotoxin-based rodent models

Several toxins are capable of inducing the death of dopaminergic neurons. Among these are 6-hydroxydopamine (6-OHDA), 1-methyl-4-phenyl-1,2,3,6-tetrahydropyridine (MPTP), lactacystin, and some pesticides, such as rotenone and paraquat (Airavaara et al., 2020). As any animal model, they present some advantages and limitations in producing relevant pathology. For example, MPTP is able to induce PD-like symptoms (including αSyn accumulation) in mice, however, rats are resistant to its toxicity (Riachi et al., 1990; Sedelis et al., 2000). Rotenone works well in rats and leads to stable motor deficits, but it requires careful application as it can cause high mortality rates (Fleming et al., 2004). 6-OHDA has been widely used for its consistency in inducing strong neurodegeneration and clear behavioural impairments in both mice and rats, as discussed in more detail below.

### *6-hydroxydopamine model*

The 6-OHDA model has now been the gold standard for studying the motor symptoms of PD for almost 60 years. Initially introduced by Ungerstedt (Ungerstedt, 1968), it has assisted scientists in the discovery and refinement of therapies that are currently used to treat PD, such as levodopa (Lundblad et al., 2002; Olsson et al., 1995). 6-OHDA can enter the dopaminergic and noradrenergic neurons via the dopamine and noradrenaline transporters, and it causes toxicity through oxidative stress by forming reactive oxygen species and inhibiting the mitochondrial respiratory chain (Glinka et al., 1997). When 6-OHDA is injected bilaterally into the brain of rodents, it causes a higher mortality rate due to consequent inability to eat (aphagia), absence of thirst (adipsia), and seizures (Sakai & Gash, 1994; Ungerstedt, 1971), therefore unilateral injections are usually

preferred. The three main target regions for modelling PD in rodents are the medial forebrain bundle (MFB) (Dunnett et al., 1981; Grealish et al., 2010; Heuer & Dunnett, 2012; Heuer, Smith, et al., 2013; Heuer et al., 2012; Lundblad et al., 2004), SNc (Heuer et al., 2012; Stanic et al., 2003), and striatum (Heuer et al., 2012; Kirik et al., 1998; Lundblad et al., 2004) and the most rapid neurodegeneration is observed when 6-OHDA is injected in the MFB or SNc. This model is highly reproducible, causes strong neurodegeneration, and displays clear motor impairments in behavioural tests. However, it is an aggressive approach, where neurodegeneration occurs quickly, with no evidence of synucleinopathy. Additionally, despite its efficacy in testing symptomatic therapies, it has shown its limitations in the identification of disease-modifying therapies (e.g., GDNF) (Choi-Lundberg et al., 1997; Hoffer et al., 1994; Wang et al., 1996; Whone, Boca, et al., 2019; Whone, Luz, et al., 2019).

## αSyn-based rodent models

Since the discovery of mutations in the SNCA gene and of the presence of αSyn in LBs (Polymeropoulos et al., 1997; Spillantini et al., 1997), researchers have started generating models based on the expression of αSyn and its toxic effects observed in PD. The first models to be developed were transgenic mice overexpressing either wild-type (WT) or mutated αSyn; however, none of these lines have reproduced the progressive neurodegeneration observed in human PD (Breger & Fuzzati Armentero, 2019). Therefore, the need to investigate the seeding and spreading properties of αSyn and its role in advanced stages of PD has led researchers to look for new alternatives. The two main approaches used nowadays involve the injection of viruses overexpressing WT or mutant αSyn in target brain regions or the direct inoculation of human or rodent aggregated αSyn in the form of preformed fibrils (PFFs) or oligomers (Carta et al., 2020).

*Viral αSyn overexpression rodent model*

Viral vector-based αSyn overexpression models have rapidly become popular amongst PD researchers as they are able to drive strong gene expression and allow for targeted gene delivery in the rodent brain. Both lentiviruses (Lauwers et al., 2003; Lo Bianco et al., 2004) and adeno-associated viruses (AAVs) have been used to overexpress WT or mutated αSyn into dopaminergic neurons, however, AAVs are the most commonly used because of their ability to target neurons more specifically, to drive stronger transgene expression, to induce more pronounced neurodegeneration, their non-pathogenicity, and the fact that their integration into the host genome is minimal (Haggerty et al., 2020). In 2002, the first pioneering study (Kirik et al., 2002) utilised the first generation AAV2/2 to overexpress αSyn in the SNc, which resulted in a strong variability in dopaminergic cell loss and behavioural outcome, suggesting that the extent of αSyn neuropathology depends

on its expression levels. Shortly after, the second generation of AAVs able to drive a stronger gene expression (e.g. AAV1/2 and AAV2/5) was introduced and tested in both SNc and striatum (Gorbatyuk et al., 2008; Koprich et al., 2011). Eventually, further modifications in the serotype and in the vector construct, such as the addition of enhancer and stabilizing elements, led to the development of the third generation of AAVs, which showed a further increase in transduction efficiency and transgene expression (Decressac, Mattsson, Lundblad, et al., 2012; Van der Perren et al., 2015). Unfortunately, while these improvements resulted in stronger nigral neurodegeneration and motor impairments, they also introduced the complication of non-specific toxicity, as the GFP-carrying AAVs used as control were shown to become toxic when used at high concentrations (Albert et al., 2019; Klein et al., 2006; Landeck et al., 2017).

Overall, despite a lack of standardisation between studies, the AAV-αSyn model recapitulates key aspects of PD pathology such as progressive neurodegeneration, behavioural impairments, axonal pathology precedent to cell loss, immune and inflammatory changes, inclusions formation, and phosphorylation of αSyn at serine 129. One aspect must be noted: these pathological changes were more evident and pronounced in rats compared to mice, making rats a better candidate for modelling αSyn pathology via AAV-based systems.

*αSyn preformed fibrils rodent model*

In PD, αSyn undergoes conformational changes, which lead to its aggregation first into oligomers, then fibrils, and eventually to the formation of LBs, which will occur in several regions of the brain. For that reason, researchers have been interested in studying the seeding and spreading properties of these toxic forms of αSyn and their ability to trigger pathology *in vivo*. Usually, the PFFs model is generated via the unilateral or bilateral inoculation of PFFs of recombinant human or rodent αSyn of various lengths into the SNc, the striatum, the cortex, or the olfactory bulb (Abdelmotilib et al., 2017; Luk et al., 2012; Peelaerts et al., 2015; Rey et al., 2016; Volpicelli-Daley et al., 2011). It has been demonstrated that PFFs can act as a template for αSyn aggregates formation by recruiting endogenous αSyn, which then propagate to functionally interconnected areas in an anterograde or retrograde manner (Luk et al., 2012; Masuda-Suzukake et al., 2013; Volpicelli-Daley et al., 2016). The aggregates contain phosphorylated αSyn resembling those observed in the human condition, and they can also trigger neuroinflammation (Abdelmotilib et al., 2017; Thakur et al., 2017). One of the major downsides of this model is the time required for the development of neuro and motor symptomatology, especially when the PFFs originate from a different species than the host (e.g., human PFFs in a rodent brain). This aspect led scientists to look for new strategies to accelerate the process. Therefore, some groups have started combining AAV-induced overexpression of human αSyn with the inoculation of human PFFs and obtained a faster appearance of symptomatic features resembling PD. In these studies, PFFs

have been injected either at the same time (Espa et al., 2019; Hoban et al., 2020; Peelaerts et al., 2015) or four weeks after the injection of an AAV expressing αSyn (Thakur et al., 2017), with the former approach being less invasive, as it requires only one surgical intervention.

## Cognition in rodent models of sporadic PD

Cognitive impairments in rodent models of PD have been studied marginally compared to motor deficits or treatment-associated dyskinesias. For example, rodents cannot process language in the same way as humans; therefore, an analogous study of this cognitive domain cannot be performed. On top of that, behavioural tests designed for rodents usually require the execution of visual and motor tasks, making the interpretation of the results more complicated as they can be in part influenced by motor impairments. Generally, but not exclusively, the cognitive deficits observed in rodent models of PD result from disrupted parallel circuits' loops between the cortex and the striatum, which sustain motor, associative, and limbic functions, and they can be studied using sensitive behavioural tests. For example, among the tests that can measure attentional deficits there are the corridor test and the lateralised choice reaction time task for unilaterally dopamine depleted animals, and the 5-choice serial reaction time task for bilaterally dopamine depleted animals. Memory impairments instead can be assessed using mazes, such as the Morris water maze, the T-maze and the Y-maze; alternatively, the novel object recognition test and the delayed matching to position task have been also utilised. For a comprehensive review about modelling cognitive deficits in rodent models of PD, please refer to (Decourt et al., 2021). Given the use of a unilateral model in this thesis, the choice of cognitive tests was restricted to those tests that rely on the dopamine imbalance between hemispheres, i.e., the corridor test and the lateralized choice reaction time task. Both tests are analogous to each other, with the second being more precise and allowing for a deeper analysis of the nature of the behavioural deficit. Thus, in this introduction, emphasis will be given to the lateralized choice reaction time task.

*Lateralized choice reaction time task*

First described by Carli et al. in 1985, this task unravelled the nature of the behavioural deficits observed in 6-OHDA unilaterally striatal dopamine-depleted rats (Carli et al., 1985). Unilaterally dopamine-depleted animals will display a contralateral deficit when tested in simple motor tests, but ipsilateral rotations when tested in the amphetamine-induced rotation test, suggesting that the deficit is not purely motor and might be due to unilateral neglect. Carli et al. trained rats to poke and hold their nose into a central hole and then to detect a random visual event presented either to the left or to the right of their head (see Materials and Methods for details). One group of rats was trained to respond in the same hole the stimulus

was presented, and one group was trained to respond in the opposite hole, away from the stimulus. All lesioned rats failed to respond contralaterally, regardless of the group they belonged to, demonstrating that their deficit results from an inability to initiate responses to the contralateral space (hemiakinesia) but not in completing them (bradykinesia). In contrast, more recent studies reported a deficit also in response completion (Dowd & Dunnett, 2004, 2005a, 2005b; Heuer & Dunnett, 2012, 2013; Heuer, Lelos, et al., 2013). This might be explained by the physical distance between the central and lateral holes; in fact, placing the lateral holes a bit further away from the central hole, forces the animal to perform a larger body movement rather than a simple head turn, thus allowing to tease out differences in movement completion. To further demonstrate the contralateral attentional deficit, other studies restricted the response to the same side by placing one response hole near and one hole far from the central location on the contralateral side (Brasted et al., 1997; Brown & Robbins, 1989; Heuer & Dunnett, 2013; Heuer, Lelos, et al., 2013). In this scenario, rats were responding to the near hole and neglecting the far location indicating that the deficit is in the relative egocentric representation of space and not in the sensory perception or in the motor execution. It has also been shown, by reward omission and reward devaluation, that the initial response to the central stimulus is goal-directed while the response to the lateral stimulus becomes habitual (Lelos et al., 2012; Wise, 2004). Additionally, this test allows for dissociation of the reaction time from the movement time, which are analogous of akinesia and bradykinesia, respectively. Interestingly, impairments in simple and choice reaction times have repeatedly been reported in PD patients as well (Evarts et al., 1981; Gauntlett-Gilbert & Brown, 1998).

As mentioned previously, the attentional deficits observed in the lateralized choice reaction time task can also be demonstrated by using a simpler test, which does not require the use of expensive operant chambers, but, at the same time, it does not allow for a deep investigation of the nature of the deficit (Dowd et al., 2005). In the corridor test, a food-deprived rat must walk through a corridor that has bowls filed with sugar pellets on each side. A rat with a unilateral dopamine lesion will retrieve the sugar pellets only from the ipsilateral side while ignoring the food on the contralateral side. In general, cognitive deficits in preclinical models of PD have been extensively characterised in 6-OHDA lesioned rats and mice, but they have been modelled with limited success in AAV-αSyn or PFFs injected animals. Few studies have reported deficits in spatial working and reference memory, inhibitory control, and attention, but none of them accounted for deficits in movement initiation or motivation (Decourt et al., 2021).

# Neurotrophic factors as potential treatment for PD

Neurotrophic factors (NTFs) are small proteins that can promote the survival, maturation, and development of dopaminergic neurons (Chmielarz & Saarma, 2020). Together with cell transplantation, they have been of great interest for disease-modifying therapies in contrast to the current available symptomatic treatments for PD. The first NTF being studied was the nerve growth factor (NGF), which was tested on one PD patient after adrenal medullary autografting resulting in functional improvements (Olson et al., 1991). However, negative side effects have been reported in Alzheimer's Disease patients, and no further clinical trials have been conducted on PD patients since then (Eriksdotter Jönhagen et al., 1998). After that, four additional NTFs have been tested in PD patients: glial cell line-derived neurotrophic factor (GDNF), neurturin (NRTN), platelet-derived growth factor BB (PDGF-BB), and the cerebral dopamine neurotrophic factor (CDNF). Table 1 summarizes past and current clinical trials using these NTFs and their major outcomes.

**Table 1 | Current NTFs being tested in clinical trials.** List of past and ongoing clinical trials utilizing NTFs and major outcomes in Unified Parkinson's Disease Rating Scale (UPDRS) score improvements, and [18F]DOPA and [11C]PE21 uptake. LV, lateral ventricle; PUT, putamen; SN, substantia nigra.

| NTF | Delivery | Method | N | Phase | UPDRS | [$^{18}$F]DOPA | [$^{11}$C]PE21 | Reference |
|---|---|---|---|---|---|---|---|---|
| GDNF | LV | rhGDNF | 50 | I-II | - | N/A | N/A | (Nutt et al. 2003) |
| | PUT | rhGDNF | 5 | I | ↑ | ↑ | N/A | (Gill et al. 2003) |
| | PUT | rhGDNF | 10 | I | ↑ | N/A | N/A | (Slevin et al. 2005) |
| | PUT | rhGDNF | 34 | II | - | ↑ | N/A | (Lang et al. 2006) |
| | PUT | rhGDNF | 41 | II | - | ↑ | N/A | NCT03652363 |
| | PUT | AAV2-GDNF | 25 | I | - | ↑ | N/A | NCT01621581 |
| | PUT | AAV2-GDNF | 12 | I | N/A | N/A | N/A | NCT04167540 |
| NRTN | PUT | AAV2-NRTN | 12 | I | ↑ | - | N/A | NCT00252850 |
| | PUT | AAV2-NRTN | 58 | II | - | - | N/A | NCT00400634 |
| | PUT, SN | AAV2-NRTN | 51-57 | I | - | - | N/A | NCT00985517 |
| PDGF-BB | LV | rhPDGF-BB | 12 | I-II | - | - | ↑ | NCT02408562 |
| CDNF | PUT | rhCDNF | 17 | I-II | ↑ | N/A | ↑ | NCT03295786 |

Among them, GDNF has been the most studied and promising, with seven clinical trials being conducted so far (see Table 1). However, conflicting results have emerged from these studies, complicating the possibility of making a clear conclusion about its neuroprotective effects. This partial insuccess could be ascribed to several reasons, such as differences in the delivery site and method, the dosage, the age of the patients, and the stage of the disease. Additionally, preclinical

data showed that GDNF can protect dopaminergic neurons in the 6-OHDA toxin model but failed to exert neuroprotection in the αSyn rat model (Choi-Lundberg et al., 1997; Decressac et al., 2011; Hoffer et al., 1994; Wang et al., 1996). Taken together, these results highlight the need for further studies at the preclinical level to elucidate the cellular and molecular effects of GDNF, as well as the need to look for NTFs with different modes of action. For example, it has been shown that αSyn induces downregulation of *Ret*, a gene encoding for a tyrosine kinase receptor critical for the neuroprotective effect of GDNF, in the substantia nigra of PD patients (Decressac, Kadkhodaei, et al., 2012; Drinkut et al., 2016). This has led to many questions regarding the signalling pathways involved with NTFs and how they are affected in PD patients. Because of this, 30 might be wise to shift the attention to novel targets and especially to those which are RET-independent. In this regard, the growth differentiation factor 5 (GDF5) has recently gained attention as alternative therapeutic agent for PD as it has shown its potential in protecting dopaminergic neurons both *in vitro* and *in vivo*.

## Growth Differentiation Factor 5

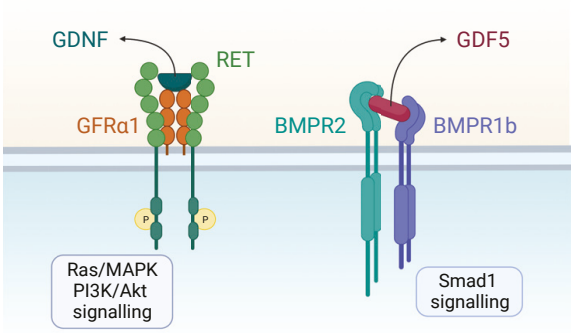


**Figure 4 | Schematic representation of GDNF vs. GDF5 mode of action.** GDNF signals through the RET tyrosine kinase receptor, which is activated only if the GDNF is first bound to the GDNF family receptor-α (GFRα) receptor 1. Its activation then triggers the Ras/MAPK and PIK3K/Akt pathways. GDF5 binds to a heterocomplex formed by BMPR1b and BMPR2 receptors, which in turn activates the Smad1 signalling. (created with BioRender.com.)

The Growth Differentiation Factor 5 (GDF5) belongs to the transforming growth factor β (TGF-β) superfamily. This superfamily includes many cytokines (including GDNF), which play an important role during tissue development and after maturation. GDF5 is strongly involved in skeletal development, and mutations in its gene can cause pathological conditions such as brachydactyly type C and chondrodysplasias in humans (Polinkovsky et al., 1997; Thomas et al., 1997; Thomas et al., 1996). Its mechanism of action is mediated by a heterocomplex of bone morphogenetic protein receptors (BMPR) type 1b (BMPR1b) and type 2 (BMPR2), which in turn activates the Smad1 signalling pathway (Figure 4) (Hegarty et al., 2014; Hegarty et al., 2013). Besides its activity on limb development, GDF5 has also been shown to be present in the central nervous system, suggesting that it may also be important during its development (Storm et

al., 1994). Studies performed on rat embryos and adults showed that GDF5 expression begins at E12, peaks at E14, and is maintained during the postnatal period in several brain regions, including the striatum and midbrain (O'Keeffe, Hanke, et al., 2004). *In vitro*, GDF5 can increase the number of dopaminergic neurons and promote neurite growth in cell cultures of E14 rat ventral mesencephalon (Clayton & Sullivan, 2007; Krieglstein et al., 1995; O'Keeffe, Dockery, et al., 2004). *In vivo*, GDF5 can protect and regenerate the nigrostriatal pathway and support grafted ventral mesencephalic neurons in the 6-OHDA rat model, similarly to what was observed for GDNF (Hurley et al., 2004; Sullivan et al., 1997; Sullivan et al., 1998). Recently, it has been shown to exert neuroprotection in the αSyn rat model as well (Goulding et al., 2021). Taken together, these results demonstrate the potential of GDF5 as a candidate for neuroprotective studies on PD patients.

# Aims of the thesis

The focus of this thesis has been the development and characterisation of a rat model of PD based on the AAV-induced overexpression of αSyn for the assessment of therapeutic interventions. To achieve this, we designed four studies with the following aims:

I. To compare different strategies for producing αSyn-based rat models of PD using AAV vectors and preformed fibrils and assess their ability to induce relevant pathology and behavioural deficits.

II. To model early-stage PD in a rat model based on AAV-induced αSyn overexpression and characterise motor and non-motor impairments using simple drug-free behavioural tests.

III. To assess, for the first time, motor and cognitive deficits on a lateralised choice reaction time task in the AAV-αSyn-based rat model of PD.

IV. To investigate the potential neuroprotective effects of a GDF5-based gene therapy in the AAV-αSyn rat model of PD.

# Key results

## Paper I

Preclinical rat models for PD based on viral human αSyn overexpression mimic some of the pathological hallmarks seen in patients, such as progressive neurodegeneration and the presence of synucleinopathy; however, their consistency between experiments is low and needs further optimization. In the attempt to generate a more reliable model, recent studies have injected viral vector-based overexpression of human wild-type αSyn and human derived αSyn PFFs either sequentially or simultaneously (Hoban et al., 2020; Peelaerts et al., 2018; Thakur et al., 2017). The aim of this project was to compare these experimental paradigms and assess their ability to induce relevant pathology and behavioural deficits.

*Experimental setup*

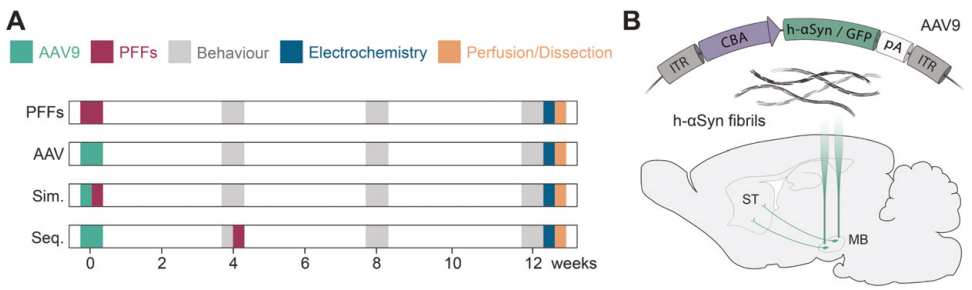


**Figure 5 | Experimental setup. A)** Schematic of the groups and timepoints for behavioural tests, electrochemical analysis, perfusions, and dissections. One group received PFFs only (PFFs), two groups were injected with either AAV-αSyn or AAV-GFP (AAV), two groups received AAV-αSyn or AAV-GFP and PFFs at the same time (Sim.), and two groups received AAV-αSyn or AAV-GFP and 4 weeks later PFFs (Seq.). **B)** Schematic of the viral genome and the brain region injected. ITR, inverted terminal repeat; CBA, chicken β-actin; pA, polyadenylation site; h-αSyn, human alpha-synuclein; GFP, green fluorescent protein; PFFs, preformed fibrils; MB, midbrain; ST, striatum.

Sprague-Dawley rats were divided into four experimental groups and injected unilaterally in the midbrain as follows: one received PFFs (PFFs), one AAV-αSyn (h-αSyn), one AAV-αSyn and PFFs simultaneously (h-αSyn/PFFs), and one AAV-αSyn and 4 weeks later PFFs (h-αSyn+PFFs). For ease of reading, h-αSyn, h-αSyn/PFFs, and h-αSyn+PFFs groups will be collectively called AAV9-αSyn injected groups. Additionally, three control groups were also included: one injected with AAV-GFP (GFP), one with AAV-GFP and PFFs simultaneously (GFP/PFFs),

and one with AAV-GFP and 4 weeks later PFFs (GFP+PFFs). All animals underwent behavioural testing at 4-, 8- and 12-weeks post AAV injection. After the last behavioural timepoint, we performed electrochemical recordings for dopamine release on three animals per group. Eventually, the brains were either perfused or dissected for immunohistochemical analysis and protein quantification, respectively (Figure 5 A-B).

*Robust AAV-induced αSyn overexpression leads to TH loss along the nigrostriatal pathway*

At the nigro-striatal level, all AAV-αSyn injected groups showed strong immunoreactivity for αSyn211 on the ipsilateral side (Figure 6 C), as further demonstrated by densitometry on αSyn211 immunolabelled striatal sections, indicating that the virus was successfully delivered to the substantia nigra with evident spread to the striatum (Figure 6 E). Concomitantly, the overexpression of αSyn resulted in a reduction in TH, the rate-limiting enzyme in dopamine production (Figure 6 D). We observed a decrease in TH immunoreactivity on the ipsilateral side, which was quantified by densitometry in the striatum and stereology in the SN (Figure 6 F and G). In particular, AAV-αSyn injected groups displayed a decrease in striatal TH staining intensity of about 50% and in SN $TH^+$ dopaminergic cells of 30-40 %. The PFFs group did not show any detectable $αSyn211^+$ signal (Figure 6 A and E) or $TH^+$ loss along the nigrostriatal pathway (Figure 6 B, F and G).

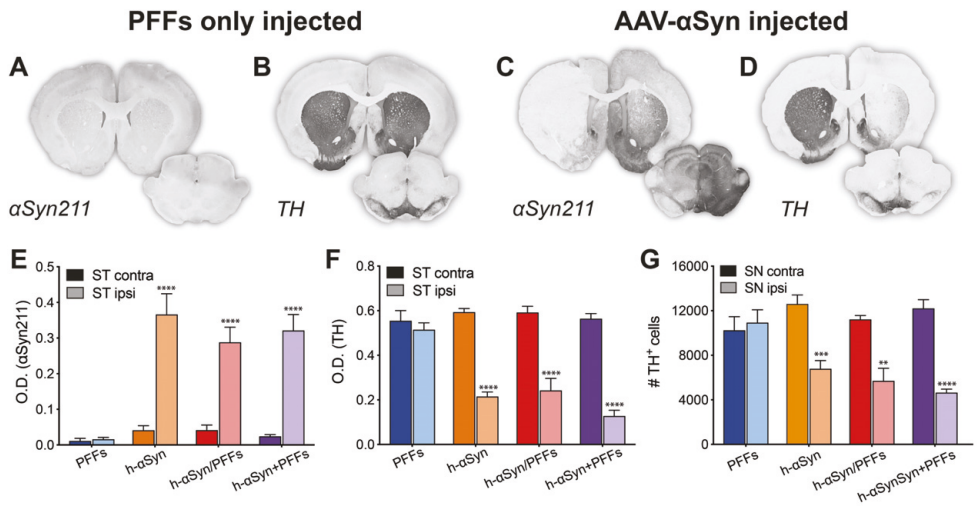


**Figure 6 | Transgene overexpression and TH loss in striatum and substantia nigra. A-D)** Representative images for striatal and midbrain sections of PFFs only injected group and AAV-αSyn injected groups (h-αSyn, h-αSyn/PFFs, and h-αSyn+PFFs) stained for either αSyn211 or TH. **E, F)** Densitometric analysis for αSyn211 or TH immunolabeled striatal sections comparing contralateral vs ipsilateral sides. **G)** Stereological quantification of $TH^+$ cells in the contralateral vs ipsilateral substantia nigra. ST, striatum; SN, substantia nigra. Data are expressed as mean ± SEM. (**p <0 .01, ***p < 0.001, ****p < 0.0001)

*AAV-αSyn injected animals show motor impairments*

Strong αSyn overexpression and TH loss resulted in the development of motor deficits over time. Animals were tested in three motor tasks, i.e., stepping, cylinder, and *d*-amphetamine-induced rotations at 4-, 8-, and 12-weeks post-surgery. Except for the PFFs only group, the remaining groups behaved similarly in each test and displayed a tendency to a contralateral bias in the cylinder and stepping tests and ipsilateral drug-induced rotational behaviour over time (Figure 7 A-C).

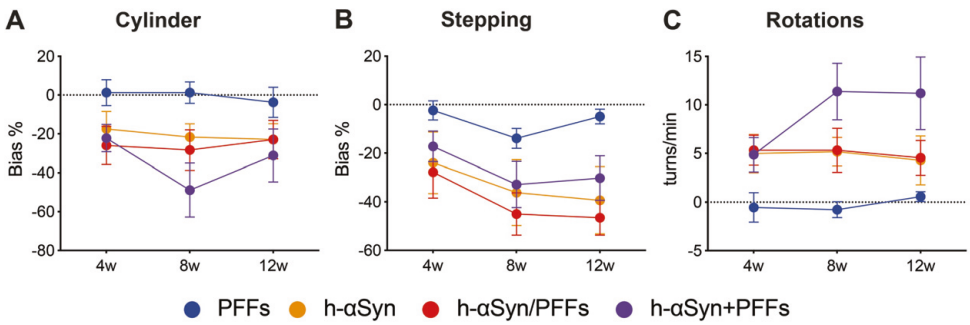


**Figure 7 | Motor impairments and axonal pathology. A-C)** Cylinder (A), stepping (B), and *d*-amphetamine-induced rotation (C) tests performed to assess motor function at 4-, 8-, and 12- weeks post injection. Data are expressed as mean ± SEM.

*The combination of AAV-αSyn and PFFs results in enhanced PD-like pathology and inflammation*

Despite the lack of differences in the level of TH loss and behavioural impairments between the h-αSyn, h-αSyn/PFFs, and h-αSyn+PFFs groups, a higher formation of αSyn aggregates and a strong inflammatory response could be observed in those groups that received both AAV-h-αSyn and PFFs. Increased midbrain levels of phosphorylated αSyn (p-αSyn) and αSyn aggregates were detected by TR-FRET (Figure 8 C, D). Moreover, p-αSyn colocalised with Thioflavin S and Ubiquitin, two markers commonly used for characterising Lewy bodies (Figure 8 A-$B_{III}$). At the striatal level, the injection of AAV-αSyn with or without additional insult with PFFs enhanced axonal pathology, which resulted in a higher number of αSyn211$^{+}$ and TH$^{+}$ positive axonal swellings compared to the PFFs only group and was further demonstrated by their quantification (Figure E-$F_{II}$). Additionally, the presence of high levels of p-αSyn and aggregates triggered an inflammatory response, and amoeboid microglia immunoreactive for Ox42 could be observed at the site of injection in the h-αSyn/PFFs and h-αSyn+PFFs groups (Figure 8 G-J). The densitometric analysis confirmed this observation, as a 50-60 % increase in Ox42 staining intensity in the ipsilateral midbrain compared to the contralateral side was measured in those groups (Figure 8 K).

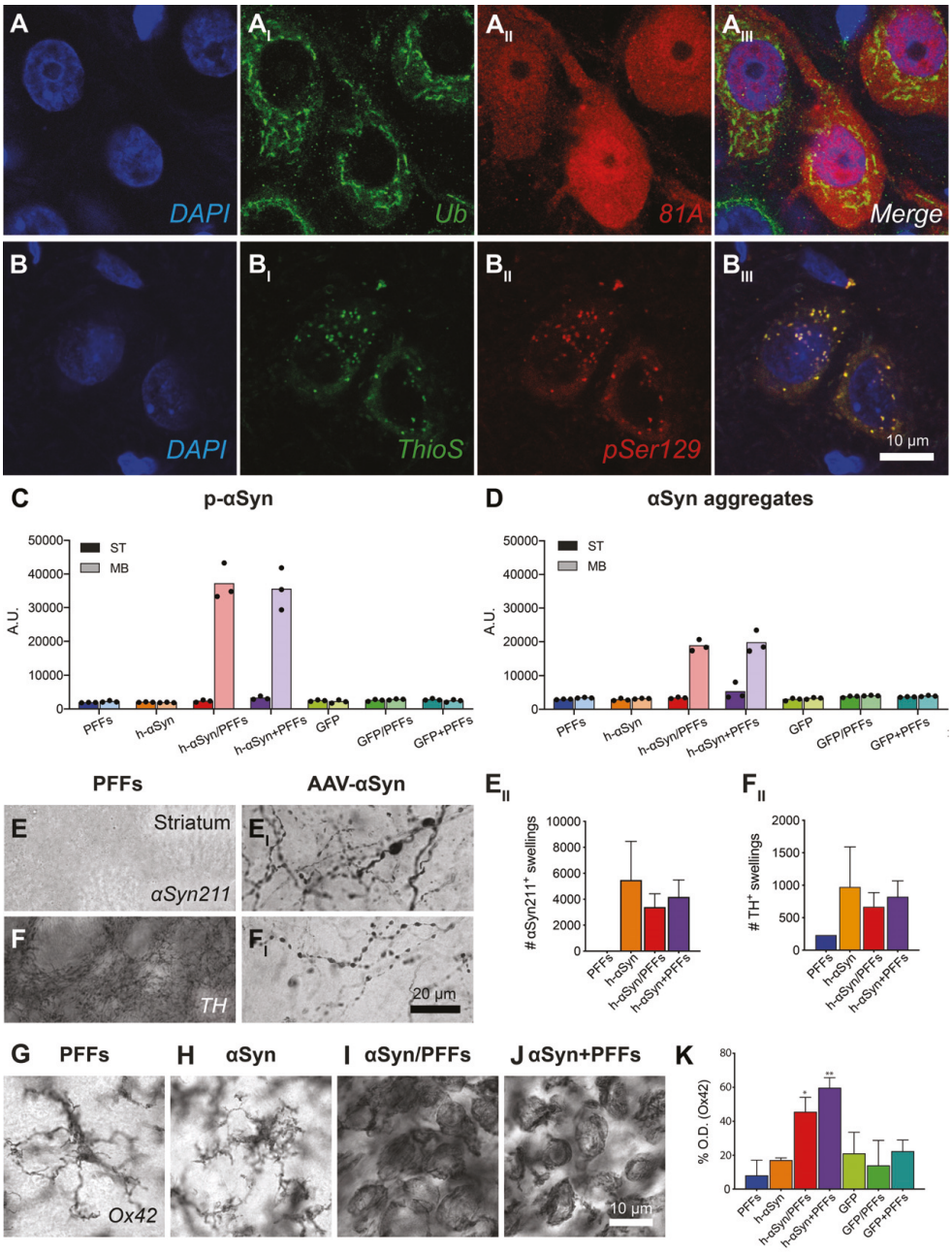


**Figure 8 | PD-like pathology and inflammatory response. A-A$_{III}$)** Triple fluorescent labelling for DAPI, Ubiquitin and pSer81A in the SN. **B-B$_{III}$)** Triple fluorescent labelling for DAPI, Thioflavin S and pSer129 in the SN. **C, D)** TR-FRET quantification for phosphorylated (C) and aggregated (D) αSyn in the ipsilateral midbrain and striatum. **E-E$_I$)** Representative images taken from the striatum of PFFs and AAV-αSyn groups showing αSyn211$^+$ axonal swellings. **E$_{II}$)** Quantification of αSyn211$^+$ axonal swellings in the ipsilateral striatum. **F-F$_I$)** Representative images taken from the striatum of PFFs and AAV-αSyn groups show TH$^+$ axonal swellings. **F$_{II}$)** Quantification of TH$^+$ axonal swellings in the ipsilateral striatum. **G-J)** 63X magnification images taken from the ipsilateral SN immunolabelled for Ox42 for the PFFs,

h-αSyn, h-αSyn/PFFs, and h-αSyn+PFFs groups. **K)** Densitometric analysis showing the increase in the percentage of Ox42 staining intensity in the ipsilateral midbrain for all the experimental groups. ST, striatum; MB, midbrain. Data are expressed as mean ± SEM. (*p < 0.05, **p <0.01)

### *AAV-induced GFP overexpression led to neurotoxicity and behavioural impairments*

A major drawback of this and many other studies was the toxicity caused by GFP in the control groups. AAV-GFP injected animals showed strong immunoreactivity for GFP with evident spread to the striatum, as demonstrated by densitometry on GFP immunolabeled striatal sections (Figure 9 A). This resulted in reduced levels of TH in the striatum and midbrain, similarly to what was observed for the AAV-αSyn injected groups. TH staining intensity in the striatum was reduced by about 70%, and the loss of $TH^+$ dopaminergic cells in the SN was around 45-50% (Figure 9 B and C). As expected, this caused the development of motor deficits over time. AAV-GFP injected groups displayed a reduced use of the contralateral paw in the cylinder and stepping tests, as well as ipsilateral rotational behaviour in the *d*-amphetamine rotation test (Figure 9 D-F). However, the three control groups did not show any synucleinopathy or inflammatory response in the midbrain or enhanced axonal swellings in the striatum (data not shown).

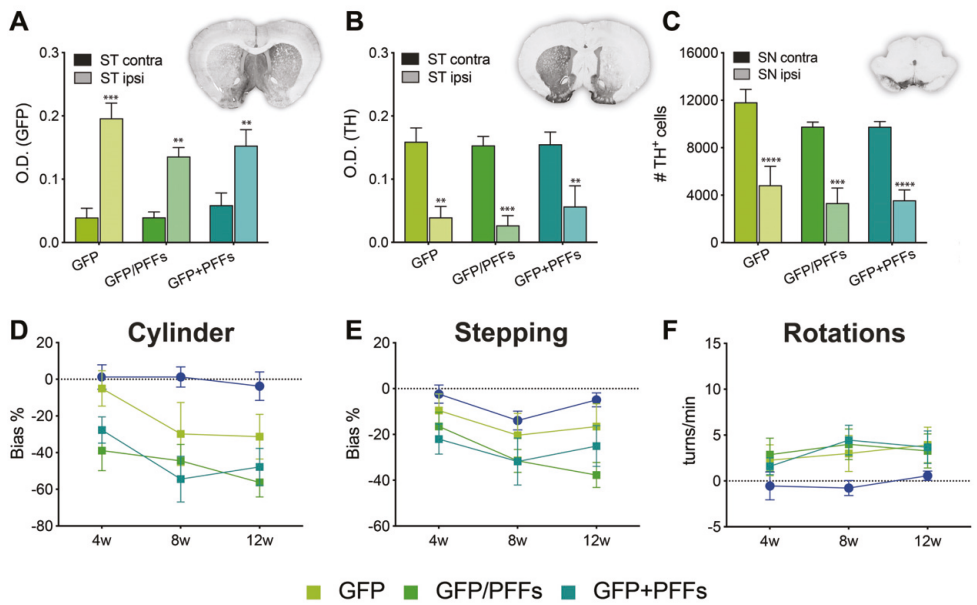


**Figure 9 | GFP overexpression results in TH loss and motor impairments. A, B)** Densitometric analysis for GFP or TH immunolabeled striatal sections comparing contralateral vs ipsilateral sides. **C)** Stereological quantification of $TH^+$ cells in the contralateral vs ipsilateral substantia nigra. **D-F)** Behavioural tests performed to assess motor impairments over time (cylinder, stepping and amphetamine-induced rotations). ST, striatum; SN, substantia nigra. Data are expressed as mean ± SEM.

# Paper II

In Paper I, we showed that the additional insult with PFFs did not exacerbate TH loss or behavioural impairments when compared to the group injected with AAV-αSyn only. Therefore, we wanted to further investigate the potential of our AAV-αSyn vector in modelling early stages of human PD, as it would be relevant for studying disease-modifying therapies and disease onset and progression. Additionally, we aimed to characterise motor as well as non-motor deficits using simple drug-free tests which rely on spontaneous behaviour. We also compared our model to the gold standard 6-OHDA model from a histopathological and behavioural point of view.

*Experimental setup*

Sprague-Dawley rats were divided equally into three experimental groups according to their behavioural performance at baseline. All groups were injected unilaterally along the nigrostriatal pathway, two groups received injections of either AAV-h-αSyn or AAV-noTG (i.e., missing the transgene) in the substantia nigra, and one group received an injection of 6-OHDA along the medial forebrain bundle (MFB). After surgery, we evaluated the behavioural phenotype using the cylinder and stepping tests at 4-, 8-, and 22-weeks post-injection and the corridor test at 8- and 22-weeks post-injection. We then performed electrochemical recordings for dopamine release on a subgroup of animals and eventually, all of them were perfused and their brains collected for post-mortem analyses (Figure 10 A, B).

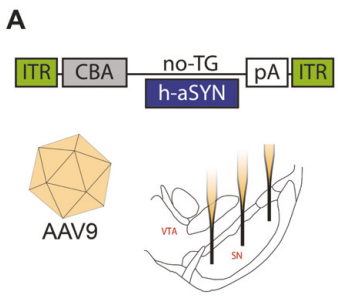


B

| Group | Capsid / Transgene | Description | Abbreviation |
|---|---|---|---|
| noTG | AAV9/ - | No viral genome | AAV-noTG |
| h-aSyn | AAV9 / h-aSYN | Human Wild Type aSYN | AAV-h-aSYN |
| 6-OHDA | n/a | Toxin | 6-OHDA |

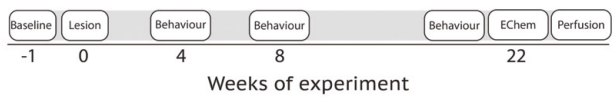


**Figure 10 | Experimental setup. A)** Schematic of the viral construct and the sites of injection in the substantia nigra (SN) of rats. **B)** Description of the groups and timepoints for injection, behaviour, electrochemical recordings, and perfusion. noTG, no transgene; h-αSyn, human alpha-synuclein; pA, polyadenylation; ITR, Inverted Terminal Repeat; CBA, Chicken β-Actin; Echem, electrochemistry.

*AAV-αSyn injection resulted in neurodegeneration of dopaminergic cells*

After confirming that αSyn was strongly expressed in both midbrain and striatum by immunohistochemistry and densitometry on αSyn211 labelled striatal and midbrain sections (Figure 11 A-$B_I$), we investigated whether this expression induced any changes in the dopamine system. TH immunolabeled striatal and midbrain sections revealed a reduction in TH density for the AAV-h-αSyn and 6-OHDA groups (Figure 11 C-$F_I$), which was measured by densitometry (Figure 11 G and H). Stereological quantification of $TH^+$ cells in the SN revealed a 28% and 75% ipsilateral reduction in $TH^+$ cell number compared to the contralateral side for the AAV-h-αSyn and 6-OHDA groups, respectively (Figure 11 I). To verify whether this reduction was due to a mere TH downregulation or to actual neurodegeneration, we counted $NeuN^+$ cells in the SN. We observed a slight reduction of $NeuN^+$ cells on the ipsilateral SN of both groups, which, however, was not nearly as strong as the observed $TH^+$ loss (Figure 11 L).

*Overexpression of αSyn resulted in PD-like pathology*

To assess whether αSyn was inducing some of the typical histological hallmarks observed in humans, we performed histological analysis to investigate the presence of αSyn aggregation and axonal degeneration in the AAV-h-αSyn group. We found colocalization between p-αSyn, Thioflavin S, and Ubiquitin, markers that are commonly used for human LBs (Figure 12 A-$B_{III}$). Additionally, αSyn was found to be proteinase K (pK) resistant both in midbrain (Figure 12 C and D) and striatum (data not shown), indicating that it is present in its aggregated and insoluble form. At the striatal level, axons and dendrites with beaded morphology could be observed and their quantification revealed high numbers of both $TH^+$ and $αSyn211^+$ axonal swellings in the contralateral side (Figure 12 E and F). We then investigated the presence of neuroinflammation and its potential link to αSyn pathology. Midbrain sections immunolabelled for IBA1 showed no visible difference between the three experimental groups in terms of microglia morphology; however, slightly higher numbers of $IBA1^+$ cells could be counted in the ipsilateral side of all the groups, suggesting an effect of the surgical procedure rather than being related to the presence of αSyn (Figure 12 G-J).

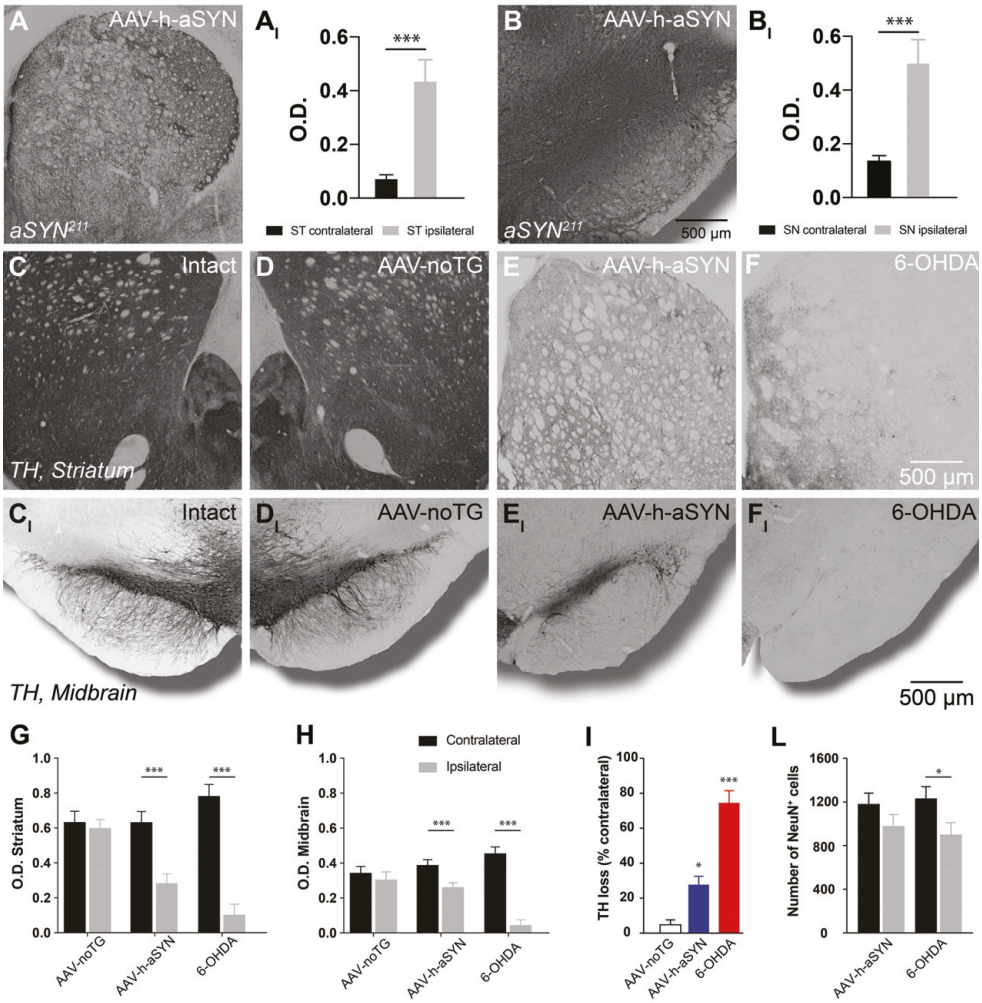


**Figure 11 | αSyn overexpression and loss of TH along the nigrostriatal pathway. A, B)** Representative images of αSyn211 immunoreactivity in the striatum (A) and midbrain (B). **$A_I$, $B_I$)** Densitometric analysis for αSyn211 staining intensity in striatum and SN comparing left vs right side. **C-F)** Representative images of TH immunoreactivity in striatal sections for the intact side (C) and injected side of the three experimental groups (D-F). **$C_I$-$F_I$)** Representative images of TH immunoreactivity in midbrain sections for the intact side ($C_I$) and injected side of the three experimental groups ($D_I$-$F_I$). **G, H)** Densitometry for TH staining intensity in striatum and midbrain comparing contralateral vs ipsilateral side. **I)** Percentage loss of $TH^+$ cells in SN quantified via stereology. **L)** Quantification of $NeuN^+$ cells in SN comparing contra vs ipsilateral side. ST, striatum; SN, substantia nigra. Data are expressed as mean ± SEM. (*p <0 .05, ***p < 0.001)

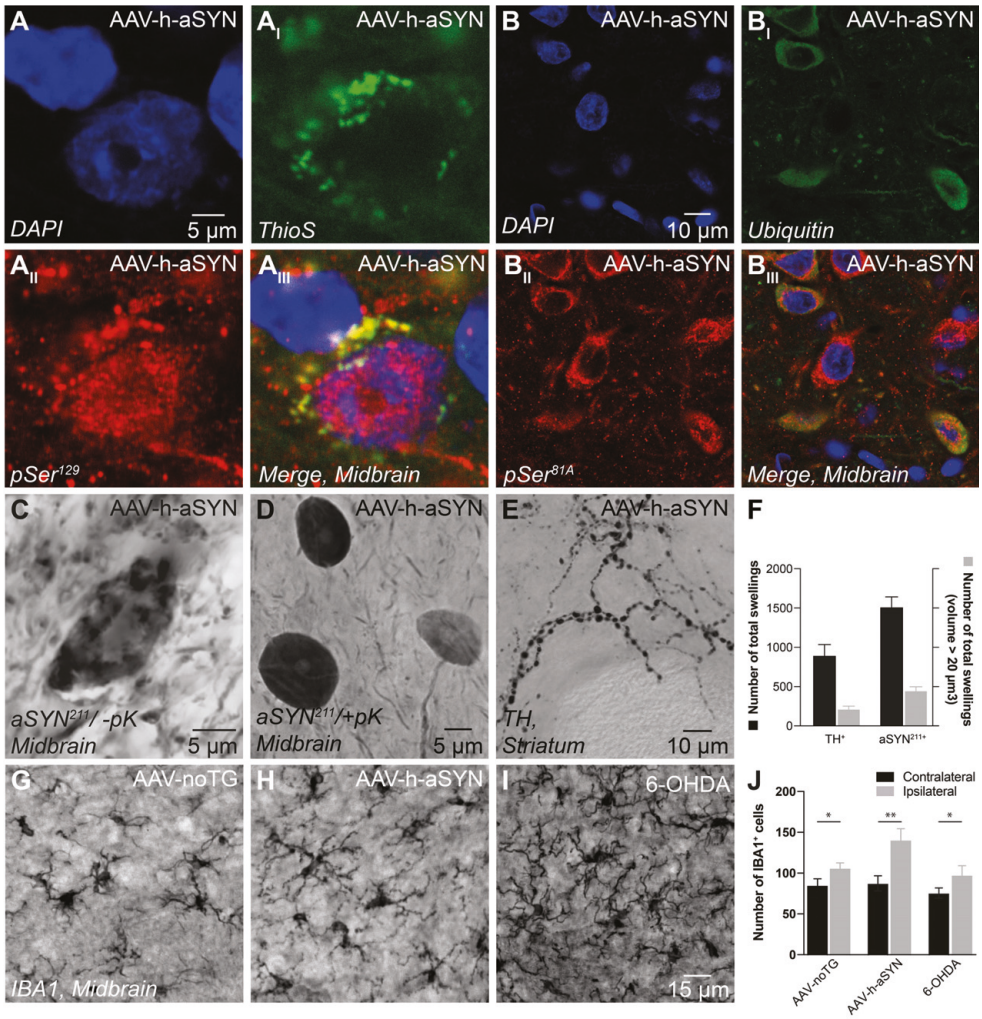


**Figure 12 | PD-like pathology and inflammation. A-A$_{III}$)** Triple immunofluorescence for DAPI, Thioflavin S and pSer129 in midbrain. **B-B$_{III}$)** Triple immunofluorescence for DAPI, Ubiquitin and pSer81A in midbrain. **C,D)** αSyn211 immunoreactivity before (-pK) and after (+pK) Proteinase K treatment in the midbrain. **E)** Representative image TH immunolabelling in striatum. **F)** Axonal swelling quantification for total and >20 µm$^3$ particles in TH and αSyn211 labelled striatal sections. **G-I)** Representative images taken from IBA1 stained ipsilateral midbrain sections of the three experimental groups. **J)** Quantification of IBA1$^+$ cells in the midbrain comparing contralateral vs ipsilateral side. Data are expressed as mean ± SEM. (*p < 0.05, **p <0 .01)

*αSyn overexpression led to motor and cognitive impairments*

Over time the AAV-h-αSyn and 6-OHDA groups displayed motor and non-motor impairments. The corridor test revealed a lateralized attentional neglect bias to the contralateral side, which increased over time and reached 40% and 70% at week 22 for the AAV-h-αSyn and 6-OHDA groups, respectively (Figure 13 A). The cylinder and stepping tests showed the development over time of forelimb asymmetry and akinesia, respectively (Figure 13 B and C). In the cylinder test, the 6-OHDA group started showing a reduced use (66 %) of the contralateral paw already at week 4, which remained stable over time (Figure 13 B). On the other side, the bias in the AAV-h-αSyn group developed progressively and reached 47% at week 22. Similar results were observed for the stepping test, where the 6-OHDA group developed impairments earlier than the AAV-h-αSyn group. In particular, the 6-OHDA group had a 60 % bias at 4 weeks which remained stable; the AAV-h-αSyn group instead had a significant 37 % bias starting from week 8, which then worsened to 50 % at week 22 (Figure 13 C).

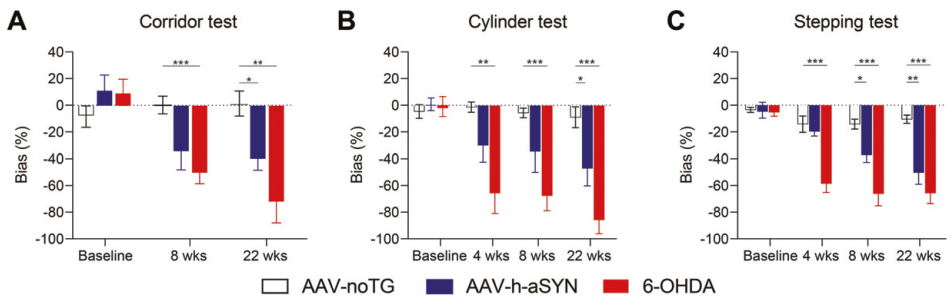


**Figure 13 | Drug-free motor and non-motor behavioural tests. A-C)** Behavioural analysis for corridor (A), cylinder (B), and stepping (C) tests over time for the three experimental groups. Data are expressed as mean ± SEM. (*p < 0.05, **p <0 .01, ***p < 0.001)

# Paper III

In Paper I and II, we characterised our AAV-αSyn overexpression model and demonstrated the development of behavioural deficits on simple and commonly used behavioural tests and of PD-like histopathological features. However, PD is a rather complex disease affecting both motor and non-motor domains. In PD patients, voluntary movement initiation and execution are more affected than muscle strength per se (Rogers & Chan, 1988). Here, for the first time in an AAV-αSyn overexpression model, we addressed deficits on a lateralised choice reaction time task which allows for the investigation of movement times, reaction times, as well as accuracy towards lateralised stimuli.

*Experimental setup*

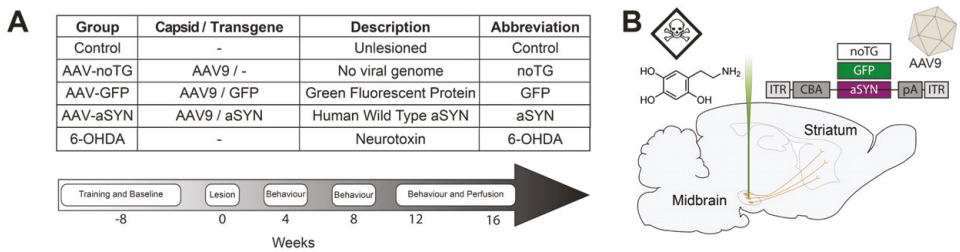


**Figure 14 | Experimental setup. A)** descriptions of groups and timepoints for behaviour, surgeries and perfusions. **B)** Schematic of the viral genome and the brain region injected. noTG, no transgene; GFP, green fluorescent protein; αSyn, alpha-synuclein; 6-OHDA, 6-hydroxydopamine; pA, polyadenylation; ITR, Inverted Terminals Repeat; CBA, Chicken β-Actin.

Sprague-Dawley rats were matched into the following six experimental groups depending on their combined behavioural performance at baseline: one non-injected group (control), one injected with an AAV carrying no transgene (AAV-noTG), one with AAV-GFP (AAV-GFP), one with AAV-αSyn (AAV-αSyn), and one with 6-OHDA (6-OHDA). Injections were made unilaterally in the SN for the AAV injected groups and in the MFB for the 6-OHDA group. We performed stepping and cylinder at 4-, 8-, and 12-weeks post-injection, corridor at 8- and 12-weeks post-injection, and the lateralised choice reaction time task at 12-weeks post injection for 15 consecutive days. According to the deficit levels observed in the simple behavioural tests, the AAV-h-αSyn group was further divided into a mild a moderate group. The moderate group includes subjects that presented a bias score bigger than 20 % on the cylinder, stepping, and corridor tests, while the remaining rats were assigned to the mild group. Animals were eventually perfused, and brains extracted for immunohistochemical analyses (Figure 14 A and B).

*Stable protein overexpression following AAV injection in midbrain and striatum*

The injection of either AAV-αSyn or AAV-GFP led to strong transgene overexpression both in the striatum and midbrain, as shown in the high magnification images taken after DAB-IHC for GFP and αSyn211 (Figure 15 A-C, E-G). Additionally, densitometric analysis of striatal and midbrain sections immunolabeled for GFP and αSyn211 revealed a significantly higher staining intensity in the ipsilateral side than the contralateral side in the GFP, mild and moderate groups (Figure D and H).

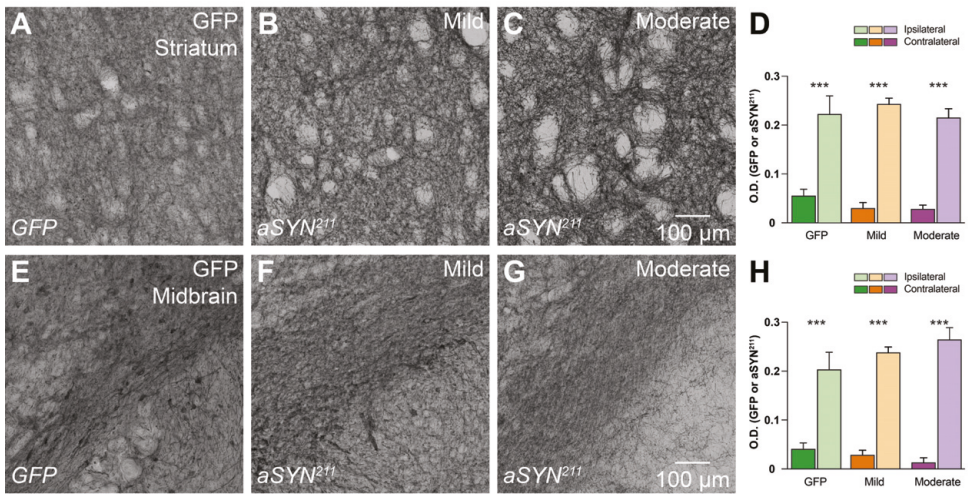


**Figure 15 | Transgene overexpression along the nigrostriatal pathway. A-C, E-G)** Representative images of GFP and αSyn211 immunoreactivity in striatum (A-C) and midbrain (E-G) for the GFP, mild and moderate group. **D, H)** Densitometric analysis for GFP and αSyn211 staining intensity in striatum and midbrain comparing contra vs ipsilateral side. (***p < 0.001)

*Transgene overexpression led to neurodegeneration of the dopaminergic system*

The presence of high levels of the transgene as well as the injection of 6-OHDA caused neurodegeneration along the nigrostriatal pathway on the ipsilateral side of the brain, as shown in the representative high magnification images taken from striatal and midbrain sections labelled for TH (Figure 16 A-$F_I$). Optical density quantification revealed a significant reduction in ipsilateral TH staining intensity in the GFP, mild, moderate, and 6-OHDA groups (Figure 16 G). Stereological quantification of $TH^+$ cells in the SN showed a significant loss of dopaminergic cells on the side of injection for the GFP (44 %), moderate (37 %), and 6-OHDA (85 %) groups (Figure 16 H). Quantification of $NeuN^+$ cells in the SN was in line with the observed TH loss, even though to a lower extent, demonstrating the presence of actual neuronal death and not only of TH enzymatic activity loss. The groups which displayed the highest neuronal degeneration were the moderate and the 6-OHDA groups, with around 25-30 % loss in $NeuN^+$ cells on the ipsilateral side (Figure 16 I).

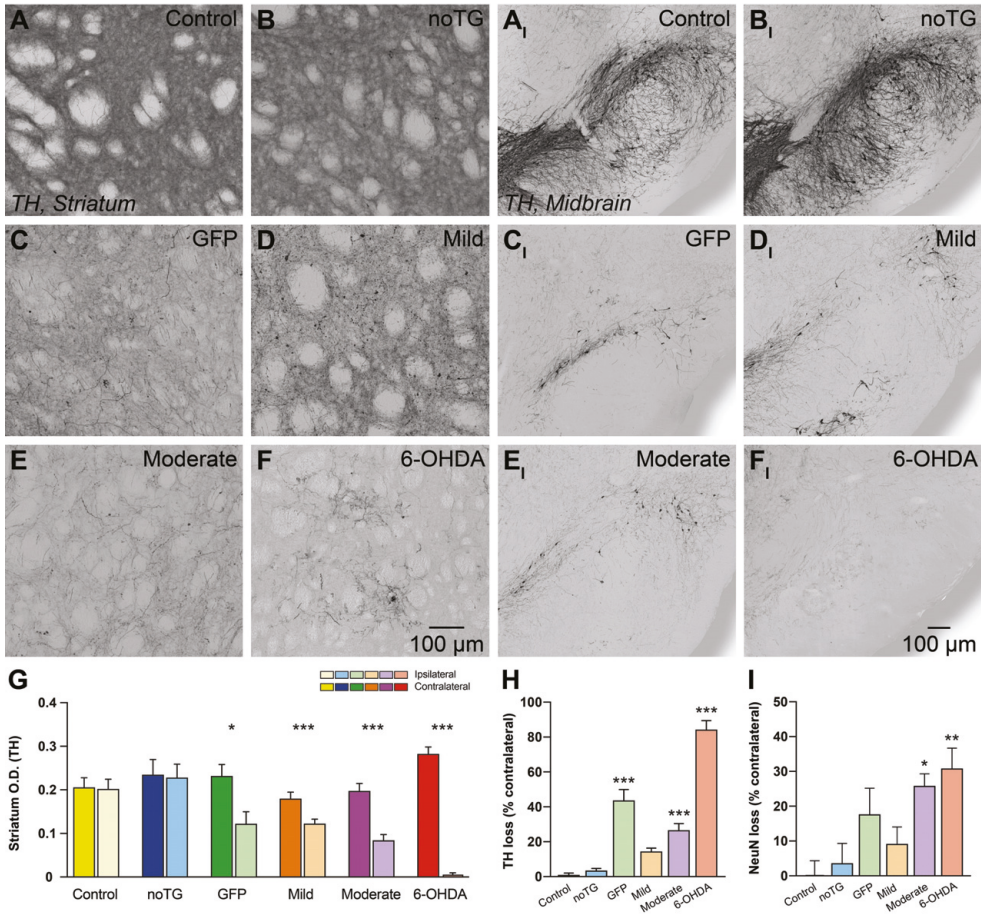


**Figure 16 | TH loss in striatum and midbrain. A-F$_I$)** Representative images of TH immunoreactivity in striatum (A-F) and midbrain (A$_I$-F$_I$) in the six experimental groups. **G)** Densitometric analysis for TH staining intensity in striatum comparing left vs right side. **H)** Percentage loss of TH$^+$ cells in the ipsilateral SN quantified via stereology (vs contralateral side). **I)** Percentage loss of NeuN$^+$ cells in the ipsilateral SN (vs contralateral side). Data are expressed as mean ± SEM. (*p < 0.05, **p <0 .01, ***p < 0.001)

*Overexpression of αSyn led to nigral and axonal pathology*

In line with previous results, we report nigral pathology by the presence of pK resistant αSyn (Figure 17 A-A$_I$), phosphorylated αSyn (Figure 17 B) and abnormal cell conformation (Figure 17 C), as well as Thioflavin S positive inclusions (data not shown) in the SN. In addition to nigral pathology, we report the presence of axonal swellings in αSyn211 and TH labelled striatal sections of the mild and moderate groups, as depicted in the representative images taken from the ipsilateral striatum of the moderate group (Figure 17 D and E). Subsequent quantification of >20 µm$^3$ αSyn211$^+$ and TH$^+$ axonal swellings in the ipsilateral striatum revealed elevated numbers in the mild and moderate groups (Figure 17 D$_I$). The GFP group

also displayed some swellings when immunostained for TH, but it did not reach a statistical difference when compared to the control groups. The control, noTG and 6-OHDA groups did not display any $TH^+$ axonal pathology (Figure $E_I$). Additionally, in the mild and moderate groups, high levels of $\alpha Syn211^+$ swellings could also be found in the prefrontal cortex, the region that receives most of the dopaminergic input from the VTA (data not shown).

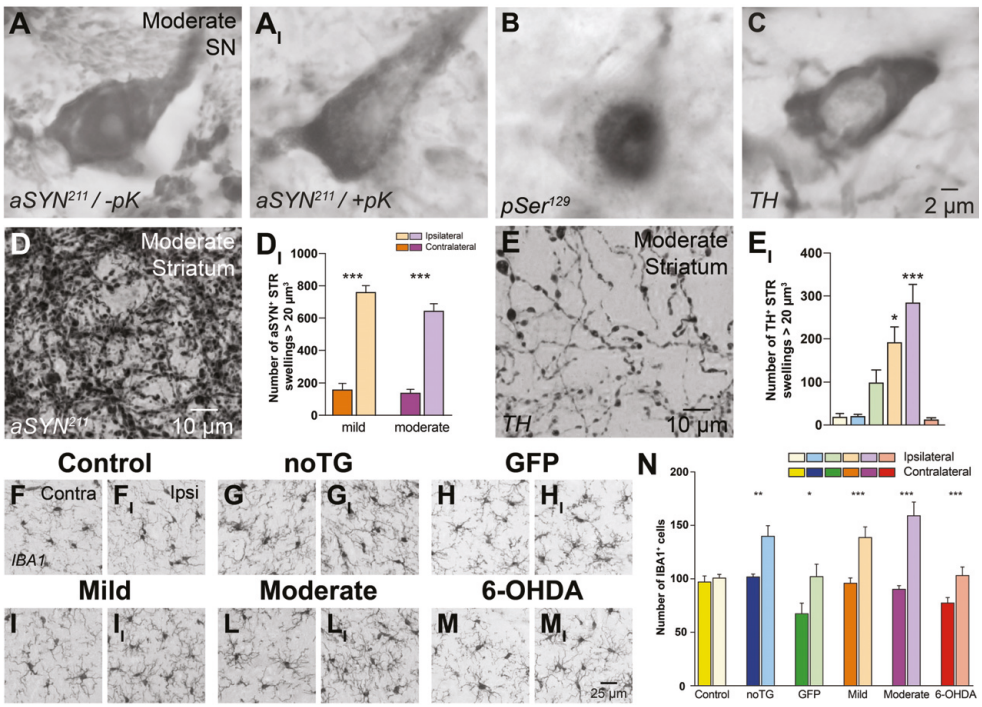


**Figure 17 | Nigrostriatal pathology and inflammation. A, $A_I$)** $\alpha$Syn211 immunoreactivity before (-pK) and after (+pK) Proteinase K treatment in the midbrain. **B, C)** Representative images of midbrain cellular pathology revealed by pSer129 (B) and TH (C) immunolabelling. **D, $D_I$)** Representative image of the striatum for the moderate group immunostained for $\alpha$Syn211 (D) and respective quantification of >20 $\mu m^3$ $\alpha Syn211^+$ axonal swellings for the mild and moderate AAV-$\alpha$Syn groups ($D_I$). **E, $E_I$)** Representative image of the striatum for the moderate group immunostained for TH (E) and respective quantification of >20 $\mu m^3$ $TH^+$ axonal swellings for the six experimental groups ($E_I$). **F-$M_I$)** Representative images taken from the ipsi and contralateral SN immunolabelled for IBA for all the experimental groups. **N)** Quantification of $IBA1^+$ cells in the left and right side of the midbrain. STR, striatum. Data are expressed as mean ± SEM. (*p < 0.05, **p <0 .01, ***p < 0.001)

*Behavioural impairments on simple and complex behavioural tasks*

We evaluated the development of cognitive and motor impairments using simple behavioural tasks over a period of 12 weeks. In the cylinder and stepping tests, the 6-OHDA group displayed a deficit at the earliest timepoint, which remained stable over time (70-80 %). On the other hand, the moderate group displayed a deficit, which worsened over time, starting from 40 % at week 4 and reaching 60-70 % at week 8 (Figure 18 A and B). In the corridor test, animals from the 6-OHDA and moderate groups displayed a similar deficit at week 8 (50%), which increased at week 12 (80-90 %). The remaining groups (control, noTG, and GFP) did not display any significant deficit in any of the previously mentioned tests (Figure 18 C). To characterise in depth the deficits observed, we tested the rats on the lateralised choice reaction time task for 15 consecutive days and subsequently divided them into 5-days blocks for analysis (i.e., Lx-I, Lx-II, and Lx-III). We report increased contralateral reaction times for the 6-OHDA group starting from Lx-I and for the moderate group from Lx-II (Figure 18 D). Contralateral accuracy was also affected. The noTG group recovered to similar levels of the control group (89 %) over the three timepoints. The GFP group recovered as well, but despite its accuracy being above 81% at Lx-III, it remained significantly lower compared to the control group (88 %). On the other hand, the mild, moderate, and 6-OHDA groups' accuracy did stay stable over the three timepoints and did not recover to baseline levels. Their accuracy stayed around 60 %, 40 %, and 7 %, respectively (Figure 18 E). When looking at the movement times, we found differences both on the ipsilateral and contralateral sides. To a different extent, the mild, moderate, and 6-OHDA groups were slower in moving to both sides (Figure 18 F and G). However, the deficit seemed to be more enhanced on the contralateral side, especially for the moderate and 6-OHDA groups at Lx-III. As for the reaction time, the 6-OHDA group was the most impaired, followed by the moderate group. The mild group was slower in moving at Lx-I and Lx-II but recovered at Lx-III. The bias observed in the cylinder, stepping, and corridor tests, as well as the decrease in contralateral accuracy, correlated significantly with the loss of $TH^+$ cells in the SN (data not shown).

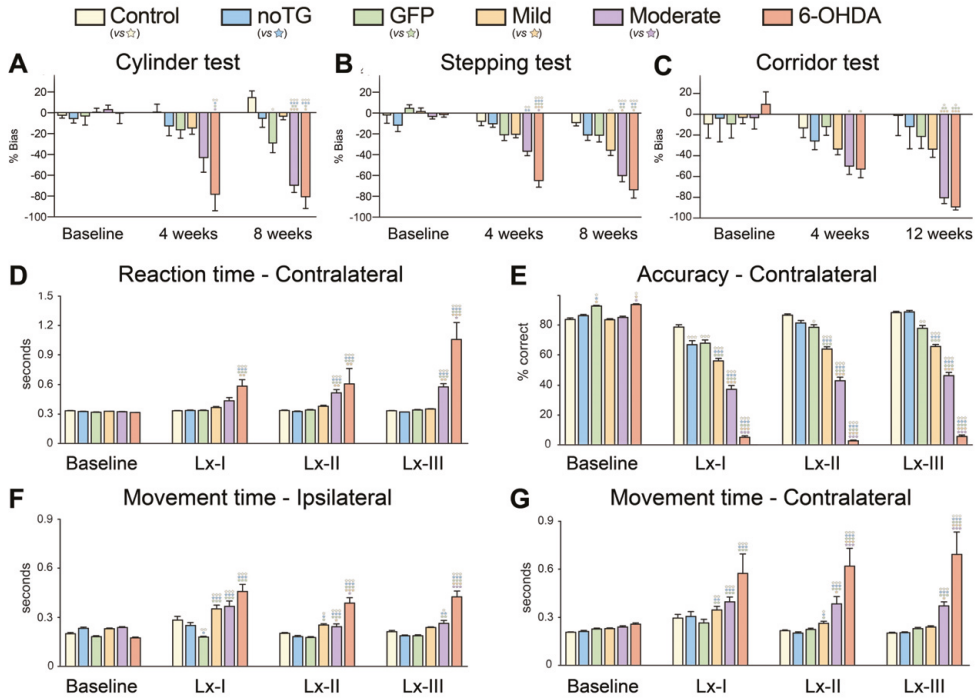


**Figure 18 | Motor and cognitive deficits. A-C)** Simple behavioural tests to assess forelimb akinesia and asymmetry (A, B) and attentional neglect (C). **D-G)** Main outcome measures recorded from the lateralised choice reaction time task: contralateral reaction time (D), contralateral accuracy (E), ipsilateral (F), and contralateral movement time (G). The 15 consecutive days of testing were divided into three 5-days blocks (Lx-I, Lx-II, and Lx-III). Data are expressed as mean ± SEM. (*p < 0.05, **p <0 .01, ***p < 0.001)

# Paper IV

The main goal of developing preclinical models of PD is to be able to study the pathological changes and test potential therapeutic treatments. Therefore, after developing and characterising a rat model of PD, we investigated whether gene therapy using neurotrophic factors could exert any neuroprotective effect. In particular, we tested the effects of AAV-based delivery of GDF5 from a histopathological and behavioural point of view.

*Experimental setup*

**A**

| Group | Virus Injected | N Total | N Behaviour | N IHC | N qPCR |
|---|---|---|---|---|---|
| **Control** | none | 12 | 12 | 11 | 5 |
| **GDF5** | AAV9-GDF5 | 13 | 13 | 13 | 5 |
| **αSyn** | AAV9-αSyn | 11 | 11 | 10 | 5 |
| **αSyn+GDF5** | AAV9-αSyn + AAV9-GDF5 | 12 | 12 | 12 | 5 |

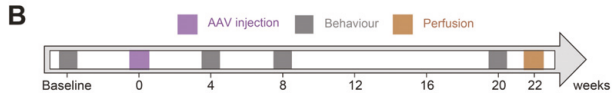


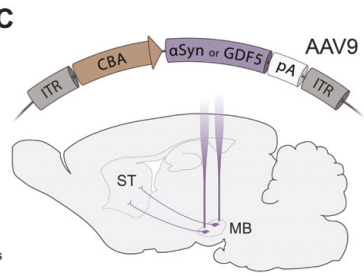


**Figure 19 | Experimental outline. A)** Name of the group names with details about the type of virus injected, total number of animals per group and sample size for the behavioural and IHC analyses. **B)** Time course for behaviour, surgery and perfusion. **C)** Schematic of the viral genome and injection site. ST, striatum; MB, midbrain; αSyn, alpha-synuclein; GDF5, growth differentiation factor 5; pA, polyadenylation; ITR, Inverted Terminals Repeat; CBA, Chicken β-Actin; IHC, immunohistochemistry.

Sprague-Dawley female rats were assigned to four experimental groups according to their performance at baseline in simple (stepping, cylinder, and *d*-amphetamine-induced rotations) and complex (lateralised choice reaction time) behavioural tasks. After baseline acquisition, rats received a unilateral injection in the SN of AAV-αSyn, AAV-GDF5, or a combination of the two depending on the group they were assigned to. One group did not receive any brain surgery and was used as a control. Animals were then re-tested on stepping, cylinder, and *d*-amphetamine-induced rotations tests at 4- and 8-weeks post-injection, and on the lateralized choice reaction time task at 8- and 20-weeks post-injection. The 20-weeks timepoint is currently under revision and data are missing. At last, we perfused the animals, and their brains were collected for histological and gene expression analyses (Figure 19 A-C).

*The injection of GDF5 did not alter αSyn levels in striatum and midbrain*

The injection of AAV-αSyn resulted in strong immunoreactivity for αSyn211 in the midbrain and striatum in αSyn and αSyn+GDF5 groups (Figure 20 A-D). Densitometric analysis revealed a significant and similar increase in the optical density in the ipsilateral striatum and midbrain for those groups (Figure 20 E).

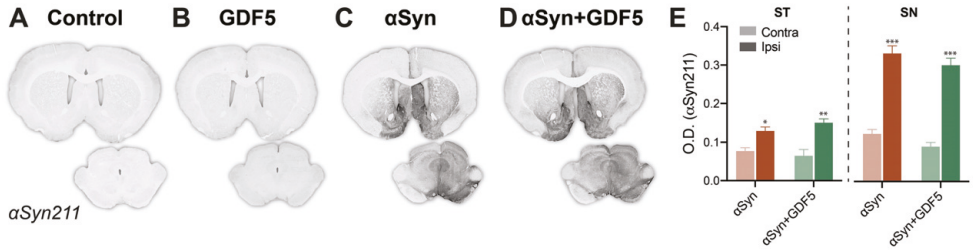


**Figure 20 | AAV-induced αSyn overexpression in the nigrostriatal system. A-D)** Representative images of striatum and midbrain for αSyn211 immunoreactivity in the four experimental groups. **E)** Densitometric analysis for αSyn211 staining intensity between contralateral and ipsilateral striatum and substantia nigra in the two AAV-αSyn injected groups, respectively. ST, striatum; SN, substantia nigra. Data are expressed as mean ± SEM. (*p < 0.05, **p > 0.01, ***p < 0.001).

*Treatment with GDF5 did not reduce TH loss in AAV-αSyn injected rats*

To investigate whether GDF5 had a neuroprotective effect on our αSyn model, we immunolabeled striatal and midbrain sections for TH. αSyn and αSyn+GDF5 groups, and to a minor extent the GDF5 group, showed TH loss in the ipsilateral striatum (Figure 21 A-D). Accordingly, densitometric analysis of TH staining intensity on striatal sections revealed a significant decrease in optical density on the side of injection (Figure 21 E). At the nigral level, quantification of $TH^+$ cells in the SN showed a 40 % cell loss in the ipsilateral SN compared to the contralateral side for both the αSyn and αSyn+GDF5 groups. The GDF5 group had a 15 % reduction in $TH^+$ cells on the side of injection and was not significantly different from the control group (Figure 21 J). The loss in TH immunoreactivity was accompanied by a reduction in $NeuN^+$ cells, suggesting the presence of actual neurodegeneration (Figure 21 F-I).

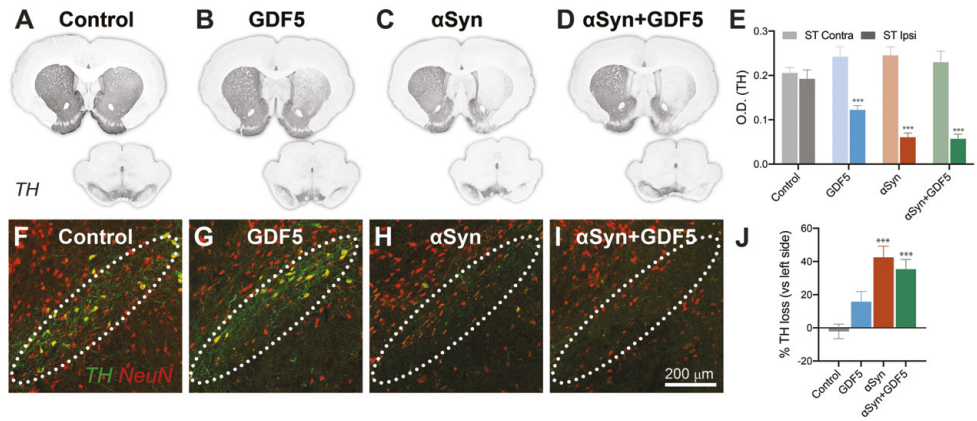


**Figure 21 | TH expression along the nigrostriatal pathway. A-D)** Representative images for striatum and midbrain immunolabeled for TH of the four experimental groups. **E)** Densitometric analysis comparing TH staining intensity of ipsilateral vs contralateral side of striatum. **F-I)** Double immunofluorescence for TH and NeuN in the substantia nigra (dotted area). **J)** Quantification of TH+ cells in the SN using Aiforia. ST, striatum. Data are expressed as mean ± SEM. (***p < 0.001).

*Gene expression analysis in the substantia nigra*

We tested the expression levels of the genes encoding for αSyn, GDF5, TH, dopamine transporter (DAT), and RET in the injected SN of five rats per group. Groups that received AAV-αSyn showed a strong *αSyn* gene expression when compared to the control group (Figure 23 A). Accordingly, groups that received AAV-GDF5 showed a strong *Gdf5* gene expression when compared to the control group (Figure 23 B). Additionally, all the groups, except for the control group, had a reduction in the dopamine-related genes *Th* and *Dat* (Figure 23 C and D). We then investigated if αSyn was downregulating *Ret*, as previously reported (Decressac, Kadkhodaei, et al., 2012; Goulding et al., 2021). Even though we did not find statistical differences between groups, we observed a trend in reduced *Ret* expression levels in the αSyn group only (Figure 23 E).

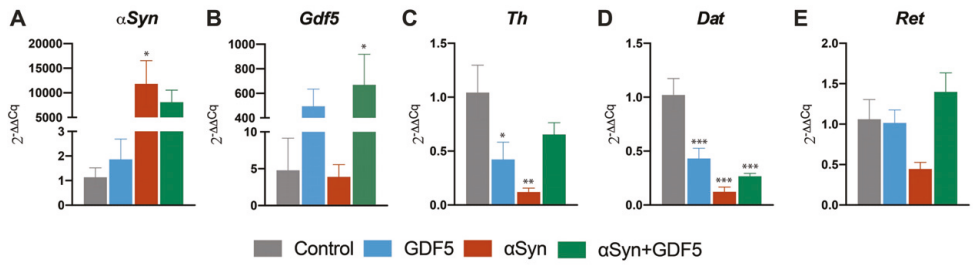


**Figure 23 | Gene expression analysis in the SN. A-E)** Relative fold gene expression for *αSyn* (A), *Gdf5* (B), *Th* (C), *Dat* (D), and *Ret* (E) in the injected SN. Data are expressed as mean ± SEM. (*p < 0.05, **p < 0.01, ***p < 0.001).

*GDF5 did not ameliorate motor and cognitive deficits in AAV-αSyn injected animals*

We tested animals on simple and complex behavioural tasks to assess for motor and cognitive recovery after the administration of AAV-GDF5. In the stepping test, the αSyn and the αSyn+GDF5 groups performed fewer contralateral adjusting steps, which were 56 % and 26 % less than the ipsilateral steps at 8 weeks, respectively (Figure 22 A). In the cylinder test, αSyn and the αSyn+GDF5 groups had a 15 % and 20 % reduced use of the contralateral forepaw at 4 weeks which then increased to 30 % and 25 % at 8 weeks, respectively. The GDF5 group also had a 13 % reduced use of the contralateral paw at 8 weeks (Figure 22 B). In the *d*-amphetamine-induced rotation test, a rotational behaviour could be observed at 8 weeks, when the αSyn and the αSyn+GDF5 groups performed 5 or more ipsilateral rotations per minute (Figure 22 C). In the lateralised choice reaction time task, we found differences between groups in the contralateral accuracy. The αSyn and the αSyn+GDF5 groups dropped their contralateral accuracy to 50 % at 8 weeks compared to baseline (Figure 22 D).

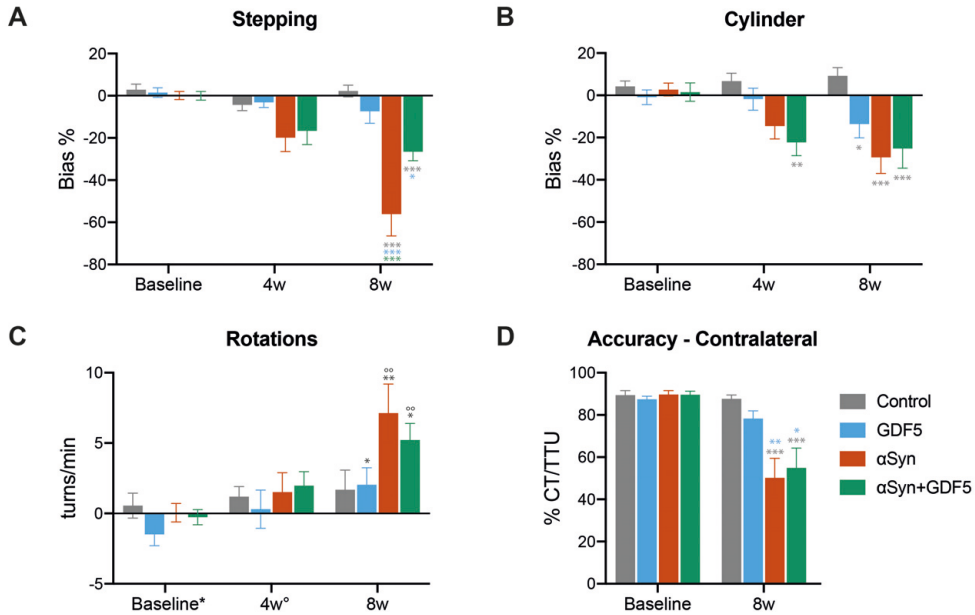


**Figure 22 | Simple and complex behavioural tests. A-C)** Simple behavioural tests used to assess motor function at week 4 and 8 post-surgery, i.e., stepping, cylinder and amphetamine-induced rotations. **D)** Outcome for the lateralized choice reaction time task, i.e., contralateral accuracy. TTU, total trial usable; CT, correct trials; w, weeks. CT, correct trials; TTU, total trials usable. Data are expressed as mean ± SEM. (*p < 0.05, **p < 0.01, ***p < 0.001, colors and simbols indicate to which group or timepoint that p-value is referring to).

# Discussion

AAV vectors are a useful tool for overexpressing proteins *in vivo*, and they are widely used to model PD in preclinical studies. They have a relatively simple design, they are low immunogenic, and their structure can be easily modified at will (Haggerty et al., 2020). In PD preclinical research, AAV-based strategies have gone through several generations, and the differences in the experimental setup and in the viral constructs have generated a large variability in AAV-αSyn mediated histopathological and phenotypical changes (Kirik et al., 2002; Klein et al., 2002; Lo Bianco et al., 2002). Overall, the injection of AAV-αSyn into rodents' midbrain can lead to $TH^+$ dopaminergic cell loss and dopaminergic denervation in the striatum (Chung et al., 2009; Decressac, Mattsson, & Bjorklund, 2012; Decressac, Mattsson, Lundblad, et al., 2012; Decressac et al., 2011; Gombash et al., 2013; Koprich et al., 2010; Lundblad et al., 2012; Oliveras-Salva et al., 2013). In the attempt to achieve a more robust and reproducible pathology, recent studies have combined viral AAV-based αSyn overexpression with the sequential or simultaneous inoculation of PFFs, which seed αSyn inclusions (Espa et al., 2019; Hoban et al., 2020; Thakur et al., 2017).

In **Paper I**, we compared for the first time different synucleinopathy models based on AAV-αSyn and PFFs. The addition of PFFs to the AAV-αSyn injection generated additional cell body pathology that shares some of the characteristics of human LBs and triggered inflammation, suggesting the presence of a synergistic effect between AAV-αSyn and PFFs. Since we found no differences in terms of pathology when the PFFs were injected either simultaneously or sequentially, we suggest that the first strategy might be a better choice for future applications as it requires a single surgical intervention, making this approach less invasive. Interestingly, the injection of AAV-αSyn with or without additional inoculation of PFFs resulted in the loss of $TH^+$ dopaminergic cells, axonal pathology, and produced a stable motor phenotype. Therefore, we decided to further characterize the use of AAV-induced αSyn overexpression to model early and late stages of PD, as well as motor and cognitive impairments and its potential use for the assessment of therapeutic interventions.

In **Paper II**, we developed a rat model of early-stage PD by reducing the viral load utilized in **Paper I**. We observed a moderate but significant loss of $TH^+$ neurons accompanied by progressively increasing behavioural impairments over a period of 22 weeks, as well as axonal pathology, and phosphorylation and aggregation of

αSyn into insoluble Lewy-like inclusions, similar to what is observed in the human condition.

In **Paper III**, for the first time, we report deficits in a complex behavioural task in the AAV-αSyn overexpression model and provide a thorough characterisation of the behavioural impairments thereof. We used a choice reaction time task to demonstrate attentional deficits, as well as deficits in movement initiation (akinesia) and movement completion (bradykinesia), which have been previously reported in PD patients (Evarts et al., 1981; Gauntlett-Gilbert & Brown, 1998; Jahanshahi et al., 1992). In line with our previous results, we also report deficits on simple behavioural tasks, as well as TH loss and axonal and nigral αSyn pathology.

In **Paper IV**, we combined our previous observations to assess the beneficial effects of GDF5 in our AAV-αSyn model. GDF5 is a newly emerging neurotrophic factor that has already shown its potential in protecting dopaminergic neurons both *in vitro* and *in vivo* (Clayton & Sullivan, 2007; Costello et al., 2012; Goulding et al., 2021; Hurley et al., 2004; Krieglstein et al., 1995; O'Sullivan et al., 2010; Sullivan et al., 1997; Sullivan et al., 1998). We report no significant improvements in dopaminergic cell survival as well as in motor and cognitive deficits in the group that received both AAV-αSyn and AAV-GDF5, in contrast to what was observed in a recent similar study (Goulding et al., 2021).

Taken together, these results represent a detailed characterisation of a rat model based on AAV-induced αSyn overexpression and highlight its advantages and limitations. We were able to obtain consistent results between studies and generate a model with stable behavioural deficits in motor and cognitive domains. We were also able to model early and late stages of PD by modulating the viral load. The early-stage PD model (**Paper II**) had a more moderate TH loss than the late-stage PD model (**Paper I**, **III** and **IV**) and the behavioural impairments observed developed more gradually. Importantly, we demonstrated that the behavioural impairments correlated with the dopaminergic cell loss and the axonal dysfunction observed at the nigrostriatal level (**Paper III**). Additionally, we showed the presence of αSyn phosphorylation and aggregation similarly to what is observed in Lewy pathology (**Paper I**, **II** and **III**). However, the protein expression levels necessary for the generation of our model complicated the choice of an appropriate control vector. In **Paper I** and **III**, GFP overexpression caused toxicity, as already reported by others (Albert et al., 2019; Koprich et al., 2011; Landeck et al., 2017). Additionally, in **Paper IV**, we also report some minor toxicity caused by AAV-induced GDF5 overexpression, which resulted in a moderate loss of $TH^+$ signal in the striatum.

This made the identification of the pathological features caused by αSyn more difficult because it showed that general transgene overexpression can be toxic per se. To overcome this issue, some studies have decreased the viral titer of the control vector (Decressac et al., 2011; Kirik et al., 2002; Mulcahy et al., 2012), but we

believe that this is not an ideal approach to follow when conducting studies that are aiming to induce cell loss by protein overexpression. The use of AAV-noTG in **Paper II** did not result in neurotoxicity, however, this control vector does not address the effects of general transgene overexpression. One remedy for this would be to search for mammalian proteins that are not prone to aggregation and that are more tolerated by the host species (Airavaara et al., 2020). Alternatively, a scrambled αSyn genomic sequence or an inducible expression cassette might be also considered.

An interesting observation was that even though the TH loss in the AAV-GFP group was larger than the one measured in the AAV-αSyn group, the behavioural impairments were smaller (**Paper III**). In human PD, it has been reported that around 30% of dopaminergic neurons in the SNc and 50-70 % of axonal terminals in the striatum are lost at the time of motor symptoms onset (Fearnley & Lees, 1991; Greffard et al., 2006; Ma et al., 1997). Additionally, it has been shown that axonal dysfunction precedes neuronal loss in the AAV-αSyn model (Chung et al., 2009; Phan et al., 2017). In **Paper I**, **II,** and **III**, we report that the injection of AAV-αSyn caused more denervation in the striatum than TH loss in the SNc, similarly to what happens in the human condition. Moreover, it triggered the formation of elevated numbers of swellings in the remaining axons, something that was not observed after AAV-GFP injection. Our results also suggest that the loss of TH phenotype is not necessarily indicative of neuronal death, as concomitant smaller levels of $NeuN^+$ cell loss in the SN were observed. Indeed, it seems that the pathological changes observed in our model derive from a combination of axonal dysfunction, TH downregulation, and actual neuronal death.

Creating and validating an appropriate PD model is of utmost importance in order to generate reliable results that are representative of the human condition, and the selection of the model should be done carefully depending on the research question. For example, the 6-OHDA model is ideal for investigating the effects of dopamine depletion but does not address for αSyn pathology. On the other side, the AAV-αSyn model develops synucleinopathy and can be useful in determining the role of αSyn in inducing pathology; however, the strong expression levels induced by AAVs might not be representative of the human condition and might result in general toxicity. Examples demonstrating this concept are the clinical and preclinical studies using GDNF therapy. Promising results were obtained in the 6-OHDA model (Choi-Lundberg et al., 1997; Hoffer et al., 1994; Wang et al., 1996) and prompted the start of a clinical trial, which unfortunately did not meet its primary endpoint (Whone, Luz, et al., 2019). In parallel, a preclinical study reported that GDNF failed to exert any neuroprotective effect in the AAV-αSyn model, suggesting the involvement of αSyn in reducing GDNF's beneficial effects (Decressac et al., 2011). Similarly, in **Paper IV**, we report opposite results from what was observed in a recent study which assessed the neuroprotection induced by AAV5-GDF5 in an AAV6-αSyn rat model (Goulding et al., 2021). In this study,

they report that AAV-GDF5 was able to reduce TH and DAT loss in the SN, and TH and dopamine loss in the striatum of AAV6-αSyn injected rats; however, they do not address behavioural impairments and behavioural recovery. These results further indicate that variability within similar models is possible.

Overall, the increase in the number of laboratories utilizing the AAV-αSyn model calls for the need for a standardized and reproducible methodology to make the results easily comparable between studies. For example, in our iteration of the AAV-αSyn model, we opted for an AAV9 carrying the human αSyn gene under the control of a CBA promoter. We determine the viral genome copies by ddPCR, and we work with concentrations from $2x10^{12}$ to $6x10^{12}$ gc/mL. We inject 2 µL unilaterally in two to three sites of the midbrain. Every variation from this setup might result in different outcomes than the ones reported by us and should be taken into consideration when replicating this model. As a matter of fact, reproducibility of published results has generated serious concerns in the past decade as it has been reported that more than half of former studies cannot be reproduced (Begley & Ellis, 2012; Hartshorne & Schachner, 2012; Prinz et al., 2011). The omission of negative or inconclusive data contributes to this replication crisis (Baker, 2016) and it secures that repetitive or biased theories will be pursued, resulting in laboratories wasting time and resources on projects that could have been more fruitful if that knowledge would had been accessible. This is heavily counterproductive, and proper execution, robust statistics, and experimental design should be valued more than the novelty per se.

To conclude, this thesis contains more than four years of research (and some negative data) that resulted in the generation of an AAV-αSyn rat model of PD, which presents some of the typical changes observed in the human condition. If used properly and until proven otherwise, this model represents a useful tool to assess disease progression and future therapeutic interventions.

# Methods

## AAV viral production

AAVs are produced according to two different protocols, one based on chloroform precipitation and one on iodixanol gradient ultracentrifugation (Negrini et al., 2020; Sandoval et al., 2019). We published a study showing that no difference in terms of toxicity, inflammation and transgene expression can be observed between these two methods; hence they are used interchangeably (Davidsson et al., 2020).

*Transfection*

HEK293T cells are seeded in culture flasks and grown until 70-80% confluency. Cells are transfected using polyethylenimine (PEI) and following a three-plasmid system. In this system, a plasmid either carrying the transgene (αSyn or GFP) or not (noTg), a helper plasmid (pXX6) and a packaging plasmid (pAAV2/9n) at a 1:2:1 molar ratio are incubated together with PEI (3 ug PEI for 1 ug of DNA) for 15 min at room temperature. The transgene plasmid is flanked by ITRs, and the expression is driven by the CBA promoter.

*Chloroform precipitation*

For details about this method, please refer to our recent publication (Negrini et al., 2020). One batch of virus consists of two T175 flasks and results in around 50 µL of purified AAV vector. Briefly, 24 h after transfection, the media is replaced with serum-free medium. 72 h post-transfection, AAVs are precipitated from cell lysate and media by centrifugation with polyethylene glycol 8000 (PEG 8000) at 4°C. After that, the precipitate is incubated with DNAse I to eliminate any unwanted unpackaged plasmid and AAVs are eventually extracted by centrifugation with chloroform. Extracted AAVs are then washed 3-4 times through PBS centrifugation in Amicon Ultra 0.5 Centrifugal filters (Merck Millipore). Purified AAVs are then stored either in glass vials or sigma-coated plastic tubes at 4°C.

*Iodixanol gradient*

For details about this method, please refer to Sandoval et al. (Sandoval et al., 2019). One batch of virus consists of six T500 flasks and results in around 200 µL of purified AAV vector. Briefly, 72 h post-transfection, AAVs are precipitated from media by centrifugation with polyethylene glycol 8000 (PEG 8000) at 4°C.

After that, the precipitate, together with the cell lysate, go through freeze/thaw cycles and they are eventually incubated with benzonase, centrifuged and the supernatant is collected. AAVs are then extracted through iodixanol gradient ultracentrifugation. Extracted AAVs are then washed 5 times through PBS centrifugation in wet concentrator columns and eventually stored either in glass vials or sigma-coated plastic tubes at 4°C.

*Virus titration*

Virus titration is performed using droplet digital PCR (ddPCR), which provides an absolute count of viral genomes, with primers specific for the ITRs (forward primer 5'-CGG CCT CAG TGA GCG A-3′ and reverse primer 5′-GGA ACC CCT AGT GAT GGA GTT-3′). Viruses are diluted to the working concentration using PBS $Mg^{++}/Ca^{++}$.

# Animals

Sprague-Dawley female rats weighing around 220-250 g are purchased from Janvier Labs, France. Rats are kept under standard caging conditions with unlimited access to food and water, except during behavioural testing that required food restriction (see Papers I, II and III for details). All procedures are approved by the Ethical Committee for the use of laboratory animals in the Lund and Malmö region and in accordance with Swedish guidelines (Jordbruksverket) and the European directive 2010/63/EU on the protection of animals used for scientific purposes.

# Stereotactic surgery

All surgical procedures are conducted under 2-3% isoflurane anaesthesia. Before starting, the rat is anesthetized in an induction chamber with 4-5% isoflurane. The head then is shaved and fixed to a digital stereotactic frame by the ear and tooth bars, whose height is adjusted so that the head is flat (in this setup, the tooth bar was set - 4.5 mm lower that the ear bars). The tooth bar is attached to a nosepiece which is connected to the anaesthesia apparatus. A vertical incision along the centre of the head is performed and the underneath skull is revealed. The coordinates for injection are taken starting from Bregma, i.e., the point where the coronal and sagittal sutures of the skull meet. Once the point of injection has been identified, a hole is drilled into the skull, so that it is possible to access the brain. The injection is made by using a 10 μL Hamilton syringe connected to a pulled glass capillary (Cat. No. 50811, Stoelting Co.) at a rate of 0.5 or 1 μL/min, after which the capillary is left in place

for additional 3-4 min to allow for complete diffusion. Once the syringe has been slowly retracted, the wound is cleaned and sutured with coated VICRYL sutures. Please refer to the attached papers and manuscripts for details about concentrations, volumes, coordinates, and infusion rates.

# Behavioural testing

*Stepping*

Akinesia is one of the main motor symptoms observed in patients diagnosed with PD and the stepping test is a behavioural method for the assessment of forelimb akinesia for both bilateral and unilateral dopaminergic lesioned animals. Different versions of this test have been developed (Olsson et al., 1995; Schallert et al., 1992).

In this thesis, the rat is held by the researcher so that the hind legs are held firmly in the palm of one hand and the other hand securely holds one forelimb against the rat's chest, leaving the other forelimb free to move. The free leg is then dragged sideways along a flat surface for about 90 cm at a constant speed. The researcher then counts the number of adjusting steps taken by the rat moving forward and backward. For each forelimb and direction, the test is repeated three times and then the counts for left and right leg are averaged. Unilaterally lesioned animals will perform fewer adjusting steps with the limb contralateral to the side of the lesion. To not introduce any bias, any distracting objects from the testing surface are removed and similar external environmental conditions are maintained between tests. Additionally, the researcher is blinded to the treatment and control groups. The data are presented as percentage bias, calculated as follows:

$$Bias\ \% = \frac{(\bar{N}\ \text{of left adjusting steps} - \bar{N}\ \text{of right adjusting steps})}{(\bar{N}\ \text{of left adjusting steps} + \bar{N}\ \text{of right adjusting steps})} \times 100$$

*Cylinder*

The cylinder test is another behavioural method that assess forelimb asymmetry and akinesia, and unlike the stepping test, it takes advantage of the natural exploratory behaviour of rats in novel environments (Schallert et al., 2000). In this test, a rat is placed inside a glass cylinder with a base diameter of 20 cm. While exploring, a rat will get up and touch the cylinder wall with its front paws. A healthy rat will use equally both front paws, while a unilaterally lesioned rat will predominantly use its ipsilateral paw. In this thesis, a camera is positioned in front of the cylinder and a 90 ° angled mirror is placed behind the cylinder to allow for a 360° recording of the apparatus. A test lasts 5 min, and the quantification is performed by re-watching the videos and scoring the first 20 touches or the 5 min, whichever happened first. Animals touching the wall with both paws at the same time are scored as two touches, one left and one right.

The data are presented as percentage bias, calculated as follows:

$$Bias\ \% = \frac{(\text{N of left touches} - \text{N of right touches})}{(\text{N of left touches} + \text{N of right touches})} \times 100$$

*Corridor*

As already described in the introduction, the corridor test is a drug-free behavioural method to assess lateralised neglect and it is sensitive to unilateral dopaminergic lesions (Dowd et al., 2005). The corridor is a long rectangular box provided with a clear perforated Plexiglas removable roof. Along the corridor, adjacent plastic lids are glued along the corridor floor on each side at 13 cm intervals for a total of 10 pairs. Each lid is filled with 5 sugar pellets. Rats are kept on food restriction and maintained above 80% of their free food weight during the whole testing. To minimise the exploratory behaviour, rats are placed into an identical but empty corridor for 5-10 min prior to testing. Similar to the cylinder test, a trial begins when a rat is placed into the corridor, and lasts for 5 min, during which the first 20 retrievals or the 5 min are scored, whichever happened first. The scoring is performed by counting how many retrievals are made on the left and right sides of the rat's body. A 'retrieval' is defined as a nose poke into the bowl, whether or not the rat actually ate any sugar pellet. Subsequent retrievals from the same bowl are counted as one retrieval, but alternate retrievals from adjacent bowls are counted as multiple. The data are presented as percentage bias, calculated as follows:

$$Bias\ \% = \frac{(\text{N of left retrievals} - \text{N of right retrievals})}{(\text{N of left retrievals} + \text{N of right retrievals})} \times 100$$

*Lateralised choice reaction time task*

This task paradigm was adapted from Carli et al (Carli et al., 1989). During the entire training and testing period, rats are maintained on food restriction, but monitored so that their weight stayed above 80% of their free food body weight. The apparatus consists of a box with nine response holes on one side and a food dispenser flanked by house lights on the opposite side and it is connected to a computer with MED-PC IV software (Med Associates Inc – USA) installed. The nine holes and the food dispenser can produce a light stimulus and they have installed an infrared beam so that it is possible to detect when a rat pokes its nose into them. For this task, the central, the third from the left and the third from the right holes are open. Rats are initially trained over a six-week period, during which the delay is gradually increased from 50 ms to 200 ms and the stimulus duration is decreased from 5000 ms to 300 ms. Importantly, an error-correction procedure is implemented in order to minimise any natural bias towards one side. In this procedure, whenever a rat makes an incorrect response to one side, the same side is presented in the next trials until the rat makes a correct response. In the final protocol, a trial begins when a rat pokes its nose in the central hole after it is illuminated.

Subsequently, the rat must maintain the position for a delay of 200 ms until the central hole light turns off and randomly, a stimulus light of 300 ms is presented in one of the two lateral response holes (Figure 24). If a rat pokes its nose into the illuminated location, the food dispenser lights up and a sugar pellet (45 mg, Sandown Scientific) is delivered. If a rat responds in the wrong location, withdraws prematurely, is slower than 300 ms or repeatedly pokes into the central hole, there will be a time-out interval of 5 seconds where all the lights go off. Each daily trial session lasted 30 min, during which about an equal number of left and right stimuli are presented.

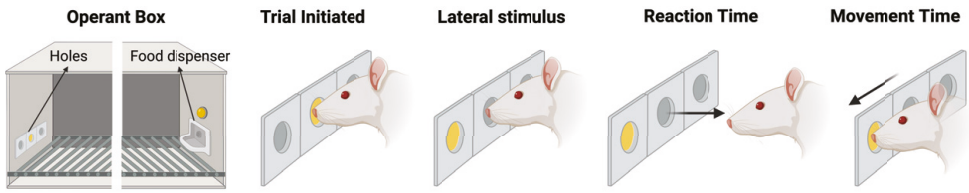


**Figure 24 | Schematic of the lateralised choice reaction time task.** The operant box has a food dispenser on one side and holes producing light stimuli on the other side. A trial is initiated when the rat pokes its nose into the central illuminated hole. A lateral stimulus is then presented, the rat reacts to it (reaction time) and produces a lateral response (movement time). If the response is correct, the rat obtains a sugar pellet delivered from the food dispenser.

The main measurements obtained from each session are:

*Total trial initiated (TTI):* defined as those in which the rat responded to the illuminated central hole.

*Total trial usable (TTU):* defined as those in which the rat responded to the illuminated central hole and sustained the poke for the required delay and executed the lateralised response.

*Reaction time (RT):* defined as the time that occurs between the onset of the lateral light stimulus and the withdrawal from the central hole.

*Movement time (MT):* defined as the time that occurs between the onset of the withdrawal from the central hole and the nose-poke to the correct or incorrect lateral hole.

*Accuracy (ACC):* defined as the number of correct responses (CT) divided by the number of TTU expressed in percentage, for each side.

*Efficiency (EFF):* defined as the number of TTU divided by the number of TTI expressed in percentage, for each side.

*d-amphetamine induced rotation test*

The *d*-amphetamine-induced rotation test was initially developed by Ungerstedt and Arbuthnott in the late 1960s (Ungerstedt & Arbuthnott, 1970). It is a non-biased, rapid, and quantitative behavioural test which relies on the rotational asymmetry observed in unilaterally dopamine-depleted animals. *D*-amphetamine increases the dopamine concentration at the synaptic cleft level by modulating its release and reuptake. It reduces dopamine reuptake by binding the dopamine transporter (DAT) and by triggering its phosphorylation, which results in both its internalisation and the reversal of dopamine transport (i.e., efflux). It can also bind to the vesicular monoamine transporter 2 (VMAT2) and cause changes in the vesicular pH, which results in dopamine release from the synaptic vesicles through VMAT2 and subsequent dopamine efflux through the phosphorylated DAT. When unilaterally dopamine-depleted rats are administered amphetamine, they start rotating in circles in the direction ipsilateral to the lesion reaching the peak of rotations after 40-60 min and lasting for about 3 hours. This test can be used to assess the level of degeneration of dopaminergic neurons, even though the number of rotations does not always correlate with the degree of cell loss. This mismatch might be due to the extent of fiber loss in the dorsolateral striatum, the subregion responsible for the rotational behaviour. Variations in the size and extent of denervated areas in the striatum can result in different behavioural outcomes as a range of 5–20 turns/min have been observed in rats with cell loss that spans from 40% to over 90%.

In this thesis, the rotational behaviour is measured by using an automated RotoMax rotometer (Omnitech Electronics, Inc.). The apparatus consists of a round plastic bowl underneath a rotating harness which is attached to a sensor connected to a computer with the Fusion Software (Omnitech Electronics, Inc.) installed. The harness is placed around the rat's chest before being injected with 2.5 mg/kg of *d*-amphetamine (diluted in saline solution). One recording session lasts 90 min, during which clockwise turns (positive values), counterclockwise turns (negative values) and net turns are measured. Data are presented as net turns/min over the 90 min recording session.

# Electrochemistry

In comparison to other techniques, such as microdialysis, electrochemistry has the particular benefit of enabling the measurement of target analytes with high temporal resolution. This is required to detect rapid events like neurotransmitter release and reuptake, which occur in milliseconds to seconds. In vivo electrochemical chronoamperometric recordings have been described previously (Hoffman & Gerhardt, 1998; Lundblad et al., 2012). Here, we use Nafion®-coated carbon fiber electrodes (Ø 30m, L 150m, Quanteon) combined with the FAST-16mkIII hardware

(Quanteon). Nafion coating is impermeable to ascorbic acid and anionic metabolites and thus improves selectivity for cationic neurotransmitters, such as dopamine. A glass capillary is attached to the electrode's tip using sticky wax at a distance of 50-100 μm, then filled with KCl (120 mM, pH = 7.4), and eventually connected to a picospritzer (Aldax) micropressure system. We apply a square wave potential (0 V to + 0.55 V) with respect to an Ag/AgCl reference electrode and determine the electrode's linearity (r2), selectivity and limit of detection (LOD) by three serial additions of 2 μM dopamine solution in 0.1 M PBS (pH = 7.4). The electrodes utilised has r2 > 0.995, selectivity higher than 100:1 for dopamine over ascorbate, and LOD < 0.01 μM. Animals are kept under 2-3% isoflurane anaesthesia during the whole procedure and the electrode-capillary assembly is implanted in the ipsilateral striatum. An Ag/AgCl electrode is used as reference which is previously prepared by electroplating an Ag wire in 1 M HCl solution saturated with NaCl for at least 20 min. Before stimulating, the assembly is left in the recording target region for at least 30 min to stabilize. We induce dopamine release by injecting locally 220–240 nL KCl (15-20 PSI, 0.1-0.5 s) four times at 10 min intervals. We analyse the resulting oxidation and reduction currents using the F.A.S.T. analysis software. Dopamine concentration is measured by subtracting baseline value (i.e., before KCl injection) to the maximum peak amplitude value. The reuptake-rate represents the rate of dopamine clearance from the extracellular space and is calculated by multiplying the Michaelis-Menten first-order rate constant with the peak amplitude (μM/s). The area under the curve represents the amount of extracellular dopamine available over time and is calculated from KCl injection until the signal is back to baseline.

## Tissue processing

All animals are euthanised with a lethal dose of Sodium Pentobarbital (1 mg/kg) injected intraperitoneally. The upper body blood circulation is then flushed with 150 mL of 0.9 % saline solution at room temperature by transcardial perfusion at a rate of 50 rpm, followed by infusion of cold 250 mL 4% paraformaldehyde solution (PFA) diluted in 0.1 M phosphate buffer. When in solution, PFA depolymerizes into formaldehyde, which acts as a fixative by cross-linking proteins and DNA molecules and preserves tissue and cell structure for subsequent immunostaining. The brain is eventually extracted and stored for 24 h in 4% PFA after which is moved to a 25-30% sucrose solution diluted in 0.1 M phosphate buffer until sunk. Sucrose cryopreserves the tissue, and if long storage is expected, 0.01% $NaN_3$ can be added to prevent bacterial growth. Brains are eventually sectioned using a freeing sledge microtome (SM200R, Leica) at 40 μm thickness and divided into 12 series and stored at -20°C in antifreeze solution until further use.

# Immunohistochemistry

*DAB staining*

On Day I, Sections are initially rinsed 3 times in potassium phosphate buffered saline (KPBS, pH = 7.4) and then incubated in a solution of 3% $H_2O_2$ and 10% methanol in KPBS for 15 min to block any endogenous peroxidase activity. Sections are then washed again for 3 times with KPBS and incubated for 1 h in a blocking solution made of 5% serum in KPBs containing 0.25% Triton X-100 (T-KPBS, pH = 7.4) to reduce any unspecific binding of the antibodies. The selection of the serum is dependent on the specie the secondary antibody is raised in. Eventually, sections are incubated overnight at room temperature in primary antibody diluted in 5% serum T-KPBS.

On Day II, sections are rinsed 2 times in KPBS and later incubated in blocking solution (5% serum T-KPBS). After that, they are left for 1 h at room temperature in biotinylated secondary antibody diluted in 5% serum T-KPBS. Other 3 washes in KPBS then precede the incubation of 1 h in avidin-biotin-peroxidase complex (ABC, Vector Laboratories) diluted in KPBS to amplify the target antigen signal. Additional 3 KPBS washes are performed, after which sections are incubated for 2-10 min in 3,3'-diaminobenzidine (DAB) substrate working solution (Vector® DAB, Vector Laboratories) prepared in distilled water. DAB substrate will form a brown precipitate in the presence of the HRP enzyme and $H_2O_2$. Three other KPBS washes are performed to remove any trace of DAB and sections are mounted on gelatine-coated glass slides. Once dry, glass slides are dehydrated in increasing ethanol concentrations (70%, 95%, 99.5%, 99.5%) and twice in pure Xylene for 2 min each step to clear sections and remove any trace of lipids. Glass slides are eventually cover-slipped using DPX mounting medium and left at least 24 h air drying before being used for microscopy.

*Fluorescent staining*

The protocol for fluorescent staining is similar to the DAB protocol except for the following steps.

On Day I, the incubation with 3% $H_2O_2$ and 10% methanol is omitted.

On Day II, the ABC incubation, the DAB reaction, and the dehydration steps are skipped. A fluorophore-conjugated secondary antibody is used instead of the biotinylated secondary antibody. For nuclei fluorescence, sections are incubated for 5 min at room temperature in DAPI diluted in KPBS and eventually rinsed before being mounted on gelatine-coated glass slides and cover-slipped with freshly thawed PVA/DABCO as soon as they dry. Antibodies utilised in this thesis can be found in Table 2.

**Table 2 | List of antibodies.**

| Antibody | Species | Cat. no | Concentration |
|---|---|---|---|
| αSyn211 | Mouse | SC-12767 | 1:10000 |
| GFP | Chicken | A10262 | 1:10000 |
| αSynuclein, p-S129 | Rabbit | ab51253 | 1:100000 |
| αSynuclein 81A (p-S129) | Mouse | AB184674 | 1:10000 |
| CD11b (Ox42) | Mouse | MCA275G | 1:500 |
| Iba1 | Rabbit | 019-19741 | 1:1000 |
| NeuN | Rabbit | AB177487 | 1:10000 |
| TH | Sheep | ab113 | 1:750 - 1:1000 |
| TH | Chicken | AB134461 | 1:1000 |
| TH | Rabbit | AB152 | 1:1000 |
| TH | Mouse | MAB318 | 1:1000 |
| VMAT2 | Rabbit | 20042 | 1:10000 |
| Ubiquitin | Rabbit | AB7780 | 1:200 |
| DAPI | - | D9542–1MG | 1:2000 |
| Anti-rabbit Biotinylated | Goat | BA6000 | 1:200 |
| Anti-mouse Biotinylated | Horse | BA2001 | 1:200 |
| Anti-chicken Biotinylated | Goat | BA9010 | 1:200 |
| Anti-mouse Alexa 488 | Goat | A11001 | 1:500 |
| Anti-sheep Alexa 488 | Donkey | A11015 | 1:500 |
| Anti-chicken Alexa 488 | Chicken | A11039 | 1:500 |
| Anti-rabbit Alexa 488 | Goat | A11008 | 1:500 |
| Anti-rabbit Alexa 568 | Goat | A11011 | 1:500 |
| Anti-mouse Alexa 568 | Goat | A11004 | 1:500 |
| Anti-mouse Alexa 647 | Donkey | A31571 | 1:500 |
| Anti-rabbit Alexa 647 | Goat | A21245 | 1:500 |

# Image analysis

*Optical Density*

Densitometry allows for quantitative measurement of optical density (OD) in stained tissue samples. Scans of the samples are taken using a flatbed scanner (Epson V850 Pro) at 600 DPI. Optical density is measured from 3-4 consecutive striatal (AP +1.6, +0.7, -0.26, and -0.6 mm) or 1-3 midbrain (AP -4.8, -5.6, -6.5) sections. Quantification is performed using Fiji Software (NIH, v1.0). Before measuring, scans are converted to 8-bit grayscale images and the software is calibrated following the protocol that can be found at https://imagej.nih.gov/ij/docs/examples/calibration/. Briefly, the first 19 steps of a step-tablet with a density range of 0.05 to 3.05 OD are measured and converted to known density values by using a Rodbard function. Background OD is measured from the corpus callosum, and its mean value is subtracted from the values measured from the regions of interest.

*Stereology*

Stereology allows for reliable quantification by sampling the region of interest following the optical fractionator principle. Before starting, 20X z-stack images of left and right sides of the midbrain are acquired using a Leica DMi8 inverted microscope. Cell counting is performed using Fiji Software (NIH, v1.0) and following a protocol adapted from Ip et al. (Ip et al., 2017). Eight to ten midbrain sections immunostained for TH for each rat are analysed (section sampling fraction, ssf = 1/6). The changes that are made to the above-mentioned protocol are in the grid area, counting frame size and optical dissector height. In Paper I, grid area is 170x170 µm, counting frame size is 55x55 µm and optical dissector height is 12 µm, with 3 µm guard zones. In Paper II, grid area is 200x200 µm, counting frame size is 100x100 µm and optical dissector height is 20 µm, without guard zones. In Paper III, grid area is 170x170 µm, counting frame size is 55x55 µm and optical dissector height is 20 µm, without guard zones.

*Axonal swellings quantification*

Before starting, three 63X z-stack images of dorsomedial, central and dorsolateral regions of the left and right striatum are acquired using a Leica DMi8 inverted microscope as previously described (Decressac, Mattsson, Lundblad, et al., 2012). Counting is performed using Fiji Software (NIH, v1.0) and applying a macro developed in-house (Quintino et al., 2022). The macro is based on the 3D object count tool and is able to identify swellings and measure their number and volume. Particles smaller than 4 $\mu m^3$ are excluded and the circularity is set between 0.3-1.0 (Paper I, is 0.5-1.0). In Paper I, swellings are additionally divided into small (4-10 $\mu m^3$), medium (10-20 $\mu m^3$), and large (>20 $\mu m^3$). In Paper II and III, results are expressed as the total number of swellings larger than 20 $\mu m^3$.

# Gene expression analysis

*RNA and cDNA preparation*

Total RNA is extracted from the right side of 3 PFA-fixed midbrain sections using E.Z.N.A.® FFPE RNA Kit (Omega Bio-tek) following the heat method with some minor modifications: sections are placed in lysing matrix tubes (MP Biomedicals) containing GPL buffer and homogenized for 20 s at 4.0 M/s, tubes are spinned for about 30 s to reduce foam, the supernatant is transferred to clean 1.5 mL tubes, the 80 °C incubation step is skipped. RNA concentration is measured using NanoDrop and stored at -80°C. 300 ng of RNA are then reverse transcribed using the iScript cDNA Synthesis Kit (Bio-Rad) following the manufacturer's protocol. Final cDNA volumes are eventually diluted 1:10 in DEPC-treated water and stored at -20°C until use.

*Quantitative Polymerase Chain Reaction (qPCR)*

qPCR is conducted using the PowerUp™ SYBR™ Green Master Mix (Applied Biosystems) diluted as follows: 4 µL of 1:10 cDNA, 5 µL of Master Mix, 0.25 µL of each primer, and 0.5 µL of DEPC-treated water for a total volume of 10 µL. The qPCR protocol is set according to the following conditions: 50°C 1 min, 95 °C 1 min, 40 cycles of 95 °C 15 s and 60 °C 30 s. Quantification cycle values (Cq) of target genes are first normalised to the Cq values of a reference gene (glyceraldehyde phosphate dehydrogenase, *GAPDH*), resulting in ΔCq values. Subsequently, ΔCq values for a target gene are normalised to the average ΔCq of the same gene in a control group (ΔΔCq). The results are reported as $2^{-\Delta\Delta Cq}$, which represents the e relative fold gene expression of that target gene compared to a control group. Primers utilised can be found in Table 3.

**Table 3 | List of qPCR primers**

| Target gene | Primer Forward (5'-3') | Primer Reverse (5'-3') |
|---|---|---|
| *αSyn* | CAG GGA GCA TTG CAG CA | GTG GGG CTC CTT CTT ATT C |
| *Dat* | CGG GGT CCT TCC GGG AGA AAC | GTG AAT TGG CGC ACC TCC CCT |
| *Gapdh* | CAA CTC CCT CAA GAT TGT CAG CAA | GGC ATG GAC TGT GGT CAT GA |
| *Gdf5* | CAC CTG GAG CCC ACG AAT C | CAG GTG GGT GGT GTG GA |
| *Ret* | GTG AAG AAA AGC AAG GGC CG | AGC ACT CCA AAG GAC CAC AC |
| *Th* | CTT TGA CCC AGA CAC AGC A | TGG ATA CGA GAG GCA TAG TTC |

# Acknowledgements

I would like to acknowledge those people that have assisted, encouraged, and guided me during these past years, and without whom I would have not succeeded.

**Andi**, without you this would not have been possible, you are my main scientific mentor and that will not be forgotten. We have been through a lot during such a short time, but this thesis is the proof that challenges can be overcome successfully. I have always appreciated your perseverance, and I am sure it will be the key to success in your future endeavours. I am also glad that you brought so many students to the lab, which have been a precious addition to the team.

**Giuseppe**, **Irene**, **Andrea**, **Febe**, **Cécile**, **Swantje** and **Diego**, you helped me the most in getting closer to the goal. Being a supervisor has been an amazing learning experience and made me understand the importance of educating the next generation of scientists. I hope you felt enriched as I did. Of course, I have not forgotten all the others. You were many, and each of you has contributed to making this experience more stimulating and delightful. To you, I dedicate this thesis.

**Fra**, you have been the first Postdoc in our lab, and I could not have been happier about it. You came when I most needed it and you brought some quiet in my messy mind. You are among the pillars without which I could have not built this thesis. Thanks to you I am also addicted to FlightRadar24.

**Marcus**, I met you as the king of cloning and you did not disappoint me. Thank you for teaching me all the molecular and viral part of my PhD and for the support in the making of this thesis. I promise I'll be better at adding references in the future.

**Tomas B**., you welcomed me in your team back in the days when I was unsure about my future, and it is also thanks to that good time that I decided to pursue a PhD.

**Tomas D**., **Olga**, and **Lisette**, you are the backbone of EMV. Thank you for your precious advice and availability, as well as understanding.

. . .

**Alex**, you have been a constant presence since the beginning of this Swedish experience. You taught me patience, kindness, curiosity, and some more trivial stuff like MtG. You'll always be my first consultant when I'll need to deal with complicated matters that require diplomacy.

**Maria, Myri, Sid, Kat, Marta, Oscar, Ana, Jordi, Mo, Lavanya** and **Martina**, you are the coziness of a Sunday lunch with family. Thank you all for the support, the laughs, the dinners, and all the small gestures which made me smile. Sometimes, I wish I would have been more present, so that we would have more shared good memories that I can carry with me. Stay true to yourselves because you are great.

**Vale, Paola, Miriana,** and **Michael,** il gruppo dei grandi. I named you like that not because of the age difference, but rather for the wise advice I receive whenever we see each other. You often helped me putting things into perspective and your positive attitude is refreshing for the mind.

**Tiago** and **Edo** (with **Sonny**) the other human and non-human flat mates I had beside my sambo. Sharing my everyday life with other *cervelli in fuga* made me feel less lonely in this foreign adventure.

**Albert, David, Eliška, Fabio, Isak, Jessica, Laura, Marcus, Marija, Nadia, Nic, Roberta, Scott,** and **Tiago,** the Be Creative survivors. Despite the fun of the first years has now faded and we all became quieter (or maybe just older), you played an important part in lightening up my mood back in the days. Skål.

**Andreas, Frenki**, **Julie**, and **Radhika**, the B10ers who managed to reach me despite my tendency to isolate in my office. Thank you for stopping by and reminding me that it does not hurt to have a chat here and there.

**Sarah**, **Fra**, **Enrico T.**, **Edoardo, Sara** and **Enrico S.**, grazie per essere rimasti, nonostante tutti questi anni che sono rimasta lontana da casa. Non sono stata molto presente nelle vostre vite, ma siete i primi che ogni volta che torno ho voglia di rivedere e sono sicura che questo significhi qualcosa di importante.

. . .

**Martino**, you have seen all my colours and shapes. You were there when I cheered, and you were there when I cried. Thank you from preventing me from slipping away during these challenging years, you have been like a warm sunny day in this Swedish weather. E ricorda: *la vita è come er vino, più lo bevi e più te frega*.

**Mamma**, **Papà** e **Sorella**, mi avete letteralmente risollevata con viti e barre e rispedita a finire quello che ho cominciato. E per fortuna, altrimenti non so come avrei fatto senza di voi. Grazie per avermi lasciata sperimentare questi anni all'estero e, nonostante ciò, di non avermi mai fatto sentire sola.

. . .

I feel I should eventually thank **the laboratory rats**. Over these years, I had the privilege to study these creatures and their behaviour and you would be surprised to know how interesting and clever they are. It is also thanks to their sacrifice that I could collect the data presented in this thesis.

# References


Abdelmotilib, H., Maltbie, T., Delic, V., Liu, Z., Hu, X., Fraser, K. B., . . . West, A. (2017). alpha-Synuclein fibril-induced inclusion spread in rats and mice correlates with dopaminergic Neurodegeneration. *Neurobiol Dis, 105*, 84-98. doi:10.1016/j.nbd.2017.05.014

Airavaara, M., Parkkinen, I., Konovalova, J., Albert, K., Chmielarz, P., & Domanskyi, A. (2020). Back and to the Future: From Neurotoxin-Induced to Human Parkinson's Disease Models. *Curr Protoc Neurosci, 91*(1), e88. doi:10.1002/cpns.88

Albert, K., Voutilainen, M. H., Domanskyi, A., Piepponen, T. P., Ahola, S., Tuominen, R. K., . . . Airavaara, M. (2019). Downregulation of tyrosine hydroxylase phenotype after AAV injection above substantia nigra: Caution in experimental models of Parkinson's disease. *J Neurosci Res, 97*(3), 346-361. doi:10.1002/jnr.24363

Albin, R. L., Young, A. B., & Penney, J. B. (1989). The functional anatomy of basal ganglia disorders. *Trends Neurosci, 12*(10), 366-375. doi:10.1016/0166-2236(89)90074-x

Alexander, G. E., DeLong, M. R., & Strick, P. L. (1986). Parallel organization of functionally segregated circuits linking basal ganglia and cortex. *Annu Rev Neurosci, 9*, 357-381. doi:10.1146/annurev.ne.09.030186.002041

Baker, M. (2016). 1,500 scientists lift the lid on reproducibility. *Nature, 533*(7604), 452-454. doi:10.1038/533452a

Barone, P. (2010). Neurotransmission in Parkinson's disease: beyond dopamine. *Eur J Neurol, 17*(3), 364-376. doi:10.1111/j.1468-1331.2009.02900.x

Begley, C. G., & Ellis, L. M. (2012). Drug development: Raise standards for preclinical cancer research. *Nature, 483*(7391), 531-533. doi:10.1038/483531a

Bjorklund, A., & Dunnett, S. B. (2007). Dopamine neuron systems in the brain: an update. *Trends Neurosci, 30*(5), 194-202. doi:10.1016/j.tins.2007.03.006

Bolam, J. P., Hanley, J. J., Booth, P. A., & Bevan, M. D. (2000). Synaptic organisation of the basal ganglia. *J Anat, 196 ( Pt 4)*, 527-542. doi:10.1046/j.1469-7580.2000.19640527.x

Braak, H., Del Tredici, K., Rub, U., de Vos, R. A., Jansen Steur, E. N., & Braak, E. (2003). Staging of brain pathology related to sporadic Parkinson's disease. *Neurobiol Aging, 24*(2), 197-211. doi:10.1016/s0197-4580(02)00065-9

Brasted, P. J., Humby, T., Dunnett, S. B., & Robbins, T. W. (1997). Unilateral lesions of the dorsal striatum in rats disrupt responding in egocentric space. *J Neurosci, 17*(22), 8919-8926.

Breger, L. S., & Fuzzati Armentero, M. T. (2019). Genetically engineered animal models of Parkinson's disease: From worm to rodent. *Eur J Neurosci, 49*(4), 533-560. doi:10.1111/ejn.14300

Brown, V. J., & Robbins, T. W. (1989). Deficits in response space following unilateral striatal dopamine depletion in the rat. *J Neurosci, 9*(3), 983-989.

Carli, M., Evenden, J. L., & Robbins, T. W. (1985). Depletion of unilateral striatal dopamine impairs initiation of contralateral actions and not sensory attention. *Nature, 313*(6004), 679-682. doi:10.1038/313679a0

Carli, M., Jones, G. H., & Robbins, T. W. (1989). Effects of unilateral dorsal and ventral striatal dopamine depletion on visual neglect in the rat: a neural and behavioural analysis. *Neuroscience, 29*(2), 309-327. doi:10.1016/0306-4522(89)90059-6

Carlsson, A., Falck, B., & Hillarp, N. A. (1962). Cellular localization of brain monoamines. *Acta Physiol Scand Suppl, 56*(196), 1-28.

Carta, A. R., Boi, L., Pisanu, A., Palmas, M. F., Carboni, E., & De Simone, A. (2020). Advances in modelling alpha-synuclein-induced Parkinson's diseases in rodents: Virus-based models versus inoculation of exogenous preformed toxic species. *J Neurosci Methods, 338*, 108685. doi:10.1016/j.jneumeth.2020.108685

Cazorla, M., de Carvalho, F. D., Chohan, M. O., Shegda, M., Chuhma, N., Rayport, S., . . . Kellendonk, C. (2014). Dopamine D2 receptors regulate the anatomical and functional balance of basal ganglia circuitry. *Neuron, 81*(1), 153-164. doi:10.1016/j.neuron.2013.10.041

Chmielarz, P., & Saarma, M. (2020). Neurotrophic factors for disease-modifying treatments of Parkinson's disease: gaps between basic science and clinical studies. *Pharmacol Rep, 72*(5), 1195-1217. doi:10.1007/s43440-020-00120-3

Choi-Lundberg, D. L., Lin, Q., Chang, Y. N., Chiang, Y. L., Hay, C. M., Mohajeri, H., . . . Bohn, M. C. (1997). Dopaminergic neurons protected from degeneration by GDNF gene therapy. *Science, 275*(5301), 838-841. doi:10.1126/science.275.5301.838

Chung, C. Y., Koprich, J. B., Siddiqi, H., & Isacson, O. (2009). Dynamic changes in presynaptic and axonal transport proteins combined with striatal neuroinflammation precede dopaminergic neuronal loss in a rat model of AAV alpha-synucleinopathy. *J Neurosci, 29*(11), 3365-3373. doi:10.1523/JNEUROSCI.5427-08.2009

Clayton, K. B., & Sullivan, A. M. (2007). Differential effects of GDF5 on the medial and lateral rat ventral mesencephalon. *Neurosci Lett, 427*(3), 132-137. doi:10.1016/j.neulet.2007.09.025

Costello, D. J., O'Keeffe, G. W., Hurley, F. M., & Sullivan, A. M. (2012). Transplantation of novel human GDF5-expressing CHO cells is neuroprotective in models of Parkinson's disease. *J Cell Mol Med, 16*(10), 2451-2460. doi:10.1111/j.1582-4934.2012.01562.x

Crosby, N. J., Deane, K. H., & Clarke, C. E. (2003). Amantadine for dyskinesia in Parkinson's disease. *Cochrane Database Syst Rev*(2), CD003467. doi:10.1002/14651858.CD003467

Cui, G., Jun, S. B., Jin, X., Pham, M. D., Vogel, S. S., Lovinger, D. M., & Costa, R. M. (2013). Concurrent activation of striatal direct and indirect pathways during action initiation. *Nature, 494*(7436), 238-242. doi:10.1038/nature11846

Dahlstroem, A., & Fuxe, K. (1964). Evidence for the Existence of Monoamine-Containing Neurons in the Central Nervous System. I. Demonstration of Monoamines in the Cell Bodies of Brain Stem Neurons. *Acta Physiol Scand Suppl*, SUPPL 232:231-255.

Damier, P., Hirsch, E. C., Agid, Y., & Graybiel, A. M. (1999). The substantia nigra of the human brain. II. Patterns of loss of dopamine-containing neurons in Parkinson's disease. *Brain, 122 ( Pt 8)*, 1437-1448. doi:10.1093/brain/122.8.1437

Davidsson, M., Negrini, M., Hauser, S., Svanbergsson, A., Lockowandt, M., Tomasello, G., . . . Heuer, A. (2020). A comparison of AAV-vector production methods for gene therapy and preclinical assessment. *Sci Rep, 10*(1), 21532. doi:10.1038/s41598-020-78521-w

Decourt, M., Jimenez-Urbieta, H., Benoit-Marand, M., & Fernagut, P. O. (2021). Neuropsychiatric and Cognitive Deficits in Parkinson's Disease and Their Modeling in Rodents. *Biomedicines, 9*(6). doi:10.3390/biomedicines9060684

Decressac, M., Kadkhodaei, B., Mattsson, B., Laguna, A., Perlmann, T., & Bjorklund, A. (2012). alpha-Synuclein-induced down-regulation of Nurr1 disrupts GDNF signaling in nigral dopamine neurons. *Sci Transl Med, 4*(163), 163ra156. doi:10.1126/scitranslmed.3004676

Decressac, M., Mattsson, B., & Bjorklund, A. (2012). Comparison of the behavioural and histological characteristics of the 6-OHDA and alpha-synuclein rat models of Parkinson's disease. *Exp Neurol, 235*(1), 306-315. doi:10.1016/j.expneurol.2012.02.012

Decressac, M., Mattsson, B., Lundblad, M., Weikop, P., & Bjorklund, A. (2012). Progressive neurodegenerative and behavioural changes induced by AAV-mediated overexpression of alpha-synuclein in midbrain dopamine neurons. *Neurobiol Dis, 45*(3), 939-953. doi:10.1016/j.nbd.2011.12.013

Decressac, M., Ulusoy, A., Mattsson, B., Georgievska, B., Romero-Ramos, M., Kirik, D., & Bjorklund, A. (2011). GDNF fails to exert neuroprotection in a rat alpha-synuclein model of Parkinson's disease. *Brain, 134*(Pt 8), 2302-2311. doi:10.1093/brain/awr149

DeLong, M. R. (1990). Primate models of movement disorders of basal ganglia origin. *Trends Neurosci, 13*(7), 281-285. doi:10.1016/0166-2236(90)90110-v

Dougherty, D. D. (2018). Deep Brain Stimulation: Clinical Applications. *Psychiatr Clin North Am, 41*(3), 385-394. doi:10.1016/j.psc.2018.04.004

Dowd, E., & Dunnett, S. B. (2004). Deficits in a lateralized associative learning task in dopamine-depleted rats with functional recovery by dopamine-rich transplants. *Eur J Neurosci, 20*(7), 1953-1959. doi:10.1111/j.1460-9568.2004.03637.x

Dowd, E., & Dunnett, S. B. (2005a). Comparison of 6-hydroxydopamine-induced medial forebrain bundle and nigrostriatal terminal lesions in a lateralised nose-poking task in rats. *Behav Brain Res, 159*(1), 153-161. doi:10.1016/j.bbr.2004.10.010

Dowd, E., & Dunnett, S. B. (2005b). Comparison of 6-hydroxydopamine-induced medial forebrain bundle and nigrostriatal terminal lesions in rats using a lateralised nose-poking task with low stimulus-response compatibility. *Behav Brain Res, 165*(2), 181-186. doi:10.1016/j.bbr.2005.06.036

Dowd, E., Monville, C., Torres, E. M., & Dunnett, S. B. (2005). The Corridor Task: a simple test of lateralised response selection sensitive to unilateral dopamine deafferentation and graft-derived dopamine replacement in the striatum. *Brain Res Bull, 68*(1-2), 24-30. doi:10.1016/j.brainresbull.2005.08.009

Drinkut, A., Tillack, K., Meka, D. P., Schulz, J. B., Kugler, S., & Kramer, E. R. (2016). Ret is essential to mediate GDNF's neuroprotective and neuroregenerative effect in a Parkinson disease mouse model. *Cell Death Dis, 7*(9), e2359. doi:10.1038/cddis.2016.263

Dubach, M. (1994). Telencephalic dopamine cells in monkeys, humans, and rats. *Cambridge University Press, Phylogeny and Development of Catecholamine Systems in the CNS of Vertebrates*, 273– 287.

Dunnett, S. B., Bjorklund, A., Stenevi, U., & Iversen, S. D. (1981). Behavioural recovery following transplantation of substantia nigra in rats subjected to 6-OHDA lesions of the nigrostriatal pathway. I. Unilateral lesions. *Brain Res, 215*(1-2), 147-161. doi:10.1016/0006-8993(81)90498-4

Eriksdotter Jönhagen, M., Nordberg, A., Amberla, K., Backman, L., Ebendal, T., Meyerson, B., . . . Wahlund, L. O. (1998). Intracerebroventricular infusion of nerve growth factor in three patients with Alzheimer's disease. *Dement Geriatr Cogn Disord, 9*(5), 246-257. doi:10.1159/000017069

Espa, E., Clemensson, E. K. H., Luk, K. C., Heuer, A., Bjorklund, T., & Cenci, M. A. (2019). Seeding of protein aggregation causes cognitive impairment in rat model of cortical synucleinopathy. *Mov Disord, 34*(11), 1699-1710. doi:10.1002/mds.27810

Evarts, E. V., Teravainen, H., & Calne, D. B. (1981). Reaction time in Parkinson's disease. *Brain, 104*(Pt 1), 167-186. doi:10.1093/brain/104.1.167

Falck, B., Hillarp, N. A., Thieme, G., & Torp, A. (1962). Fluorescence of catechol amines and related compounds condensed with formaldehyde. *Brain Res Bull, 9*(1-6), xi-xv. doi:10.1016/0361-9230(82)90113-7

Fearnley, J. M., & Lees, A. J. (1991). Ageing and Parkinson's disease: substantia nigra regional selectivity. *Brain, 114 ( Pt 5)*, 2283-2301. doi:10.1093/brain/114.5.2283

Fleming, S. M., Zhu, C., Fernagut, P. O., Mehta, A., DiCarlo, C. D., Seaman, R. L., & Chesselet, M. F. (2004). Behavioral and immunohistochemical effects of chronic intravenous and subcutaneous infusions of varying doses of rotenone. *Exp Neurol, 187*(2), 418-429. doi:10.1016/j.expneurol.2004.01.023

Fujiwara, H., Hasegawa, M., Dohmae, N., Kawashima, A., Masliah, E., Goldberg, M. S., . . . Iwatsubo, T. (2002). alpha-Synuclein is phosphorylated in synucleinopathy lesions. *Nat Cell Biol, 4*(2), 160-164. doi:10.1038/ncb748

Gaspar, P., Berger, B., Febvret, A., Vigny, A., Krieger-Poulet, M., & Borri-Voltattorni, C. (1987). Tyrosine hydroxylase-immunoreactive neurons in the human cerebral cortex: a novel catecholaminergic group? *Neurosci Lett, 80*(3), 257-262. doi:10.1016/0304-3940(87)90464-2

Gauntlett-Gilbert, J., & Brown, V. J. (1998). Reaction time deficits and Parkinson's disease. *Neurosci Biobehav Rev, 22*(6), 865-881. doi:10.1016/s0149-7634(98)00014-1

Gerfen, C. R. (1984). The neostriatal mosaic: compartmentalization of corticostriatal input and striatonigral output systems. *Nature, 311*(5985), 461-464. doi:10.1038/311461a0

Gerfen, C. R. (1985). The neostriatal mosaic. I. Compartmental organization of projections from the striatum to the substantia nigra in the rat. *J Comp Neurol, 236*(4), 454-476. doi:10.1002/cne.902360404

Gerfen, C. R., Engber, T. M., Mahan, L. C., Susel, Z., Chase, T. N., Monsma, F. J., Jr., & Sibley, D. R. (1990). D1 and D2 dopamine receptor-regulated gene expression of striatonigral and striatopallidal neurons. *Science, 250*(4986), 1429-1432. doi:10.1126/science.2147780

Gerfen, C. R., McGinty, J. F., & Young, W. S., 3rd. (1991). Dopamine differentially regulates dynorphin, substance P, and enkephalin expression in striatal neurons: in situ hybridization histochemical analysis. *J Neurosci, 11*(4), 1016-1031.

Glinka, Y., Gassen, M., & Youdim, M. B. (1997). Mechanism of 6-hydroxydopamine neurotoxicity. *J Neural Transm Suppl, 50*, 55-66. doi:10.1007/978-3-7091-6842-4_7

Gombash, S. E., Manfredsson, F. P., Kemp, C. J., Kuhn, N. C., Fleming, S. M., Egan, A. E., . . . Sortwell, C. E. (2013). Morphological and behavioral impact of AAV2/5-mediated overexpression of human wildtype alpha-synuclein in the rat nigrostriatal system. *PLoS One, 8*(11), e81426. doi:10.1371/journal.pone.0081426

Gorbatyuk, O. S., Li, S., Sullivan, L. F., Chen, W., Kondrikova, G., Manfredsson, F. P., . . . Muzyczka, N. (2008). The phosphorylation state of Ser-129 in human alpha-synuclein determines neurodegeneration in a rat model of Parkinson disease. *Proc Natl Acad Sci U S A, 105*(2), 763-768. doi:10.1073/pnas.0711053105

Goulding, S. R., Concannon, R. M., Morales-Prieto, N., Villalobos-Manriquez, F., Clarke, G., Collins, L. M., . . . O'Keeffe, G. W. (2021). Growth differentiation factor 5 exerts neuroprotection in an alpha-synuclein rat model of Parkinson's disease. *Brain, 144*(2), e14. doi:10.1093/brain/awaa367

Graybiel, A. M., Hirsch, E. C., & Agid, Y. (1990). The nigrostriatal system in Parkinson's disease. *Adv Neurol, 53*, 17-29.

Graybiel, A. M., & Ragsdale, C. W., Jr. (1978). Histochemically distinct compartments in the striatum of human, monkeys, and cat demonstrated by acetylthiocholinesterase staining. *Proc Natl Acad Sci U S A, 75*(11), 5723-5726. doi:10.1073/pnas.75.11.5723

Grealish, S., Mattsson, B., Draxler, P., & Bjorklund, A. (2010). Characterisation of behavioural and neurodegenerative changes induced by intranigral 6-hydroxydopamine lesions in a mouse model of Parkinson's disease. *Eur J Neurosci, 31*(12), 2266-2278. doi:10.1111/j.1460-9568.2010.07265.x

Greffard, S., Verny, M., Bonnet, A. M., Beinis, J. Y., Gallinari, C., Meaume, S., . . . Duyckaerts, C. (2006). Motor score of the Unified Parkinson Disease Rating Scale as a good predictor of Lewy body-associated neuronal loss in the substantia nigra. *Arch Neurol, 63*(4), 584-588. doi:10.1001/archneur.63.4.584

Greig, S. L., & McKeage, K. (2016). Carbidopa/Levodopa ER Capsules (Rytary((R)), Numient): A Review in Parkinson's Disease. *CNS Drugs, 30*(1), 79-90. doi:10.1007/s40263-015-0306-3

Haggerty, D. L., Grecco, G. G., Reeves, K. C., & Atwood, B. (2020). Adeno-Associated Viral Vectors in Neuroscience Research. *Mol Ther Methods Clin Dev, 17*, 69-82. doi:10.1016/j.omtm.2019.11.012

Hartshorne, J. K., & Schachner, A. (2012). Tracking replicability as a method of post-publication open evaluation. *Front Comput Neurosci, 6*, 8. doi:10.3389/fncom.2012.00008

Hegarty, S. V., Collins, L. M., Gavin, A. M., Roche, S. L., Wyatt, S. L., Sullivan, A. M., & O'Keeffe, G. W. (2014). Canonical BMP-Smad signalling promotes neurite growth in rat midbrain dopaminergic neurons. *Neuromolecular Med, 16*(2), 473-489. doi:10.1007/s12017-014-8299-5

Hegarty, S. V., Sullivan, A. M., & O'Keeffe, G. W. (2013). BMP2 and GDF5 induce neuronal differentiation through a Smad dependant pathway in a model of human midbrain dopaminergic neurons. *Mol Cell Neurosci, 56*, 263-271. doi:10.1016/j.mcn.2013.06.006

Heuer, A., & Dunnett, S. B. (2012). Unilateral 6-OHDA lesions induce lateralised deficits in a 'skinner box' operant choice reaction time task in rats. *J Parkinsons Dis, 2*(4), 309-320. doi:10.3233/JPD-2012-012133

Heuer, A., & Dunnett, S. B. (2013). Characterisation of spatial neglect induced by unilateral 6-OHDA lesions on a choice reaction time task in rats. *Behav Brain Res, 237*, 215-222. doi:10.1016/j.bbr.2012.09.038

Heuer, A., Lelos, M. J., Kelly, C. M., Torres, E. M., & Dunnett, S. B. (2013). Dopamine-rich grafts alleviate deficits in contralateral response space induced by extensive dopamine depletion in rats. *Exp Neurol, 247*, 485-495. doi:10.1016/j.expneurol.2013.01.020

Heuer, A., Smith, G. A., & Dunnett, S. B. (2013). Comparison of 6-hydroxydopamine lesions of the substantia nigra and the medial forebrain bundle on a lateralised choice reaction time task in mice. *Eur J Neurosci, 37*(2), 294-302. doi:10.1111/ejn.12036

Heuer, A., Smith, G. A., Lelos, M. J., Lane, E. L., & Dunnett, S. B. (2012). Unilateral nigrostriatal 6-hydroxydopamine lesions in mice I: motor impairments identify extent of dopamine depletion at three different lesion sites. *Behav Brain Res, 228*(1), 30-43. doi:10.1016/j.bbr.2011.11.027

Hoban, D. B., Shrigley, S., Mattsson, B., Breger, L. S., Jarl, U., Cardoso, T., . . . Parmar, M. (2020). Impact of alpha-synuclein pathology on transplanted hESC-derived dopaminergic neurons in a humanized alpha-synuclein rat model of PD. *Proc Natl Acad Sci U S A, 117*(26), 15209-15220. doi:10.1073/pnas.2001305117

Hoffer, B. J., Hoffman, A., Bowenkamp, K., Huettl, P., Hudson, J., Martin, D., . . . Gerhardt, G. A. (1994). Glial cell line-derived neurotrophic factor reverses toxin-induced injury to midbrain dopaminergic neurons in vivo. *Neurosci Lett, 182*(1), 107-111. doi:10.1016/0304-3940(94)90218-6

Hoffman, A. F., & Gerhardt, G. A. (1998). In vivo electrochemical studies of dopamine clearance in the rat substantia nigra: effects of locally applied uptake inhibitors and unilateral 6-hydroxydopamine lesions. *J Neurochem, 70*(1), 179-189. doi:10.1046/j.1471-4159.1998.70010179.x

Hökfelt, T. M., R.; Björklund, A.; Kleinau, A.; Goldstein, M. (1984). Distributional maps of tyrosine-hydroxylase-immunoreactive neurons in the rat brain. *Handbook of Chemical Neuroanatomy, 2*(Classical Transmitters in the CNS), 277–379.

Hornykiewicz, O. (2002). L-DOPA: from a biologically inactive amino acid to a successful therapeutic agent. *Amino Acids, 23*(1-3), 65-70. doi:10.1007/s00726-001-0111-9

Hurley, F. M., Costello, D. J., & Sullivan, A. M. (2004). Neuroprotective effects of delayed administration of growth/differentiation factor-5 in the partial lesion model of Parkinson's disease. *Exp Neurol, 185*(2), 281-289. doi:10.1016/j.expneurol.2003.10.003

Ibanez, P., Bonnet, A. M., Debarges, B., Lohmann, E., Tison, F., Pollak, P., . . . Brice, A. (2004). Causal relation between alpha-synuclein gene duplication and familial Parkinson's disease. *Lancet, 364*(9440), 1169-1171. doi:10.1016/S0140-6736(04)17104-3

Ip, C. W., Cheong, D., & Volkmann, J. (2017). Stereological Estimation of Dopaminergic Neuron Number in the Mouse Substantia Nigra Using the Optical Fractionator and Standard Microscopy Equipment. *J Vis Exp*(127). doi:10.3791/56103

Jahanshahi, M., Brown, R. G., & Marsden, C. D. (1992). Simple and choice reaction time and the use of advance information for motor preparation in Parkinson's disease. *Brain, 115 ( Pt 2)*, 539-564. doi:10.1093/brain/115.2.539

Kalia, L. V., & Lang, A. E. (2015). Parkinson's disease. *Lancet, 386*(9996), 896-912. doi:10.1016/S0140-6736(14)61393-3

Katzenschlager, R., Sampaio, C., Costa, J., & Lees, A. (2003). Anticholinergics for symptomatic management of Parkinson's disease. *Cochrane Database Syst Rev*(2), CD003735. doi:10.1002/14651858.CD003735

Khoo, T. K., Yarnall, A. J., Duncan, G. W., Coleman, S., O'Brien, J. T., Brooks, D. J., . . . Burn, D. J. (2013). The spectrum of nonmotor symptoms in early Parkinson disease. *Neurology, 80*(3), 276-281. doi:10.1212/WNL.0b013e31827deb74

Kim, C., Ho, D. H., Suk, J. E., You, S., Michael, S., Kang, J., . . . Lee, S. J. (2013). Neuron-released oligomeric alpha-synuclein is an endogenous agonist of TLR2 for paracrine activation of microglia. *Nat Commun, 4*, 1562. doi:10.1038/ncomms2534

Kirik, D., Rosenblad, C., & Bjorklund, A. (1998). Characterization of behavioral and neurodegenerative changes following partial lesions of the nigrostriatal dopamine system induced by intrastriatal 6-hydroxydopamine in the rat. *Exp Neurol, 152*(2), 259-277. doi:10.1006/exnr.1998.6848

Kirik, D., Rosenblad, C., Burger, C., Lundberg, C., Johansen, T. E., Muzyczka, N., . . . Bjorklund, A. (2002). Parkinson-like neurodegeneration induced by targeted overexpression of alpha-synuclein in the nigrostriatal system. *J Neurosci, 22*(7), 2780-2791. doi:20026246

Klein, R. L., Dayton, R. D., Leidenheimer, N. J., Jansen, K., Golde, T. E., & Zweig, R. M. (2006). Efficient neuronal gene transfer with AAV8 leads to neurotoxic levels of tau or green fluorescent proteins. *Mol Ther, 13*(3), 517-527. doi:10.1016/j.ymthe.2005.10.008

Klein, R. L., King, M. A., Hamby, M. E., & Meyer, E. M. (2002). Dopaminergic cell loss induced by human A30P alpha-synuclein gene transfer to the rat substantia nigra. *Hum Gene Ther, 13*(5), 605-612. doi:10.1089/10430340252837206

Koprich, J. B., Johnston, T. H., Huot, P., Reyes, M. G., Espinosa, M., & Brotchie, J. M. (2011). Progressive neurodegeneration or endogenous compensation in an animal model of Parkinson's disease produced by decreasing doses of alpha-synuclein. *PLoS One, 6*(3), e17698. doi:10.1371/journal.pone.0017698

Koprich, J. B., Johnston, T. H., Reyes, M. G., Sun, X., & Brotchie, J. M. (2010). Expression of human A53T alpha-synuclein in the rat substantia nigra using a novel AAV1/2 vector produces a rapidly evolving pathology with protein aggregation, dystrophic neurite architecture and nigrostriatal degeneration with potential to model the pathology of Parkinson's disease. *Mol Neurodegener, 5*, 43. doi:10.1186/1750-1326-5-43

Krieglstein, K., Rufer, M., Suter-Crazzolara, C., & Unsicker, K. (1995). Neural functions of the transforming growth factors beta. *Int J Dev Neurosci, 13*(3-4), 301-315. doi:10.1016/0736-5748(94)00062-8

Landeck, N., Buck, K., & Kirik, D. (2017). Toxic effects of human and rodent variants of alpha-synuclein in vivo. *Eur J Neurosci, 45*(4), 536-547. doi:10.1111/ejn.13493

Lauwers, E., Debyser, Z., Van Dorpe, J., De Strooper, B., Nuttin, B., & Baekelandt, V. (2003). Neuropathology and neurodegeneration in rodent brain induced by

lentiviral vector-mediated overexpression of alpha-synuclein. *Brain Pathol, 13*(3), 364-372. doi:10.1111/j.1750-3639.2003.tb00035.x

Lelos, M. J., Dowd, E., & Dunnett, S. B. (2012). Nigral grafts in animal models of Parkinson's disease. Is recovery beyond motor function possible? *Prog Brain Res, 200*, 113-142. doi:10.1016/B978-0-444-59575-1.00006-5

Lennon, J. C., & Hassan, I. (2021). Magnetic resonance-guided focused ultrasound for Parkinson's disease since ExAblate, 2016-2019: a systematic review. *Neurol Sci, 42*(2), 553-563. doi:10.1007/s10072-020-05020-1

Lo Bianco, C., Ridet, J. L., Schneider, B. L., Deglon, N., & Aebischer, P. (2002). alpha -Synucleinopathy and selective dopaminergic neuron loss in a rat lentiviral-based model of Parkinson's disease. *Proc Natl Acad Sci U S A, 99*(16), 10813-10818. doi:10.1073/pnas.152339799

Lo Bianco, C., Schneider, B. L., Bauer, M., Sajadi, A., Brice, A., Iwatsubo, T., & Aebischer, P. (2004). Lentiviral vector delivery of parkin prevents dopaminergic degeneration in an alpha-synuclein rat model of Parkinson's disease. *Proc Natl Acad Sci U S A, 101*(50), 17510-17515. doi:10.1073/pnas.0405313101

Luk, K. C., Kehm, V. M., Zhang, B., O'Brien, P., Trojanowski, J. Q., & Lee, V. M. (2012). Intracerebral inoculation of pathological alpha-synuclein initiates a rapidly progressive neurodegenerative alpha-synucleinopathy in mice. *J Exp Med, 209*(5), 975-986. doi:10.1084/jem.20112457

Lundblad, M., Andersson, M., Winkler, C., Kirik, D., Wierup, N., & Cenci, M. A. (2002). Pharmacological validation of behavioural measures of akinesia and dyskinesia in a rat model of Parkinson's disease. *Eur J Neurosci, 15*(1), 120-132. doi:10.1046/j.0953-816x.2001.01843.x

Lundblad, M., Decressac, M., Mattsson, B., & Bjorklund, A. (2012). Impaired neurotransmission caused by overexpression of alpha-synuclein in nigral dopamine neurons. *Proc Natl Acad Sci U S A, 109*(9), 3213-3219. doi:10.1073/pnas.1200575109

Lundblad, M., Picconi, B., Lindgren, H., & Cenci, M. A. (2004). A model of L-DOPA-induced dyskinesia in 6-hydroxydopamine lesioned mice: relation to motor and cellular parameters of nigrostriatal function. *Neurobiol Dis, 16*(1), 110-123. doi:10.1016/j.nbd.2004.01.007

Ma, S. Y., Roytta, M., Rinne, J. O., Collan, Y., & Rinne, U. K. (1997). Correlation between neuromorphometry in the substantia nigra and clinical features in Parkinson's disease using disector counts. *J Neurol Sci, 151*(1), 83-87. doi:10.1016/s0022-510x(97)00100-7

Mallet, N., Micklem, B. R., Henny, P., Brown, M. T., Williams, C., Bolam, J. P., . . . Magill, P. J. (2012). Dichotomous organization of the external globus pallidus. *Neuron, 74*(6), 1075-1086. doi:10.1016/j.neuron.2012.04.027

Manzanza, N. O., Sedlackova, L., & Kalaria, R. N. (2021). Alpha-Synuclein Post-translational Modifications: Implications for Pathogenesis of Lewy Body Disorders. *Front Aging Neurosci, 13*, 690293. doi:10.3389/fnagi.2021.690293

Mastro, K. J., Bouchard, R. S., Holt, H. A., & Gittis, A. H. (2014). Transgenic mouse lines subdivide external segment of the globus pallidus (GPe) neurons and reveal distinct GPe output pathways. *J Neurosci, 34*(6), 2087-2099. doi:10.1523/JNEUROSCI.4646-13.2014

Masuda-Suzukake, M., Nonaka, T., Hosokawa, M., Oikawa, T., Arai, T., Akiyama, H., . . . Hasegawa, M. (2013). Prion-like spreading of pathological alpha-synuclein in brain. *Brain, 136*(Pt 4), 1128-1138. doi:10.1093/brain/awt037

McGregor, M. M., & Nelson, A. B. (2019). Circuit Mechanisms of Parkinson's Disease. *Neuron, 101*(6), 1042-1056. doi:10.1016/j.neuron.2019.03.004

Mulcahy, P., O'Doherty, A., Paucard, A., O'Brien, T., Kirik, D., & Dowd, E. (2012). Development and characterisation of a novel rat model of Parkinson's disease induced by sequential intranigral administration of AAV-alpha-synuclein and the pesticide, rotenone. *Neuroscience, 203*, 170-179. doi:10.1016/j.neuroscience.2011.12.011

Negrini, M., Wang, G., Heuer, A., Bjorklund, T., & Davidsson, M. (2020). AAV Production Everywhere: A Simple, Fast, and Reliable Protocol for In-house AAV Vector Production Based on Chloroform Extraction. *Curr Protoc Neurosci, 93*(1), e103. doi:10.1002/cpns.103

Noyce, A. J., Bestwick, J. P., Silveira-Moriyama, L., Hawkes, C. H., Giovannoni, G., Lees, A. J., & Schrag, A. (2012). Meta-analysis of early nonmotor features and risk factors for Parkinson disease. *Ann Neurol, 72*(6), 893-901. doi:10.1002/ana.23687

Nutt, J. G., Woodward, W. R., Beckner, R. M., Stone, C. K., Berggren, K., Carter, J. H., . . . Gordin, A. (1994). Effect of peripheral catechol-O-methyltransferase inhibition on the pharmacokinetics and pharmacodynamics of levodopa in parkinsonian patients. *Neurology, 44*(5), 913-919. doi:10.1212/wnl.44.5.913

O'Keeffe, G. W., Dockery, P., & Sullivan, A. M. (2004). Effects of growth/differentiation factor 5 on the survival and morphology of embryonic rat midbrain dopaminergic neurones in vitro. *J Neurocytol, 33*(5), 479-488. doi:10.1007/s11068-004-0511-y

O'Keeffe, G. W., Hanke, M., Pohl, J., & Sullivan, A. M. (2004). Expression of growth differentiation factor-5 in the developing and adult rat brain. *Brain Res Dev Brain Res, 151*(1-2), 199-202. doi:10.1016/j.devbrainres.2004.04.004

O'Sullivan, D. B., Harrison, P. T., & Sullivan, A. M. (2010). Effects of GDF5 overexpression on embryonic rat dopaminergic neurones in vitro and in vivo. *J Neural Transm (Vienna), 117*(5), 559-572. doi:10.1007/s00702-010-0392-9

Olanow, C. W., Agid, Y., Mizuno, Y., Albanese, A., Bonuccelli, U., Damier, P., . . . Stocchi, F. (2004). Levodopa in the treatment of Parkinson's disease: current controversies. *Mov Disord, 19*(9), 997-1005. doi:10.1002/mds.20243

Oliveras-Salva, M., Van der Perren, A., Casadei, N., Stroobants, S., Nuber, S., D'Hooge, R., . . . Baekelandt, V. (2013). rAAV2/7 vector-mediated overexpression of alpha-synuclein in mouse substantia nigra induces protein aggregation and progressive dose-dependent neurodegeneration. *Mol Neurodegener, 8*, 44. doi:10.1186/1750-1326-8-44

Olson, L., Backlund, E. O., Ebendal, T., Freedman, R., Hamberger, B., Hansson, P., . . . et al. (1991). Intraputaminal infusion of nerve growth factor to support adrenal medullary autografts in Parkinson's disease. One-year follow-up of first clinical trial. *Arch Neurol, 48*(4), 373-381. doi:10.1001/archneur.1991.00530160037011

Olsson, M., Nikkhah, G., Bentlage, C., & Bjorklund, A. (1995). Forelimb akinesia in the rat Parkinson model: differential effects of dopamine agonists and nigral transplants as assessed by a new stepping test. *J Neurosci, 15*(5 Pt 2), 3863-3875.

Ouchi, Y., Yoshikawa, E., Sekine, Y., Futatsubashi, M., Kanno, T., Ogusu, T., & Torizuka, T. (2005). Microglial activation and dopamine terminal loss in early Parkinson's disease. *Ann Neurol, 57*(2), 168-175. doi:10.1002/ana.20338

Parkinson, J. (2002). An essay on the shaking palsy. 1817. *J Neuropsychiatry Clin Neurosci, 14*(2), 223-236; discussion 222. doi:10.1176/jnp.14.2.223

Parkkinen, L., Kauppinen, T., Pirttila, T., Autere, J. M., & Alafuzoff, I. (2005). Alpha-synuclein pathology does not predict extrapyramidal symptoms or dementia. *Ann Neurol, 57*(1), 82-91. doi:10.1002/ana.20321

Parkkinen, L., O'Sullivan, S. S., Collins, C., Petrie, A., Holton, J. L., Revesz, T., & Lees, A. J. (2011). Disentangling the relationship between lewy bodies and nigral neuronal loss in Parkinson's disease. *J Parkinsons Dis, 1*(3), 277-286. doi:10.3233/JPD-2011-11046

Parkkinen, L., Pirttila, T., & Alafuzoff, I. (2008). Applicability of current staging/categorization of alpha-synuclein pathology and their clinical relevance. *Acta Neuropathol, 115*(4), 399-407. doi:10.1007/s00401-008-0346-6

Peelaerts, W., Bousset, L., Baekelandt, V., & Melki, R. (2018). a-Synuclein strains and seeding in Parkinson's disease, incidental Lewy body disease, dementia with Lewy bodies and multiple system atrophy: similarities and differences. *Cell Tissue Res, 373*(1), 195-212. doi:10.1007/s00441-018-2839-5

Peelaerts, W., Bousset, L., Van der Perren, A., Moskalyuk, A., Pulizzi, R., Giugliano, M., . . . Baekelandt, V. (2015). alpha-Synuclein strains cause distinct synucleinopathies after local and systemic administration. *Nature, 522*(7556), 340-344. doi:10.1038/nature14547

Phan, J. A., Stokholm, K., Zareba-Paslawska, J., Jakobsen, S., Vang, K., Gjedde, A., . . . Romero-Ramos, M. (2017). Early synaptic dysfunction induced by alpha-synuclein in a rat model of Parkinson's disease. *Sci Rep, 7*(1), 6363. doi:10.1038/s41598-017-06724-9

Polinkovsky, A., Robin, N. H., Thomas, J. T., Irons, M., Lynn, A., Goodman, F. R., . . . Warman, M. L. (1997). Mutations in CDMP1 cause autosomal dominant brachydactyly type C. *Nat Genet, 17*(1), 18-19. doi:10.1038/ng0997-18

Polymeropoulos, M. H., Lavedan, C., Leroy, E., Ide, S. E., Dehejia, A., Dutra, A., . . . Nussbaum, R. L. (1997). Mutation in the alpha-synuclein gene identified in families with Parkinson's disease. *Science, 276*(5321), 2045-2047. doi:10.1126/science.276.5321.2045

Prinz, F., Schlange, T., & Asadullah, K. (2011). Believe it or not: how much can we rely on published data on potential drug targets? *Nat Rev Drug Discov, 10*(9), 712. doi:10.1038/nrd3439-c1

Quintino, L., Gubinelli, F., Sarauskyte, L., Arvidsson, E., Davidsson, M., Lundberg, C., & Heuer, A. (2022). Automated quantification of neuronal swellings in a preclinical rodent model of Parkinson's disease detects region-specific changes in pathology. *J Neurosci Methods, 378*, 109640. doi:10.1016/j.jneumeth.2022.109640

Rabey, J. M., Sagi, I., Huberman, M., Melamed, E., Korczyn, A., Giladi, N., . . . Rasagiline Study, G. (2000). Rasagiline mesylate, a new MAO-B inhibitor for the treatment of Parkinson's disease: a double-blind study as adjunctive therapy to levodopa. *Clin Neuropharmacol, 23*(6), 324-330. doi:10.1097/00002826-200011000-00005

Ransmayr, G. (2011). Physical, occupational, speech and swallowing therapies and physical exercise in Parkinson's disease. *J Neural Transm (Vienna), 118*(5), 773-781. doi:10.1007/s00702-011-0622-9

Rascol, O., Brooks, D. J., Melamed, E., Oertel, W., Poewe, W., Stocchi, F., . . . group, L. s. (2005). Rasagiline as an adjunct to levodopa in patients with Parkinson's disease and motor fluctuations (LARGO, Lasting effect in Adjunct therapy with Rasagiline Given Once daily, study): a randomised, double-blind, parallel-group trial. *Lancet, 365*(9463), 947-954. doi:10.1016/S0140-6736(05)71083-7

Rey, N. L., Steiner, J. A., Maroof, N., Luk, K. C., Madaj, Z., Trojanowski, J. Q., . . . Brundin, P. (2016). Widespread transneuronal propagation of alpha-synucleinopathy triggered in olfactory bulb mimics prodromal Parkinson's disease. *J Exp Med, 213*(9), 1759-1778. doi:10.1084/jem.20160368

Riachi, N. J., Dietrich, W. D., & Harik, S. I. (1990). Effects of internal carotid administration of MPTP on rat brain and blood-brain barrier. *Brain Res, 533*(1), 6-14. doi:10.1016/0006-8993(90)91788-i

Rogers, M. W., & Chan, C. W. (1988). Motor planning is impaired in Parkinson's disease. *Brain Res, 438*(1-2), 271-276. doi:10.1016/0006-8993(88)91346-7

Sakai, K., & Gash, D. M. (1994). Effect of bilateral 6-OHDA lesions of the substantia nigra on locomotor activity in the rat. *Brain Res, 633*(1-2), 144-150. doi:10.1016/0006-8993(94)91533-4

Sandoval, I. M., Kuhn, N. M., & Manfredsson, F. P. (2019). Multimodal Production of Adeno-Associated Virus. *Methods Mol Biol, 1937*, 101-124. doi:10.1007/978-1-4939-9065-8_6

Schallert, T., Fleming, S. M., Leasure, J. L., Tillerson, J. L., & Bland, S. T. (2000). CNS plasticity and assessment of forelimb sensorimotor outcome in unilateral rat models of stroke, cortical ablation, parkinsonism and spinal cord injury. *Neuropharmacology, 39*(5), 777-787. doi:10.1016/s0028-3908(00)00005-8

Schallert, T., Norton, D., & Jones, T. A. (1992). A Clinically Relevant Unilateral Rat Model of Parkinsonian Akinesia. *Journal of Neural Transplantation and Plasticity, 3*(4), 332-333. doi:10.1155/np.1992.332

Sedelis, M., Hofele, K., Auburger, G. W., Morgan, S., Huston, J. P., & Schwarting, R. K. (2000). MPTP susceptibility in the mouse: behavioral, neurochemical, and histological analysis of gender and strain differences. *Behav Genet, 30*(3), 171-182. doi:10.1023/a:1001958023096

Singleton, A. B., Farrer, M., Johnson, J., Singleton, A., Hague, S., Kachergus, J., . . . Gwinn-Hardy, K. (2003). alpha-Synuclein locus triplication causes Parkinson's disease. *Science, 302*(5646), 841. doi:10.1126/science.1090278

Spillantini, M. G., Schmidt, M. L., Lee, V. M., Trojanowski, J. Q., Jakes, R., & Goedert, M. (1997). Alpha-synuclein in Lewy bodies. *Nature, 388*(6645), 839-840. doi:10.1038/42166

Stanic, D., Finkelstein, D. I., Bourke, D. W., Drago, J., & Horne, M. K. (2003). Timecourse of striatal re-innervation following lesions of dopaminergic SNpc neurons of the rat. *Eur J Neurosci, 18*(5), 1175-1188. doi:10.1046/j.1460-9568.2003.02800.x

Storm, E. E., Huynh, T. V., Copeland, N. G., Jenkins, N. A., Kingsley, D. M., & Lee, S. J. (1994). Limb alterations in brachypodism mice due to mutations in a new member of the TGF beta-superfamily. *Nature, 368*(6472), 639-643. doi:10.1038/368639a0

Sullivan, A. M., Opacka-Juffry, J., Hotten, G., Pohl, J., & Blunt, S. B. (1997). Growth/differentiation factor 5 protects nigrostriatal dopaminergic neurones in a rat model of Parkinson's disease. *Neurosci Lett, 233*(2-3), 73-76. doi:10.1016/s0304-3940(97)00623-x

Sullivan, A. M., Pohl, J., & Blunt, S. B. (1998). Growth/differentiation factor 5 and glial cell line-derived neurotrophic factor enhance survival and function of dopaminergic grafts in a rat model of Parkinson's disease. *Eur J Neurosci, 10*(12), 3681-3688. doi:10.1046/j.1460-9568.1998.00378.x

Sulzer, D. (2007). Multiple hit hypotheses for dopamine neuron loss in Parkinson's disease. *Trends Neurosci, 30*(5), 244-250. doi:10.1016/j.tins.2007.03.009

Tecuapetla, F., Koos, T., Tepper, J. M., Kabbani, N., & Yeckel, M. F. (2009). Differential dopaminergic modulation of neostriatal synaptic connections of striatopallidal axon collaterals. *J Neurosci, 29*(28), 8977-8990. doi:10.1523/JNEUROSCI.6145-08.2009

Thakur, P., Breger, L. S., Lundblad, M., Wan, O. W., Mattsson, B., Luk, K. C., . . . Bjorklund, A. (2017). Modeling Parkinson's disease pathology by combination of fibril seeds and alpha-synuclein overexpression in the rat brain. *Proc Natl Acad Sci U S A, 114*(39), E8284-E8293. doi:10.1073/pnas.1710442114

Thomas, J. T., Kilpatrick, M. W., Lin, K., Erlacher, L., Lembessis, P., Costa, T., . . . Luyten, F. P. (1997). Disruption of human limb morphogenesis by a dominant negative mutation in CDMP1. *Nat Genet, 17*(1), 58-64. doi:10.1038/ng0997-58

Thomas, J. T., Lin, K., Nandedkar, M., Camargo, M., Cervenka, J., & Luyten, F. P. (1996). A human chondrodysplasia due to a mutation in a TGF-beta superfamily member. *Nat Genet, 12*(3), 315-317. doi:10.1038/ng0396-315

Trétiakoff, C. (1919). Contribution a l'etude de l'Anatomie pathologique du Locus Niger de Soemmering avec quelques deduction relatives a la pathogenie des troubles du tonus musculaire et de la maladie de Parkinson. *Theses de Paris*.

Ungerstedt, U. (1968). 6-Hydroxy-dopamine induced degeneration of central monoamine neurons. *Eur J Pharmacol, 5*(1), 107-110. doi:10.1016/0014-2999(68)90164-7

Ungerstedt, U. (1971). Adipsia and aphagia after 6-hydroxydopamine induced degeneration of the nigro-striatal dopamine system. *Acta Physiol Scand Suppl, 367*, 95-122. doi:10.1111/j.1365-201x.1971.tb11001.x

Ungerstedt, U., & Arbuthnott, G. W. (1970). Quantitative recording of rotational behavior in rats after 6-hydroxy-dopamine lesions of the nigrostriatal dopamine system. *Brain Res, 24*(3), 485-493. doi:10.1016/0006-8993(70)90187-3

Van der Perren, A., Toelen, J., Casteels, C., Macchi, F., Van Rompuy, A. S., Sarre, S., . . . Baekelandt, V. (2015). Longitudinal follow-up and characterization of a robust rat model for Parkinson's disease based on overexpression of alpha-synuclein with adeno-associated viral vectors. *Neurobiol Aging, 36*(3), 1543-1558. doi:10.1016/j.neurobiolaging.2014.11.015

Volpicelli-Daley, L. A., Kirik, D., Stoyka, L. E., Standaert, D. G., & Harms, A. S. (2016). How can rAAV-alpha-synuclein and the fibril alpha-synuclein models advance our understanding of Parkinson's disease? *J Neurochem, 139 Suppl 1*, 131-155. doi:10.1111/jnc.13627

Volpicelli-Daley, L. A., Luk, K. C., Patel, T. P., Tanik, S. A., Riddle, D. M., Stieber, A., . . . Lee, V. M. (2011). Exogenous alpha-synuclein fibrils induce Lewy body

pathology leading to synaptic dysfunction and neuron death. *Neuron, 72*(1), 57-71. doi:10.1016/j.neuron.2011.08.033

Wang, S., Chu, C. H., Stewart, T., Ginghina, C., Wang, Y., Nie, H., . . . Zhang, J. (2015). alpha-Synuclein, a chemoattractant, directs microglial migration via H2O2-dependent Lyn phosphorylation. *Proc Natl Acad Sci U S A, 112*(15), E1926-1935. doi:10.1073/pnas.1417883112

Wang, Y., Tien, L. T., Lapchak, P. A., & Hoffer, B. J. (1996). GDNF triggers fiber outgrowth of fetal ventral mesencephalic grafts from nigra to striatum in 6-OHDA-lesioned rats. *Cell Tissue Res, 286*(2), 225-233. doi:10.1007/s004410050691

Whone, A., Boca, M., Luz, M., Woolley, M., Mooney, L., Dharia, S., . . . Gill, S. S. (2019). Extended Treatment with Glial Cell Line-Derived Neurotrophic Factor in Parkinson's Disease. *J Parkinsons Dis, 9*(2), 301-313. doi:10.3233/JPD-191576

Whone, A., Luz, M., Boca, M., Woolley, M., Mooney, L., Dharia, S., . . . Gill, S. S. (2019). Randomized trial of intermittent intraputamenal glial cell line-derived neurotrophic factor in Parkinson's disease. *Brain, 142*(3), 512-525. doi:10.1093/brain/awz023

Wise, R. A. (2004). Dopamine, learning and motivation. *Nat Rev Neurosci, 5*(6), 483-494. doi:10.1038/nrn1406

Wong, Y. C., & Krainc, D. (2017). alpha-synuclein toxicity in neurodegeneration: mechanism and therapeutic strategies. *Nat Med, 23*(2), 1-13. doi:10.1038/nm.4269

Wood, S. J., Wypych, J., Steavenson, S., Louis, J. C., Citron, M., & Biere, A. L. (1999). alpha-synuclein fibrillogenesis is nucleation-dependent. Implications for the pathogenesis of Parkinson's disease. *J Biol Chem, 274*(28), 19509-19512. doi:10.1074/jbc.274.28.19509